

ÉCOLE DE TECHNOLOGIE SUPÉRIEURE
UNIVERSITÉ DU QUÉBEC

THESIS PRESENTED TO
ÉCOLE DE TECHNOLOGIE SUPÉRIEURE

IN PARTIAL FULFILLMENT OF THE REQUIREMENTS FOR
THE DEGREE OF MASTER OF MECHANICAL ENGINEERING
M. Eng.

BY
POULIN, Jonathan

CONSTRUCTION OF NACELLE POWER-CURVE FOLLOWING
MARKOV'S THEORY

MONTRÉAL, OCTOBER 29 2007

© Copyright 2007 reserved by Jonathan Poulin

THIS THESIS HAS BEEN EVALUATED
BY THE FOLLOWING BOARD OF EXAMINERS

Mr. Christian Masson, Thesis Supervisor
Département de génie mécanique à l'École de technologie supérieure

Ms. Saskia Honhoff, Thesis Co-supervisor
General Electric, Wind Energy

M. Jean-Pierre Kenné, President of the Board of Examiners
Département de génie mécanique à l'École de technologie supérieure

M. Simon Joncas, Examiner
Département de génie de la production automatisée à l'École de technologie supérieure

THIS THESIS HAS BEEN PRESENTED AND DEFENDED

BEFORE A BOARD OF EXAMINERS

SEPTEMBER 28, 2007

AT ÉCOLE DE TECHNOLOGIE SUPÉRIEURE

ACKNOWLEDGMENT

First, I would like to thank my thesis supervisor Christian Masson, for giving me the opportunity to make my master's thesis in wind-turbine technology. Your support, knowledge and availability was well appreciated. You give me much more than simply answer my questions! Thank you for everything.

I also would like to thanks my thesis co-supervisor Saskia Honhoff, from General Electric, in Germany. Thank you for your hospitality, when I went 3 weeks in Germany. Also thank you for all the time you spent with me in order to realise this thesis.

Thank you to all my friends and family, especially my father Luc, my mother Carole and her husband Michel. This thesis wouldn't have been possible without you. You made me believe that it was possible to make this project and did support me on the toughest moments. I'm grateful to have you for parents... Thank you! Merci!

Special thanks to my girlfriend Marie-Josée, thank you for loving me, being with me all that time and helping me in the realisation of this thesis. The past one and half year with you was exceptional... Merci Bibi!

CONSTRUCTION OF NACELLE POWER-CURVE FOLLOWING MARKOV'S THEORY

POULIN, Jonathan

ABSTRACT

The standard procedure to construct a power curve is the IEC standard. However, this model contains some flaws. In fact, by averaging the power inside a bin speed the power obtained isn't precise, since the power is directly affected by the turbulence intensity of the wind speed. Moreover, it requires long time to evaluate the influence of different settings with this method. The solution proposed in this thesis is to implement a novel method to construct a power curve, which is by following the Markov's theory. This method calculates the stationary power with a stochastic approach, which is more precise and should take less time than the standard procedure. Nonetheless, the construction of a power curve with the meteorological-mast (MM) anemometer isn't always feasible. In addition, the distance between the MM and the turbine can reduce the correlation of the wind speed read at the MM anemometer and the one which hit the blades of the turbine. Thus, to correct that, the construction of the power curve should be implemented on the nacelle anemometer.

The final objective of this master thesis is to implement a Markov power-curve program, which will calculate the stationary power with the nacelle anemometer at each speed bin. Furthermore, this thesis will evaluate and optimise the parameters to obtain the best power curve following this novel method. Finally, the evaluation of the measurement time required to construct this type of power curve will be executed.

Albeit the power curves obtained following this new method aren't stable, this thesis proposes the median to calculate the conditional moment, since the results are less affected by the turbulence intensity. Besides, it also proposes to average the wind speed over a period of two minutes, when using the nacelle anemometer, to eliminate the fast fluctuations of the wind speed due to the blade passage. Moreover, the utilisation of the data averaged over different periods of time doesn't change the result of the power curve. However, the time required to construct a Markov power-curve isn't affected by the averaging time of the data. Nevertheless, this novel method is a little bit faster than the IEC procedure.

Further improvement should be done in the power-curve program. The software amelioration should make the results more stable and more accurate. In addition, the required time to construct a Markov power-curve might decrease again. The first recommendation is to verify with more data sets the rotor-position filter effect, when using the nacelle anemometer to construct a Markov power-curve. The second recommendation could be to correct the second minimum problem when calculating the stationary power with the minimal potential. A method to correct that will be to optimize the relaxation-time interval to determine the drift.

CONSTRUCTION OF NACELLE POWER-CURVE FOLLOWING MARKOV'S THEORY

POULIN, Jonathan

RÉSUMÉ

La procédure standard pour construire une courbe de puissance est la norme IEC. Toutefois, ce modèle contient quelques faiblesses. Une de ses faiblesses est le fait de moyenner les puissances, ce qui engendre des erreurs puisque les puissances obtenues, sur la courbe de puissance, sont grandement influencées par l'intensité de turbulence de la vitesse du vent. De plus, cette norme peut demander beaucoup de temps pour évaluer l'influence de divers paramètres sur une éolienne. La solution proposée dans ce mémoire est d'implémenter une nouvelle méthode, en suivant la théorie de Markov, pour calculer les courbes de puissance. Cette méthode calcule la puissance stationnaire avec une approche stochastique, laquelle est plus précise et s'effectue en un plus court laps de temps. Il arrive aussi que le calcul d'une courbe de puissance puisse être impossible à effectuer avec l'anémomètre à la tour météorologique, il faut donc créer une fonction de transfert pour l'implémenter à l'anémomètre à la nacelle de l'éolienne.

L'objectif final de ce mémoire est de créer un programme qui va construire une courbe de puissance, avec l'anémomètre à la nacelle, en suivant la théorie de Markov, tout en évaluant et optimisant l'influence de divers paramètres. Finalement, un autre objectif est l'analyse du temps minimum requis avec ce nouveau modèle pour construire une courbe de puissance.

Bien que les résultats obtenus ne soient pas stables, ni parfait, ce mémoire propose la médiane pour calculer le moment conditionnel, puisque les résultats sont moins affectés par l'intensité de turbulence. Par la suite, il propose aussi de moyenner les vitesses du vent sur une période de deux minutes, lorsque la vitesse du vent est lue sur l'anémomètre à la nacelle, afin d'éliminer les fluctuations rapide du vent causées par le passage des pales de l'éolienne. Cependant, le temps nécessaire à la construction d'une courbe de puissance en suivant la théorie de Markov n'est pas affectée par les données moyennées à différents intervalles de temps. Par contre, cette nouvelle méthode peut construire une courbe de puissance en un temps plus rapide que la norme IEC.

De plus amples améliorations doivent être effectuées dans le programme qui construit la courbe de puissance avec Markov. En fait, l'amélioration du programme permettrait d'obtenir des résultats plus stables, et donc plus précis. Par le fait même, cette amélioration pourrait faire en sorte d'effectuer une courbe de puissance en un temps plus court. La première recommandation est de vérifier l'impact du filtrage pour la position du rotor, avec un plus grand nombre d'éoliennes. La deuxième recommandation est de corriger l'apparition du deuxième minimum. Une méthode pour le corriger est d'optimiser l'intervalle du temps de relaxation.

TABLE OF CONTENTS

	Page
INTRODUCTION	1
CHAPTER 1 LITERATURE REVIEW	5
1.1 International Electrotechnical Commission (IEC) standard	5
1.1.1 Performance test on a wind turbine	6
1.2 IEC flaws	11
1.3 Markov process	12
1.4 GE's works	12
1.5 University of Oldenburg's contribution	15
1.5.1 Simulated-data and power-curve programs	15
1.5.2 Articles made by the University of Oldenburg	16
CHAPTER 2 MATHEMATICAL MODEL	18
2.1 Langevin equation for Brownian motion	18
2.2 Fokker-Planck equation	21
2.3 Stochastic processes	22
2.4 Markov property	23
2.5 Coefficients estimation	23
CHAPTER 3 WIND-TURBINES DESCRIPTION	27
3.1 Klondike-II	27
3.2 Wietmarschen	29
3.3 Prettin	31
CHAPTER 4 POWER CURVE CONSTRUCTED WITH THE METEOROLOGICAL- MAST ANEMOMETER	34
4.1 Default power-curve	36
4.2 Power-states range filter	40
4.3 Method to calculate the conditional moment	42
4.3.1 Median	43
4.3.2 Most frequent power-difference	45
4.3.3 Power-differences filter	48
4.4 Method to calculate the stationary power curve	50
4.5 Method to calculate the drift	52
4.6 Power-states number	54
4.7 Averaging time	56
4.8 Wind speed averaging	58
4.9 Synthesis of all parameters	61
CHAPTER 5 POWER CURVE CONSTRUCTED WITH THE NACELLE ANEMOMETER	63
5.1 Wind-speed averaging at the nacelle anemometer	64

5.2	Rotor-position filter	66
5.3	Averaging time below 1 second.....	67
CHAPTER 6 VALIDATION OF THE POWER CURVE WITH WIETMARSCHEN AND PRETTIN TURBINES.....		70
6.1	Meteorological-mast anemometer	70
6.2	Nacelle anemometer.....	75
CHAPTER 7 TIME REQUIRED TO CONSTRUCT A NACELLE POWER-CURVE FOLLOWING MARKOV'S THEORY		81
CONCLUSION.....		84
RECOMMENDATIONS		87
APPENDIX I FLOW CHART: SOFTWARE TO CONSTRUCT THE STATIONARY POWER CURVE.....		89
APPENDIX II POWER ERROR FOR THE DATA AVERAGED AT 1 SECOND.....		95
APPENDIX III POWER ERROR FOR THE DATA AVERAGED AT 0,1 SECOND		98
APPENDIX IV CONDITIONAL MOMENT IN FUNCTION OF THE RELAXATION TIME		101
BIBLIOGRAPHY.....		105

LIST OF FIGURES

	Page
Figure 1.1 Requirements as to distance of the meteorological mast and maximum allowed measurement sectors [9].	7
Figure 1.2 Sectors to exclude due to wakes of neighbouring and operating wind turbines and significant obstacles [9].	8
Figure 1.3 GE's simulated data created around a theoretical power-curve [13].	14
Figure 1.4 Power curve obtained by the University of Oldenburg with their simulated-data and power-curve programs [6].	16
Figure 1.5 Power curves obtained for a simulated data set [7].	17
Figure 2.1 Example of conditional moment in function of the relaxation time (τ).	25
Figure 2.2 Comparison of the minimal potential with the zero crossing to determine the stationary power output [13].	26
Figure 3.1 Klondike-II site located in U.S.A. in the Oregon State.	28
Figure 3.2 Scatter plot of the power in function of the MM wind speed at an averaged time of 1 second for Klondike-10.	29
Figure 3.3 Wietmarschen site located in Germany.	30
Figure 3.4 Scatter plot of the power in function of the MM wind speed at an averaged time of 1 second for Wietmarschen-1.	31
Figure 3.5 Prettin site located in Germany.	32
Figure 3.6 Scatter plot of the power in function of the MM wind speed at an averaged time of 1 second for Prettin-5.	33
Figure 4.1 Scatter plot of the simulated data around the theoretical power-curve [6].	35
Figure 4.2 Default power-curve for the simulated data.	37
Figure 4.3 Default power-curve for the MM anemometer of Klondike-10.	37
Figure 4.4 Linear-regression method to determine the power at the bin speed of 6,25 m/s for Klondike-10.	38

Figure 4.5	Minimal-potential method to determine the power at the bin speed of 6,25 m/s for Klondike-10.....	39
Figure 4.6	Conditional moment in function of the relaxation time at the bin speed of 6,25 m/s at the power state of 579 kW for Klondike-10.....	40
Figure 4.7	Comparison of different power-states range filter for the simulated data.	42
Figure 4.8	Comparison of different power-states range filter for the MM anemometer of Klondike-10.	42
Figure 4.9	Histogram of the power difference for the bin speed of 9,25 m/s, for the power state of 1450 kW and for the relaxation time (τ) of 5 seconds for Klondike-10.	43
Figure 4.10	Comparison of the mean with the median to calculate the power curve for the simulated data.	44
Figure 4.11	Comparison of the mean with the median to calculate the power curve for the MM anemometer of Klondike-10.	45
Figure 4.12	Example of distribution for the power difference.....	46
Figure 4.13	Example of distribution for the power difference at 50% of the highest number of data.	47
Figure 4.14	Comparison of the median with the most frequent to calculate the power curve for the MM anemometer of Klondike-10.....	48
Figure 4.15	Comparison of the median with the power-differences filter to calculate the power curve for the simulated data.	49
Figure 4.16	Comparison of the median with the power-differences filter to calculate the power curve for the MM anemometer of Klondike-10.....	49
Figure 4.17	Comparison of the median with the power-differences filter to calculate the power curve for the MM anemometer of Wietmarschen-2.	50
Figure 4.18	Comparison of the minimal potential with the linear regression to calculate the power curve for the simulated data.	52
Figure 4.19	Comparison of the minimal potential with the linear regression to calculate the power curve for the MM anemometer of Klondike-10.....	52
Figure 4.20	Comparison of the power curve with different methods to calculate the drift for the simulated data.	54

Figure 4.21	Comparison of the power curve with different methods to calculate the drift for the MM anemometer of Klondike-10.....	54
Figure 4.22	Comparison of different number of power states to calculate the power curve for the simulated data.....	55
Figure 4.23	Comparison of different number of power states to calculate the power curve for the MM anemometer of Klondike-10.....	56
Figure 4.24	Comparison between the averaging times higher than 1 second to construct the power curve for the MM anemometer of Klondike-10.....	57
Figure 4.25	Comparison between the averaging times shorter than 1 second to construct the power curve for the MM anemometer of Klondike-10.....	58
Figure 4.26	Comparison of different averaging times of the wind speed to construct the power curve for the simulated data.....	60
Figure 4.27	Comparison of different averaging times of the wind speed to construct the power curve for the MM anemometer of Klondike-10.....	60
Figure 4.28	Comparison of different averaging times of the wind speed to construct the power curve for the MM anemometer of Wietmarschen-2.	61
Figure 5.1	Correlation between the MM and the nacelle anemometer for Klondike-10.	63
Figure 5.2	Default power-curve constructed for the nacelle anemometer of Klondike-10.....	64
Figure 5.3	Comparison of different wind-speed averaging time for the power curve constructed for the nacelle anemometer of Klondike-10.....	66
Figure 5.4	Comparison of the rotor-position filter for the power curve constructed for the nacelle anemometer of Klondike-10.....	67
Figure 5.5	Comparison of the time averaging for the power curve constructed for the nacelle anemometer of Klondike-10.....	68
Figure 6.1	Power curve obtained with the default parameters for the MM anemometer of Prettin-4.....	71
Figure 6.2	Power curve obtained with the default parameters for the MM anemometer of Prettin-5.....	72
Figure 6.3	Power curve obtained with the default parameters for the MM anemometer of Wietmarschen-1.	73

Figure 6.4	Power curve obtained with the default parameters for the MM anemometer of Wietmarschen-2.	73
Figure 6.5	Comparison of the time averaging for the power curve constructed for the MM anemometer of Wietmarschen-1.	74
Figure 6.6	Comparison of the time averaging for the power curve constructed for the MM anemometer of Wietmarschen-2.	75
Figure 6.7	Power curve obtained with the default parameters for the nacelle anemometer of Prettin-4.	76
Figure 6.8	Power curve obtained with the default parameters for the nacelle anemometer of Prettin-5.	77
Figure 6.9	Power curve obtained with the default parameters for the nacelle anemometer of Wietmarschen-1.	77
Figure 6.10	Power curve obtained with the default parameters for the nacelle anemometer of Wietmarschen-2.	78
Figure 6.11	Comparison of the time averaging for the power curve constructed for the nacelle anemometer of Wietmarschen-1.	79
Figure 6.12	Comparison of the time averaging for the power curve constructed for the nacelle anemometer of Wietmarschen-2.	79
Figure 7.1	Power error at each bin speed in function of the time for the data averaged at 1 second.	82
Figure 7.2	Power error at each bin speed in function of the time for the data averaged at 0,1 second.	83

LIST OF SYMBOLS AND MEASURE UNITS

A	Swept area of the wind-turbine rotor [m^2]
$AE P$	Annual Energy Production [MWh]
$B_{10\text{min}}$	Measured air pressure averaged over 10 minutes [N/m^2]
C_p	Power coefficient
$C_{p,i}$	Power coefficient in bin i
d	Distance between the rotor and the anemometer [m]
D	Rotor diameter [m]
$D^{(l)}$	Drift coefficient
$D_{\text{noise-ind}}^{(l)}$	Noise-induced drift
D_e	Equivalent rotor diameter [m]
F	Force [N]
$F(V)$	Rayleigh cumulative probability distribution function for wind speed
F_c	Damping force [N]
F_f	Fluctuation force [N]
l_h	Height of obstacle [m]
l_w	Width of obstacle [m]
k_B	Boltzmann's constant [$\text{J}/^\circ\text{K}$]
L_e	Distance between the obstacle and the MM [m]
m	Mass [kg]
$M^{(l)}$	Conditional moment
N	Number of bins

N_i	Number of 10 minutes data sets in bin i
N_h	Number of hours in one year [8760 hours]
p	Fluctuation around the stationary power [W]
P	Power output [W]
P_{fix}	Stationary power [W]
P_i	Normalized an averaged power output in bin i [W]
P_n	Simulated power output [W]
$P_{n,i,j}$	Normalized power output of data set j in bin i [W]
P_{state}	Power state [W]
$P_{stationary}$	Stationary power [W]
P_{th}	Theoretical power output [W]
Q	Conditional probability
R_0	Gas constant of dry air [287.05 J/(kg x °K)]
t	Time (s)
T	Temperature (°K)
T_{10min}	Temperature averaged over 10 minutes [°K]
TI	Turbulence intensity
u_n	Simulated wind speed
U	Horizontal mean wind speed [m/s]
V	Wind speed [m/s]
V_{10min}	Measured wind speed averaged over 10 minutes [m/s]
V_{ave}	Annual average wind speed at hub height [m/s]
V_{avg}	Averaged wind speed over a certain period [m/s]

V_i	Normalized and averaged wind speed in bin i [m/s]
V_n	Normalized wind speed [m/s]
$V_{n,i,j}$	Normalized wind speed of data set j in bin i [m/s]
W	Probability-density function
α	Additional excluded sector [degree]
β	Noise influence
γ	Relaxation parameter
Γ	Fluctuating force per unit mass [N/kg]
Γ_n	Gamma function
δ	Dirac delta function
ε	Attraction from averaged wind speed
ζ	Stochastic variable
η_{GB}	Gear box ratio
η_{tot}	Total efficiency
λ	Mass flow [kg/s]
v	Speed [m/s]
\dot{v}	Acceleration [m/s ²]
ρ	Air density [kg/m ³]
ρ_0	Reference air density [kg/m ³]
ρ_{10min}	Derived 10 minutes averaged air density [kg/m ³]
σ_u	Standard deviation of the horizontal wind speed [m/s]
τ	Relaxation time [s]
τ_0	Duration time of a collision [s]

φ	Influenced rotor position [degree]
ω	Average generator speed [rpm]

INTRODUCTION

In recent years, new demand for cleaner and renewable energy sources has arrived, since the pollution has become a global warning, with his non-desirable effect on the earth, to most of the population. Indeed, coal and oil energy, fuel emissions and others sources of pollution have a negative impact on globe health. The planet has the advantage to produce natural energy, and one of them comes from the wind, which can be found anywhere around the world.

Today, more than 74 GW of wind energy are installed all around the worlds, which represent over 100 000 wind turbines in 70 countries [5]. Furthermore, the low cost of wind energy, which is less expansive than the coal, oil and nuclear, is a favourable element to continue to investigate in this field. In fact, it costs approximately 3,5 to 4 cents per kilowatt hour and declining [3].

Introduction to wind turbine

The production of wind energy is done by the exploitation of a wind turbine. Basically, when wind hits the blades of the turbine, it creates a rotation of the rotor, and this rotation coupled with the torque produce the power. Afterwards, this mechanical power is transformed in electrical power by a generator.

The wind power is a cubic function of the wind speed. However, the turbine isn't working at really low wind speed due to the fact it will cost more electricity that it will produce. Therefore, the turbine start-up occurs when the wind speed reaches a point, where there is enough energy into it to efficiently use the turbine, which is referred to as the cut-in wind speed. Once the turbine has reached the cut-in wind speed, its power will increase with a cubic relation of the wind speed, until it attains the rated power. The rated power is the power capacity of the turbine. Once it is reached, the power will stay the same, even if the wind speed continues to increase. This is a preventive measure, since the turbine stresses would be

too high if the power would continue to increase. For the same reason, the turbine will stop if the wind speed is too high, which is called the cut-off wind speed.

Objectives and methodology

Today, the wind-energy companies need to follow the IEC procedure to construct a power curve. A power curve is a curve which expresses the power of the turbine in function of the wind speed. However, this standard procedure (IEC) has some flaws, since it can take some considerable time in order to construct power curves. Moreover, by utilising an averaging method, like the IEC does, it is not accurate to calculate the power since it is a cubic function of the wind speed. Consequently, the measurements of different settings are long and the results aren't precise.

To avoid the seasonal variation when evaluating different settings and to reduce costs, these problems should be solved. One of the solutions is to evaluate a new method to construct a power curve. The method analysed in this master thesis is the construction of a power curve following Markov's theory. This method is a stochastic evaluation of the power curve. However, a problem occurs when using this method because it requires data averaged over a short period, and also because the turbine can be far away from the meteorological mast (MM). Thus, the correlation between the MM anemometer and the power output of the turbine is reduced or lost. Furthermore, the utilisation of the MM anemometer isn't always feasible, because it is too far away of the turbine, or the terrain is highly complex. For all these reasons, the analysis should be implemented on the nacelle anemometer.

This thesis proposes a program which can calculate a power curve with this novel method. In addition, it also recommends a transfer function to correlate the wind speed from the MM anemometer to the nacelle anemometer, with the respect of Markov's theory.

Thesis structure

In order to have a better understanding of the thesis, the objectives, the problems and the results; the description of the thesis structure is explained here.

In Chapter 1, a literature review, of what was made before in this field, is done. The standards and the results of the previous research from different contributors are presented. Moreover, the IEC flaws are exposed and proved, and a short introduction of the novel theory is done to acquire basic knowledge.

Then, Chapter 2 will demonstrate the mathematical model of a power curve constructed with the Markov's theory. Therefore, the equations will be shown and the method to determine different coefficients will be revealed.

Next, Chapter 3 will introduce the wind turbines analysed in this master thesis. Consequently, the location of the wind farms, the operating data and the limitation of the analysis on those turbines are described.

After that, Chapter 4 will analyse the influence of each parameter to construct a Markov power-curve with the MM anemometer. In fact, an optimisation of each parameter is done to determine the best power curve for all turbines studied.

Chapter 5 will optimise the parameters to construct the best Markov power-curve, but this time with the nacelle anemometer.

Afterwards, Chapter 6 will only validate the best parameters with other sites or turbines. Therefore, power curves following Markov's theory will be constructed with optimised parameters of others turbines and data sets, to verify the quality of the power curve for those sites or turbines.

Finally, Chapter 7 will determine the minimal amount of data required to construct a good power curve with the nacelle anemometer and compare this result with the IEC standard.

CHAPTER 1

LITERATURE REVIEW

The construction of a power curve for a specific site is well known and well defined. When constructed, this power curve is used to determine the Annual Energy Production (AEP) of the site. However, the construction of a power curve requires data collection over a certain period of time like power, wind speed, air density, wind direction, etc. This chapter presents a literature review of the standard procedure to construct a power curve on wind farms, the flaws of the standard procedure and a new method to construct a power curve.

1.1 International Electrotechnical Commission (IEC) standard

The International Electrotechnical Commission (IEC) is a worldwide organization for standardization comprising all national electrotechnical committees. The objective of IEC is to promote international co-operation on all questions concerning standardization in the electrical and electronic fields [9]. This committee is therefore present in wind-energy technology, where their standards are applied all around the world.

The official method to construct a power curve is explained in one of the IEC standard. Wind-farm and wind-turbine companies are recommended to follow this standard, otherwise customers won't have any reference when analysing which companies have the best turbines for their projects.

There are two different IEC standards in the wind-energy industry used to construct power curves. The first one (IEC 61400-12-1) is a standard utilised when the energy calculated at the turbine is made with the MM anemometer, while the second one (IEC 61400-12-2) is a standard utilised when the energy calculated at the turbine is made with the nacelle anemometer, which is normally positioned on the top of the wind turbine.

1.1.1 Performance test on a wind turbine

The performance test is used to verify if the output power giving by the turbine is the same as what was defined in the manufacturer-customer contract. This validation requires a few steps. Firstly, it is required to find a location for the MM. The second step is to determine the measurement sector. Thirdly, the measurements can be done and the wind speed needs to be normalized with respect to air density. Then, the power curve, the AEP and the power coefficient can be calculated.

Meteorological-mast location

When positioning the MM, it should not be installed too close of the wind turbine, because the wind speed will be influenced. However, it should neither be installed too far away from the turbine, since the correlation between the wind speed and the electrical power output of the wind turbine will be reduced.

The ideal distance to which the meteorological mast can be installed from the turbine is 2,5 times the rotor diameter (D) of the wind turbine. However, it also can be installed at a distance between two and four times the rotor diameter, from the wind turbine. In fact if the MM is too close of the turbine, then the wind speed read at the MM anemometer might be influenced by the blade passage, while if the MM is too far of the turbine then the correlation between the MM and the turbine could be lost. Most of the times, the best meteorological-mast position will be upwind of the turbine in the direction where the most dominant wind is expected to come during the test [9].

Measurement sector

Due to the MM being in the wake of the wind turbine for certain sectors, it is necessary to exclude those sectors during the test. Indeed, when the wind passes trough a turbine, it affects its speed. Consequently, the wind speed obtained at the MM isn't the real wind speed. Figure

1.1 shows the sectors which need to be excluded when the turbine is situated at a distance from the MM of 2, 2,5 and 4 times the rotor diameter.

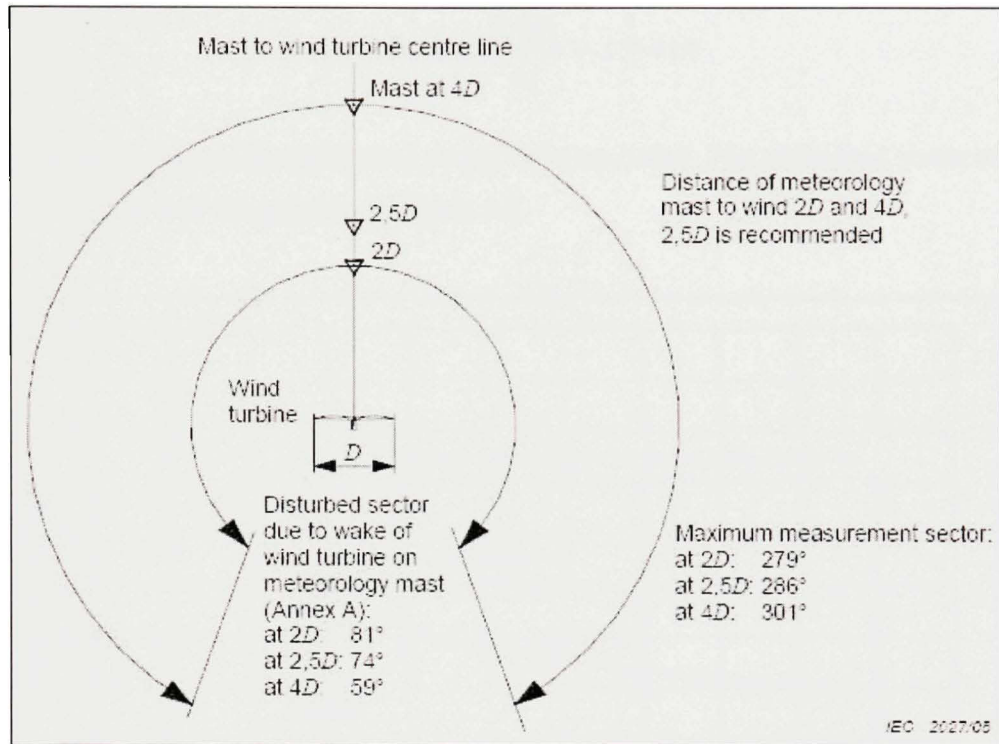


Figure 1.1 Requirements as to distance of the meteorological mast and maximum allowed measurement sectors [9].

However, those sectors might be insufficient when others turbines or significant obstacles are present on the wind farm. In fact, those obstacles affect the wind speed, so the measurement sector should be reduced. The distance (L_e) between the obstacle and the meteorological mast, the equivalent rotor diameter (D_e) and the size of the obstacle are the dimensions to be taken into account. If the obstacle isn't a wind turbine, then the equivalent rotor diameter should be calculated.

$$D_e = \frac{2l_h l_w}{l_h + l_w} \quad (1.1)$$

Afterwards, with the equivalent diameter and the distance, the disturbed sector of the obstacle can be defined.

$$\alpha = 1.3 \arctan\left(\frac{2.5D_e}{L_e} + 0.15\right) + 10 \quad (1.2)$$

In the equation (1.2), α is the additional sector to be excluded. The additional sector excluded also can be found with the graphic of Figure 1.2.

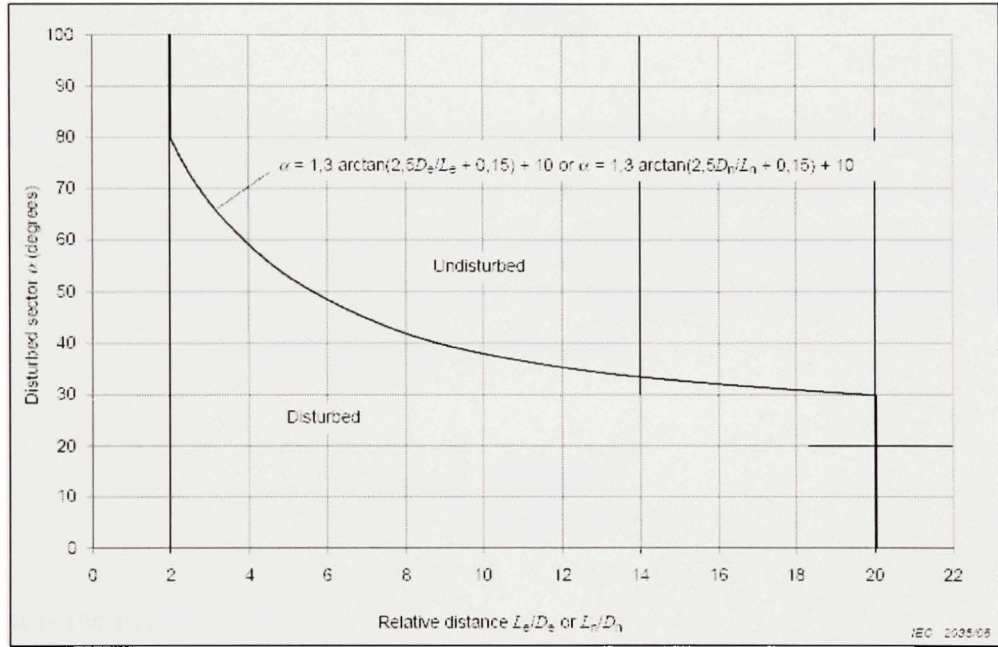


Figure 1.2 Sectors to exclude due to wakes of neighbouring and operating wind turbines and significant obstacles [9].

Data normalization

In order to execute a performance test following the IEC standard, it is necessary to average all variables measured over ten minutes. Therefore, the air density, the pressure, the wind speed, the power, and other variables are averaged on a period of ten minutes. However, the data collected aren't normalized. In fact, the calculation of the power in function of the wind speed is given by [11]:

$$P = \frac{1}{2} \rho A V^3 \eta_{tot} C_P \quad (1.3)$$

In the equation (1.3), the power is in function of the wind speed, but is also depending of the air density. The air density is in function of the atmospheric pressure and the outside temperature [9].

$$\rho_{10\min} = \frac{B_{10\min}}{R_0 T_{10\min}} \quad (1.4)$$

Because the air density isn't a constant, it is required to normalize the data to the sea level air density (ρ_0), which is 1,225 kg/m³. Moreover, GE's wind turbines are with active power-control. In that case, the normalization should be applied to the wind speed, according to the IEC procedure. However, if the turbines are with passive power-control, then the normalization should be applied to the power output [9].

$$V_n = V_{10\min} \left(\frac{\rho_{10\min}}{\rho_0} \right)^{1/3} \quad (1.5)$$

Wind-turbine performances

The turbine performances are characterized by the calculation of the power curve, the AEP and the power coefficient. According to the IEC standard, those measures of performance are determined by applying the method of bins. The first step in applying the method of bins consists of calculating the mean value of the power and the wind speed at each 0,5 m/s bins for the normalized data sets [9].

$$V_i = \frac{1}{N_i} \sum_{j=1}^{N_i} V_{n,i,j} \quad (1.6)$$

$$P_i = \frac{1}{N_i} \sum_{j=1}^{N_i} P_{n,i,j} \quad (1.7)$$

Then, it is possible to calculate the annual energy production from the wind turbine. In order to do that, a Rayleigh distribution is used as the reference wind speed frequency distribution [9].

$$AEP = N_h \sum_{i=1}^N [F(V_i) - F(V_{i-1})] \left(\frac{P_{i-1} + P_i}{2} \right) \quad (1.8)$$

$$F(V) = 1 - \exp \left(-\frac{\pi}{4} \left(\frac{V}{V_{ave}} \right)^2 \right) \quad (1.9)$$

Finally, the power coefficient can be calculated with equation (1.10). At rated power, the power coefficient will drop significantly with the respect to equation (1.10), since the wind speed is increasing while the power stays constant.

$$C_{P,i} = \frac{P_i}{\frac{1}{2} \rho_0 A V_i^3} \quad (1.10)$$

If we want to utilise the nacelle anemometer to construct a power curve, the correlation between the nacelle anemometer and the MM anemometer should be done following the IEC 61400-12-2 procedure [12]. This correlation is done because the wind is affected by the blade passage. This correlation can be executed by following the bins method. In reality, the real wind-speed, from the meteorological-mast anemometer, is in function of the nacelle wind-speed. Therefore, at each bin speed a linear regression is done between those two wind speeds.

1.2 IEC flaws

Even though the only standard method to calculate a power curve is the IEC 61400-12-1 procedure, this method contains some flaws. Indeed, an IEC power curve cannot be constructed before the data base reaches 180 hours [9]. Therefore, the performance test can be long, since the wind isn't always in the measurement sector and the turbine might not work properly for a certain period of time.

Moreover, averaging the power and the wind speed gives imprecision because it is not a linear function. In fact, the power is a cubic function of the wind speed, as shown in equation (1.3). Consequently, the power curve is obtained from those measurements by ensemble averages denoted as $\langle V(t) \rangle \rightarrow \langle P(V(t)) \rangle$ [1]. The nonlinearity of this power curve is also spoiled by turbulent winds at the specific turbine site, which is caused by the obstacles, weather, topography etc. The turbulence of the wind is described by the turbulence intensity (TI).

$$TI = \sigma_u / U \quad (1.11)$$

The turbulent winds aren't considered in the standard procedure and lead to the following inequality:

$$P(\langle V(t) \rangle) \neq \langle P(V(t)) \rangle$$

Therefore, if we focus on the instantaneous electrical wind-turbine power, instead of the ensemble averages we thus obtain [1]:

$$P(t) = P_{fix}(V) + p(t) \quad (1.12)$$

Where $P_{fix}(V)$ denotes the stationary power output as function of the wind speed and $p(t)$ denotes the respective temporal fluctuations around this stationary power output. The performance test is utilised to verify if the turbine gives the power it is suppose to give at a certain wind speed. Consequently, the power of interest is the stationary power, instead of the average power ($P(t)$), since this power doesn't include or is less influenced by the wind turbulences, pitch-angle changes, shutdown states, or others non-desirable effect, which cause the scatter plot to be greater. A method to obtain numerically the stationary power curve is to utilise Markov's theory, which is described by a generalised one-dimensional Langevin equation. The mathematical model of those equations is demonstrated in the Chapter 2.

1.3 Markov process

In order to understand the works explained in this chapter, an introduction of Markov process is described here. In fact, GE's and the University of Oldenburg works explain how they have constructed a power curve following Markov's theory. Therefore, a brief explication of Markov process is required.

The Markov process can be applied in different applications, like the physics, the statistics, the electrics or the bioinformatics. First, a Markov property is a stochastic process, with also the conditional-probability of the distribution of future states of the process, and this conditional-probability depends only of the present state and not on any past states [19]. Thus, the distribution of future states depends only of the present state and not how it occurs at the current state. Therefore, the Markov process is a memory-less process [13]. More details on this property will be done later in the Chapter 2, and also the equations of this process will be explained.

1.4 GE's works

The Wind-Energy division of General electric has developed a software to create simulated data. They also made other software to construct a power curve following Markov's theory.

A master thesis has been written on the subject by a student from GE and the title of the thesis is: “*Characterization of the wind turbine power performance curve by stochastic modelling*” [13]. The creation of simulated data is required to validate the power curve obtained with the Markov software. In fact, the simulated-data software will create data around a theoretical power-curve. Therefore, to validate the Markov software, the power curve obtained must fit with the theoretical one.

The simulated data were created following the Ornstein-Uhlenbeck equations [13]. This equation creates the simulated data of the power and the wind speed in function of the theoretical power curve, which is demonstrated by the equation (1.13) and (1.14). The variable P_{th} is the theoretical value of the power in function of the wind speed. Therefore, it is the stationary power at which the turbine would find equilibrium [14].

$$P_{n+1} = P_n - \gamma[P_n - P_{th}(u_n)] \quad (1.13)$$

$$u_{n+1} = u_n - \varepsilon[u_n - V] + \sqrt{\beta} \cdot \Gamma_n \quad (1.14)$$

Figure 1.3 illustrates the results obtained with their software. The simulated data (red) are created around the theoretical power-curve (yellow), which is a cubic function of the wind speed until the rated power.

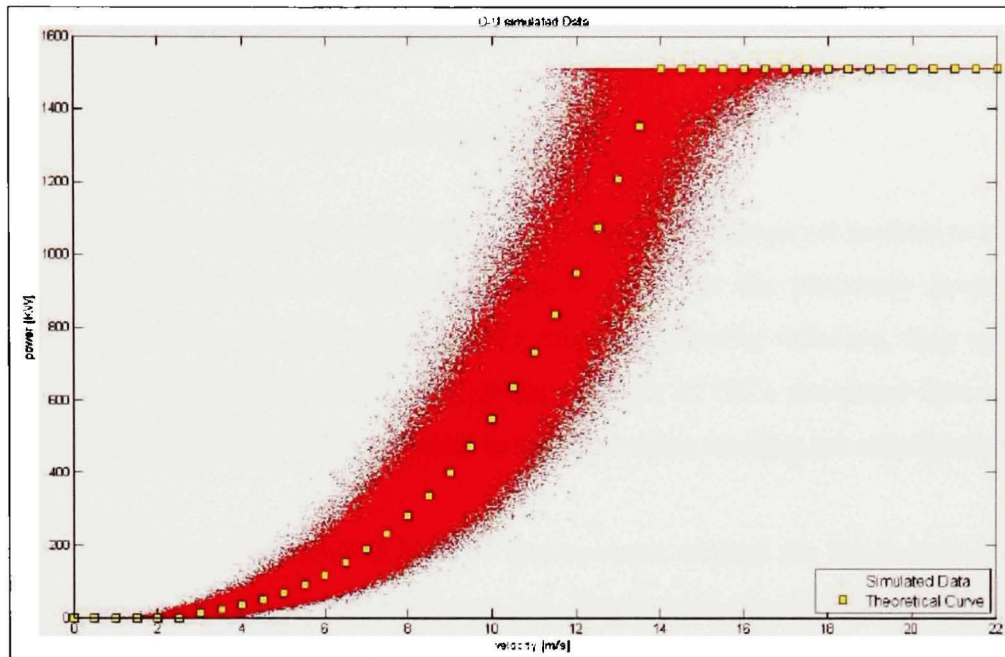


Figure 1.3 GE's *simulated data created around a theoretical power-curve [13].*

However, the creation of simulated data was done by assuming the relaxation parameter as constant. Like mentioned in the GE's student thesis, further improvement can be made by setting the relaxation parameter (γ), of the equation (1.13), in function of the wind speed and his time derivative [13]. By setting this parameter as a non-constant, it will include another parameter which is the dynamic response of a turbine, and the simulated data will be more representative of the real behaviour of a turbine.

After the creation of the simulated data, they made a program to construct a power curve following Markov's theory. However, this program didn't give good results with those data since the power curves obtained with the simulated data didn't fit with the theoretical power-curve. Moreover, the power curves obtained for the real data didn't give consistent results. Those assertions lead to the conclusion that the Markov and the simulated data software need to be improved. Mainly, in this master thesis, Markov power-curve software will be created in order to improve the previous software from GE.

1.5 University of Oldenburg's contribution

1.5.1 Simulated-data and power-curve programs

The University of Oldenburg also has made some research in this novel method to construct a power curve. They have created a program to calculate the stationary power curve following Markov's theory. To confirm their new power-curve software, they also have created their simulated-data software. But at the opposite of GE's simulated-data software, they didn't assume the relaxation parameter as constant when creating the simulated data.

After that, they have constructed a Markov power-curve around the theoretical one, with their new software, like illustrated in Figure 1.4. The results obtained have validated their two programs, since the combination of their power curve and their simulated data gives acceptable results. With the permission of the University of Oldenburg, we will utilise their simulated data to validate and determine the best parameters to construct a power curve following Markov's theory. Thus, we will assume that their simulated data are perfect. However, their power-curve software isn't available, which is one of the reasons why a new software is created in this master thesis.

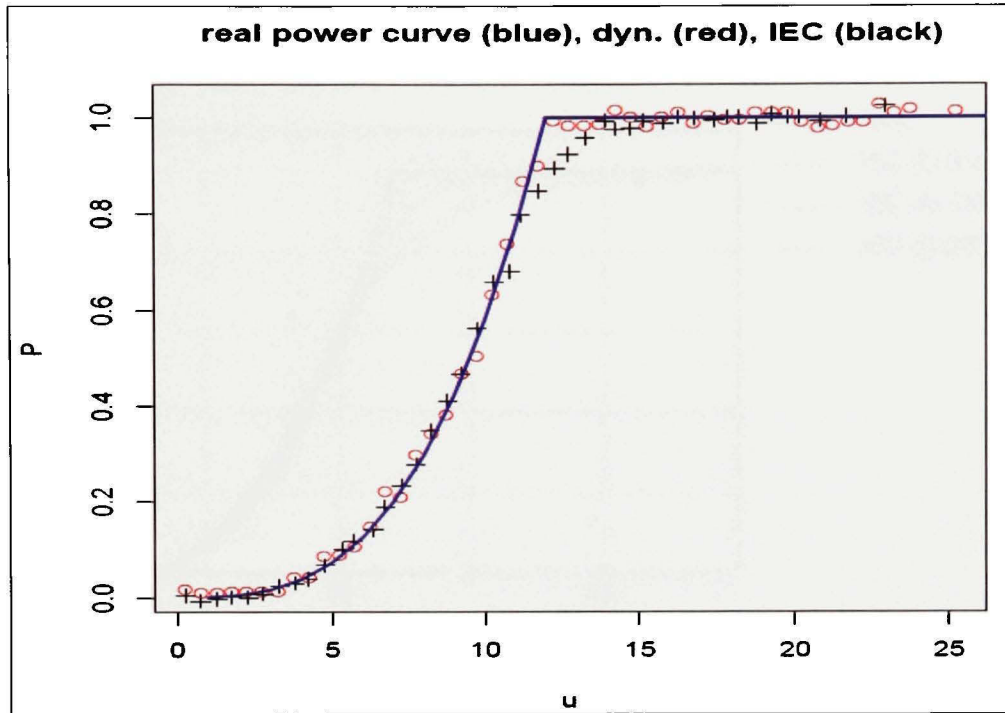


Figure 1.4 *Power curve obtained by the University of Oldenburg with their simulated-data and power-curve programs [6].*

1.5.2 Articles made by the University of Oldenburg

The University of Oldenburg also has produced several articles on the subject. Mainly, those articles expose the IEC flaws and propose a solution to correct those flaws, which is to construct the power curves by a stochastic approach [1][2][7]. They demonstrate the mathematical model they utilise to construct this power curve and developed a software to construct it with good results for the simulated and the real data.

They also have proved that the Markov power-curve, which is the red curve in Figure 1.5, isn't affected by the turbulence intensity, which is not the case with the IEC standard. Figure 1.5 shows also that the IEC power curves are affected by the turbulence intensity (ζ), since the rated power is decreasing when the turbulence intensity is increasing. Moreover, in this graphic the Markov power-curve does fit exactly the theoretical power curve, which is not shown but explained by the authors of [7].

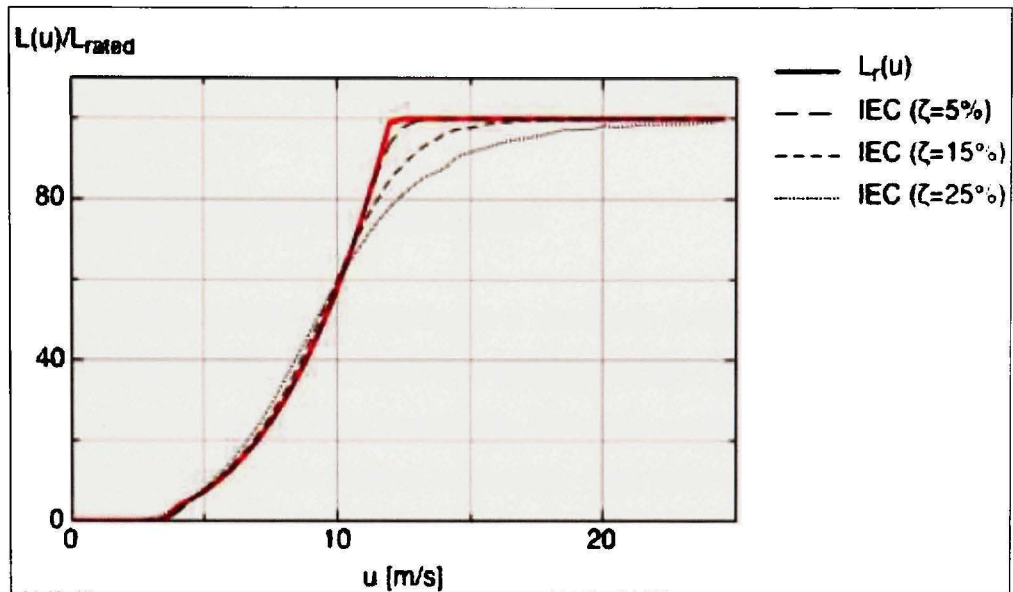


Figure 1.5 *Power curves obtained for a simulated data set [7].*

The explanation of the literature review was necessary in order to introduce the subject analysed in this thesis. This chapter explained the standard method, the flaws of this method, the introduction of the Markov's theory, and also some works done by GE and the University of Oldenburg. With all these elements, it is now possible to look at the mathematical model of the Markov's theory, by applying Langevin equation.

CHAPTER 2

MATHEMATICAL MODEL

2.1 Langevin equation for Brownian motion

In statistical physic, a Langevin equation is a stochastic differential equation describing a simple and well known Brownian motion in a potential [18]. Consequently, before analysing a Langevin equation, we will first discuss the Brownian motion of particles in its simplest form. A Brownian motion is a random movement of particles suspended in a fluid and it is also called a Wiener Process [16]. If a small particle is immersed in a fluid, then a friction force will act on the particle. The Stoke law gives the equation for this damping force [15].

$$F_c = -\lambda v \quad (2.1)$$

Also the Newton second law express that the summation of forces on an object is equal to the mass of this object multiplied by his acceleration.

$$\sum F = m\dot{v} \quad (2.2)$$

Therefore, the expression of motion for the particle of mass (m) without any additional forces is given by:

$$m\dot{v} + \lambda v = 0 \quad (2.3)$$

and the relaxation time (τ) is defined as:

$$\tau = \frac{m}{\lambda} \quad (2.4)$$

However, this equation is valid only when the mass of the particle is large enough so its velocity due to thermal fluctuations is null or negligible. The mean energy of the particle in one dimension is given by the equipartition law [17]. The original concept of equipartition was that the total kinetic energy of a system is shared equally among all of its independent part once the system has reached thermal equilibrium [17].

$$\frac{1}{2}m\langle v^2 \rangle = \frac{1}{2}k_B T \quad (2.5)$$

The equation (2.3) needs to be modified with the respect of equation (2.5), which leads to the correct thermal energy. The correction consists in adding, on the right-hand side of (2.3), a fluctuating force (F_f), which is a stochastic or random force [15].

$$F(t) = F_c(t) + F_f(t) \quad (2.6)$$

The fluctuating force occurs because the problem isn't treated exactly. If the problem was treated exactly, the coupled equations of motion for all the molecules of the fluid and for the small particle would be solved, and then, no stochastic force would occur. In reality, because of the large number of molecules in the fluid (in the order of 10^{23}), these coupled equations generally can't be solved.

Therefore, the force (F_f) varies from one system to the other, and one thing to do is to consider the average of this force for the ensemble. The fluctuating force per unit mass (Γ), which is called the Langevin force, is obtained by dividing the force (F_f) by the mass. We also divide all the remaining terms of the equation (2.6) by the mass and we thus obtain the equation of the Langevin force.

$$\dot{v} + \frac{1}{\tau}v = \Gamma(t) \quad (2.7)$$

The first assumption of this force is that its average over the ensemble should be zero, since the equation of motion for the average velocity is given by the equation (2.3).

$$\langle \Gamma(t) \rangle = 0 \quad (2.8)$$

If two Langevin forces at different times are multiplied, we then assume that the average value is zero at time differences $(t'-t)$, for a time larger than the duration of a collision (τ_0). This assumption seems to be reasonable, since the collisions between the molecules of the fluid and the particle are approximately independent.

$$\langle \Gamma(t)\Gamma(t') \rangle = 0 \quad \text{for} \quad |t-t'| \geq \tau_0 \quad (2.9)$$

Nevertheless, the duration time of a collision is usually much smaller than the relaxation time (τ) of the velocity of the particle. Therefore, the limit of $\tau_0 \rightarrow 0$ should be taken as a much more reasonable approximation.

$$\langle \Gamma(t)\Gamma(t') \rangle = q\delta(t-t') \quad (2.10)$$

Risken describes in reference [15] the apparition of the delta (δ) function. He states: “The δ function appears because otherwise the average energy of the small particle can't be finite as it should be according the equipartition law” shown at the equation (2.5). The variable (q) describes the noise strength of the Langevin force. In fact, the noise strength is the variable which describes the size of the scatter plot. More the strength is high, more the scatter plot will be large.

$$q = 2\lambda kT / m^2 \quad (2.11)$$

Once the Brownian motion is explained, the Langevin equation can be introduced. The form of the general non-linear Langevin equation, for one stochastic variable (ζ), is given by:

$$\dot{\zeta} = h(\zeta, t) + g(\zeta, t)\Gamma(t) \quad (2.12)$$

The noise strength may be absorbed in the function g , while the function h is the deterministic drift. Also, the Langevin force is again a Gaussian stochastic variable with zero mean and delta correlated function. However, a formal general solution for the stochastic differential equation (2.12) can not be given [15].

2.2 Fokker-Planck equation

The introduction of the Fokker-Planck equation is necessary to better understand the origin of the equations and variables, which will lead to construct a power curve following Markov's theory.

The probability density of the stochastic variable can be calculated with the Fokker-Planck equation. The Kramers-Moyal expansion coefficients of this Fokker-Planck equation are giving by [15]:

$$D^{(n)}(x, t) = \frac{1}{n!} \lim_{\tau \rightarrow 0} \frac{1}{\tau} \left\langle [\zeta(t + \tau) - x]^n \right\rangle \Big|_{\zeta(t)=x} \quad (2.13)$$

Therefore, the solution of (2.12) is giving by $\zeta(t + \tau)$ where $\tau > 0$. The differential equation (2.12) is then written in the form of an integration to derive these Kramers-Moyal expansion coefficients.

$$\zeta(t + \tau) - x = \int_t^{t+\tau} [h(\zeta(t'), t') + g(\zeta(t'), t')\Gamma(t')] dt' \quad (2.14)$$

After some manipulations of the equation (2.14), giving by [15], and with the limit $\tau \rightarrow 0$ we thus obtain for the drift coefficient:

$$D^{(1)}(x, t) = h(x, t) + \frac{\partial g(x, t)}{\partial x} g(x, t) \quad (2.15)$$

The term $D^{(1)}$ contains the deterministic drift and another term which is called the noise-induced drift.

$$D_{noise-ind}^{(1)} = \frac{\partial g(x, t)}{\partial x} g(x, t) = \frac{1}{2} \frac{\partial}{\partial x} D^{(2)}(x, t) \quad (2.16)$$

2.3 Stochastic processes

Let's start the stochastic processes by defining that the probability that the random variable ζ is equal or less than x is called Q ($\zeta \leq x$). Since the variable ζ is also real, then $Q(\zeta \leq \infty) = 1$. Therefore, the derivative of Q with respect to x is the probability density function (W) of the variable ζ .

$$W_{\xi}(x) = \frac{d}{dx} Q(\xi \leq x) = \langle \delta(x - \xi) \rangle \quad (2.17)$$

Also, by assuming that Q is differentiable, the probability dQ to find the continuous stochastic variable ζ in the interval $(x \leq \zeta \leq x + dx)$ is seen as follow:

$$Q(\xi \leq x + dx) - Q(\xi \leq x) = \frac{d}{dx} Q(\xi \leq x) dx = W_{\xi}(x) dx \quad (2.18)$$

The probability density of the random variable ζ at time t_n , under the condition that the random variable at the time $t_{n-1} < t_n$ has the sharp value x_{n-1} , is defined by the conditional probability density.

$$Q(x_n, t_n \mid x_{n-1}, t_{n-1}; \dots; x_1, t_1) = \langle \delta(x_n - \xi(t_n)) \rangle \Big|_{\xi(t_n-1)=x_{n-1}, \dots, \xi(t_1)=x_1} \quad (2.19)$$

$$t_n > t_{n-1} > \dots > t_1$$

2.4 Markov property

A Markov process is a type of stochastic process. The process described by the Langevin equation (2.12), with δ -correlated Langevin force, is a Markov process. Its conditional probability at time t_n depends only on the value at the next earlier time. However, if $\Gamma(t)$ is no longer δ -correlated, the Markov property is destroyed.

$$Q(x_n, t_n | x_{n-1}, t_{n-1}; \dots; x_1, t_1) = Q(x_n, t_n | x_{n-1}, t_{n-1}) \quad (2.20)$$

The interpretation of equation (2.20) may lead that there is only a memory value of the variable for the latest time. The arbitrary of the time difference $t_2 - t_1$ of the conditional probability $Q(x_2, t_2 | x_1, t_1)$ of a Markov process, affects the dependence of Q on x_1 . Indeed, if the time difference is large, then the dependence will be small, conversely if the time difference is infinitesimally small then the conditional probability will have the sharp value x_1 [15]. If $n = 2$ and the time difference is infinitesimally small, then the conditional probability will be giving by:

$$\lim_{t_2 \rightarrow t_1} Q(x_2, t_2 | x_1, t_1) = \delta(x_1 - x_2) \quad (2.21)$$

2.5 Coefficients estimation

As seen in (2.13), the Kramers-Moyal expansion coefficients of the Fokker-Planck equation are giving by:

$$D^{(n)}(x) = \frac{1}{n!} \lim_{\tau \rightarrow 0} \frac{1}{\tau} M^{(n)}(x, \tau) \quad (2.22)$$

with the conditional moment ($M^{(1)}$)

$$M_i^{(1)}(x, \tau) = \left\langle x_i(t + \tau) - x_i(t) \right\rangle_{x_i(t)=x_i} \quad (2.23)$$

Now the variable x can be replaced by P_{state} , which is the power state in a certain bin speed, while x_i can be replaced by P which is the power output of the wind turbine. In fact, there are multiple power states inside a certain bin speed.

$$M_i^{(1)}(P_{state}, \tau) = \langle P(t + \tau) - P(t) \rangle \Big|_{P(t)=P} \quad (2.24)$$

The expected power output of P_{state} is then calculated with the conditional probability density $Q(P_{n+1}, t + \tau | P_n, t)$. This conditional probability describes the probability of states P_{n+1} , of the system variable P_{state} , at time $t + \tau$ with the condition that the system is in state P_n at time t [1].

The drift coefficient ($D^{(1)}$) is then obtained by dividing the conditional moment (M) by the relaxation time (τ) and then calculating the limit $\tau \rightarrow 0$. The drift can be explained as a force that acts on each power state inside a bin speed and it is directed toward the stationary power at this bin speed. For example, if we have a strong negative force, then the power state where the calculation has been done is much higher than the stationary power. On the other hand, if we have a small positive drift, then the power state is a little bit smaller than the stationary power.

In order to calculate the drift coefficient, it is necessary to calculate the slope for an interval of τ where we assume the process to be Markovian [7]. The Figure 2.1 shows an example of the conditional moment in function of the relaxation time at a certain power state. Therefore, the drift coefficient is the slope of the linear regression.

$$D^{(1)}(P_{state}) = \frac{dM^{(1)}(P_{state}, \tau)}{d\tau} \quad (2.25)$$

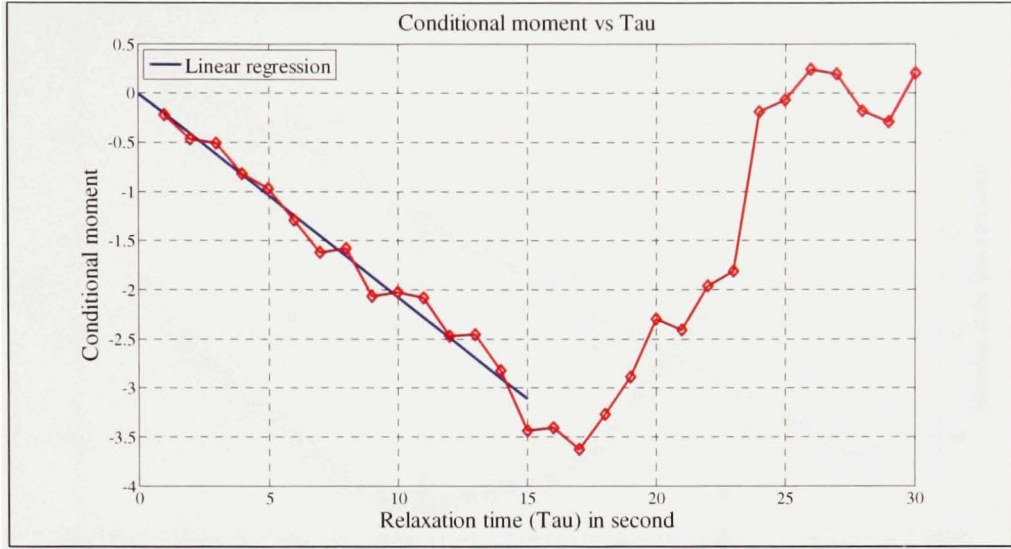


Figure 2.1 *Example of conditional moment in function of the relaxation time (τ).*

Then, the stationary power is found by the search of null crossing or the minimal potential of the deterministic coefficient $D^{(1)}(P_{state})$ [1]. The stationary power found with the minimal potential is defined as:

$$P_{stationary} = \min \left(- \int D^{(1)}(P_{state}) dP_{state} \right) \quad (2.26)$$

Even if the search of zero crossing seems easier, the minimal potential doesn't cumulate errors like the fit of the linear regression. In fact, if there is a drift value which is offset of its supposed value, then the linear regression will fit to that error, while the minimal potential will be less affected. Therefore, theoretically this method is more accurate. As shown in Figure 2.2, and explained in thesis of GE's student [13], the minimal potential and the linear regression do not give the same result when calculating the stationary power at a certain power state.

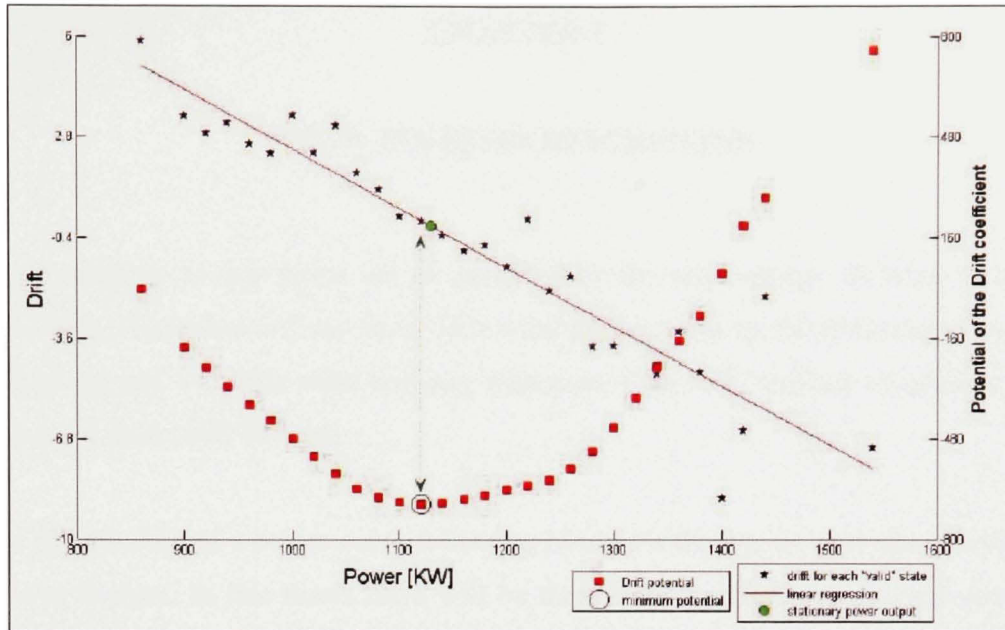


Figure 2.2 *Comparison of the minimal potential with the zero crossing to determine the stationary power output [13].*

With the mathematical model presented in this chapter, which contains the methods to calculate the conditional moments, the drift coefficients and the stationary powers, we will calculate the Markov's power curve, and analyse the impact of different parameters. This analysis will be shown in Chapter 4 for the MM anemometer and Chapter 5 for the nacelle anemometer. However, before doing any analysis, we will first introduce the turbine analysed in this thesis.

CHAPTER 3

WIND-TURBINES DESCRIPTION

The data analysed in this thesis are all supplied by the wind-energy division of General Electric (GE). Those data are also from GE's wind turbines. GE is one of the world leaders in manufacturing and assembly wind turbines, with more than 7500 turbines installation, which produce more than 9800 MW [4].

Prior to construction of a power curve following Markov's theory, we will describe the wind turbines to analyse. In this thesis there will be three wind farms and five wind turbines to evaluate. In this chapter the introduction of those wind turbines is done. This includes the description of the turbines, the MM anemometer, the wind measurement sectors, the scatter plot of the power in function of the wind speed, the location of those wind farms and more.

3.1 Klondike-II

The Klondike-II site is located in the U.S.A. in Oregon state (see Figure 3.1). It has 50 turbines, which generate a total 75 MW of wind power, including one 1.5xle and forty-nine 1.5sl. The turbine model analysed in this thesis will be the 1.5xle and it produces 1,5 MW at the rated wind speed, which is reached at 12,5 m/s. The cut-in wind speed of this turbine is 3,5 m/s, while the cut-off wind speed is 20 m/s. The rotor speed is variable, (between 10,1 and 18,7 rotation per minute (rpm)) and its diameter is 82,5 meters. The electrical frequency output of this turbine can be either 50 Hz or either 60 Hz to accommodate European and North American standard respectively.

The output power of the turbine is recorded by a measurement system at a rate of 50 times per second. The data analysed in this thesis was obtained over a three weeks period from February 5th to February 28th 2006. The anemometers for Klondike-10 are both Sonic for the

MM anemometer and for the nacelle anemometer. For the MM anemometer it is a Gill Windmaster P6032, while for the nacelle anemometer it is a Metek USA-1.



Figure 3.1 *Klondike-II site located in U.S.A. in the Oregon State.*

For the Klondike-II site, the turbine analysed will be Klondike-10. This turbine is situated at a distance of 197 meters of the meteorological mast. The wind measurement sector is between 236 and 315 degrees. The scatter plot of the power in function of the wind speed is shown at Figure 3.2.

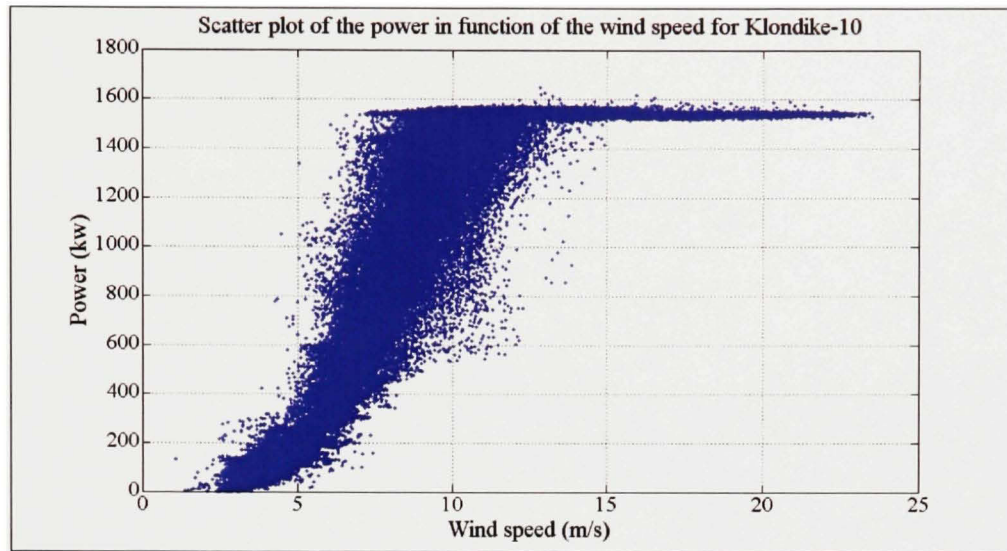


Figure 3.2 *Scatter plot of the power in function of the MM wind speed at an averaged time of 1 second for Klondike-10.*

3.2 Wietmarschen

The Wietmarschen site is situated in Germany (see Figure 3.3). It is composed of multiple 1.5sl turbines, which produces 1,5 MW of wind power at a rated wind speed of 14 m/s. The cut-in wind speed of those turbines is 3,5 m/s, while the cut-off wind speed is 20 m/s. Like Klondike-II turbines, the rotor speed is variable. In fact, it varies between 11 and 20,4 rpm and its diameter is 77 meters. The electrical frequency output of this turbine is 50 Hz, which can not be utilised in North America.

The output power of the Wietmarschen turbines is recorded at a rate of 50 times per second. The data analysed in this thesis are obtained on a 19 days period, which was collected in December 2004. The anemometers for both Wietmarschen turbines are Sonic, while it is also the same for the MM anemometer. All anemometers do have a Gill Windmaster 1086M. The Wietmarschen turbines do also have a cheap cup anemometer at the nacelle, but we won't utilise the data obtained from this anemometer in this thesis, since it is not as accurate as the Sonic anemometers.



Figure 3.3 *Wietmarschen site located in Germany.*

For Wietmarschen site, the turbines analysed will be Wietmarschen-1 and Wietmarschen-2. Those turbines are at a distance of 269 and 185 meters respectively of the meteorological mast. The wind measurement sector for both turbines is between 218 and 318 degrees. The scatter plot of the power output in function of the wind speed, for the Wietmarschen-1 turbine, is shown at Figure 3.4. It can be noticed that the scatter plot is much larger for Klondike-10 turbine. Therefore, the Markov's theory will be tested, because it will be interesting to study the behaviour of the power curve when the turbulence intensity is much larger than usual. This effect has been shown at Figure 1.5, when the IEC power curves were constructed at different turbulence intensity.

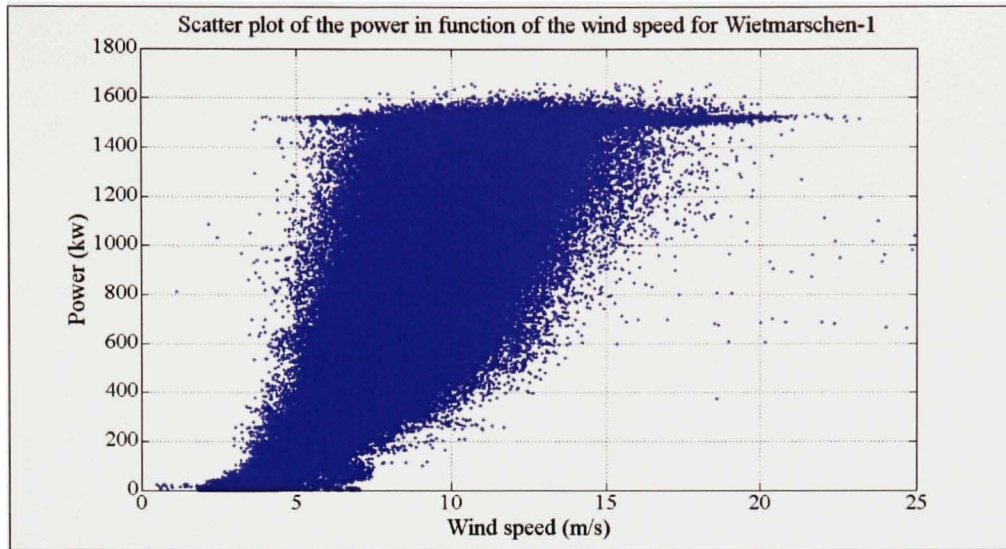


Figure 3.4 *Scatter plot of the power in function of the MM wind speed at an averaged time of 1 second for Wietmarschen-1.*

3.3 Prettin

The Prettin site is situated in Germany (see Figure 3.5). The turbines utilised for this site are the same as the Wietmarschen-site ones (1.5sl turbines). All the parameters of Prettin-site turbines are the same than the ones of Wietmarschen-site turbines. Unlike Wietmarschen and Klondike turbines, the output power of Prettin turbines is recorded at each second. The data analysed in this thesis are obtained over a 5 months period and was collected from June to November 2006. The anemometers for both Prettin turbines are the same than the ones from Wietmarschen turbines. Thus they are all Sonic anemometers of type Gill Windmaster 1086M. Also, like the Wietmarschen turbines, the Prettin turbines do have a cheap cup anemometer at the nacelle, which we won't utilise in this thesis.



Figure 3.5 *Prettin site located in Germany.*

For Prettin site, the turbines analysed will be Prettin-4 and Prettin-5. Those turbines are at a distance of 369 and 291 meters respectively of the meteorological mast, which is a long distance. Indeed, the location of the MM shouldn't be beyond four times the rotor diameter, which is 308 meters in this case. However, this long distance will test the Markov property, since the correlation between the wind speed read at the MM anemometer and the power output at the turbine will be reduced. Therefore, the scatter plot will be larger and the turbulence intensity will increase.

The wind measurement sector is between 207 and 256 degrees for Prettin-4, while it is between 210 and 305 degrees for Prettin-5. The scatter plot of the power in function of the wind speed, for the Prettin-5 machine, is shown at Figure 3.6.

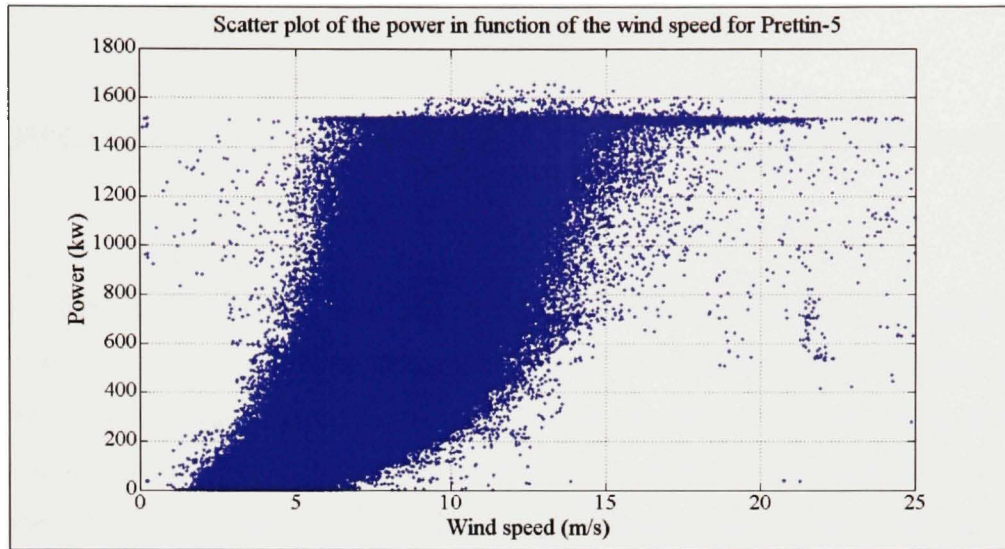


Figure 3.6 *Scatter plot of the power in function of the MM wind speed at an averaged time of 1 second for Prettin-5.*

Now, we do have a good idea of the turbines utilized in this master thesis, and we do know the differences between the equipments on each wind farms. The main difference is the measurement system of Klondike-10 and Wietmarschen turbines, which is not the same than Prettin turbines, since it can only collect the data once per second, while it is 50 times per second for the three others turbines. The data obtained from these equipments will be utilized to optimize the Markov power-curves by evaluating the effect of different parameters.

CHAPTER 4

POWER CURVE CONSTRUCTED WITH THE METEOROLOGICAL-MAST ANEMOMETER

Before constructing a nacelle power-curve following Markov's theory, it is preferable to make it with the MM anemometer, since the wind speed isn't affected by the blade passage. Moreover, it is also important to construct a power curve with the simulated data, because as shown in section 1.2, the stochastic power curve will not fit with the IEC power curve, so there won't be any reference to know if the Markov power-curve software is working or not. However, if simulated data are created following a theoretical power curve, like illustrated in Figure 4.1, then it will be possible to validate if the software and the novel theory are good to construct a power curve. Thus, knowing that the software is good, the power curve made with real data will likely be good.

In a perfect Markov power-curve we want to have a perfect cubic curve, which start from the cut-in wind speed until the rated power. This means if the curve constructed with Markov theory doesn't follow perfectly a cubic curve, then the Markov power-curve isn't considered perfect. From the rated wind speed the curve should become horizontal until the cut-off wind speed. In fact, the theoretical power curve shown in Figure 4.1 is a good example of what we want to look for in a perfect Markov power-curve.

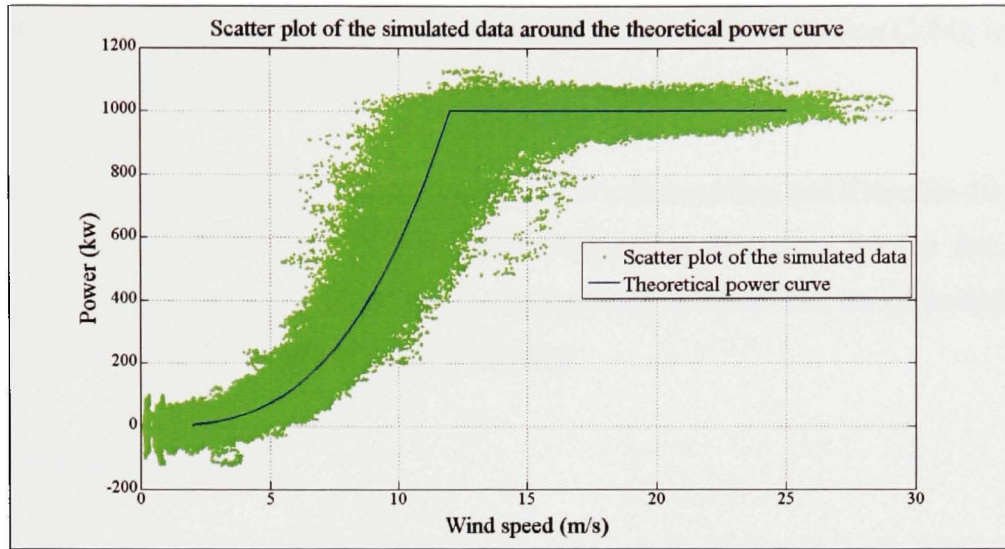


Figure 4.1 *Scatter plot of the simulated data around the theoretical power-curve [6].*

However, multiple differences are present between the real and the simulated data. The first difference is that the wind speed read at the meteorological-mast anemometer takes a certain time before reaching the turbine. Moreover, the wind turbine doesn't react instantly to the wind speed fluctuation. In order to solve the turbine reaction, it is necessary to take a relaxation time (τ), for which the values will give an appropriate linear regression in the calculation of the drift, like shown at the Figure 2.1. The relaxation time used in this thesis, is between 5 and 15 seconds, according to the research made by the University of Oldenburg [8]. In this report, we assume that the simulated data react the same way than the turbine. In fact, by making this supposition the software utilised to calculate the Markov power-curve is the same for real and simulated data.

Another difference is the apparition of holes when utilising the real data. Indeed, those holes are created either when the data at a certain moment aren't good, or when there is a period of time, more than the relaxation time, between the data recorded. The bad data appear because either the system of the turbine is malfunctioning, the wind speed is outside of the measurement sector, or there is a sensor that is not working properly or other different reasons. Nevertheless, Markov's theory doesn't accept those holes in the data, since the

calculation of the moment needs to be done with the respect of the equation (2.24), in which the power differences need to be taken at each relaxation time.

To lighten the report, only the power curves from the simulated data and Klondike-10 turbine are presented in graphic form. However, the analyses are also done for the four others turbines. The final results of the power curve for those turbines will be presented in the Chapter 6 to verify Markov power-curve efficiency.

4.1 Default power-curve

To start the analysis, we will set a default power-curve. This default power-curve can be modified in further section depending on results obtained. Therefore, if we find out that parameter A is better than parameter B, then parameter A will be kept in all further sections of this thesis. For the moment, the default power-curve is constructed with:

- the mean to calculate the conditional moment;
- the minimal potential to calculate the stationary power;
- ten power states at each bin speed;
- the relaxation time constant between 5 and 15 seconds;
- the bins speed set at 0,5 m/s;
- the averaged time of the data at 1 second.

The flowchart of the Markov power-curve software is shown in the APPENDIX I. Figure 4.2 and Figure 4.3 illustrate the default power-curve for the simulated data and for the meteorological-mast anemometer of Klondike-10 respectively. The power curve constructed with the IEC standard, for the simulated data, is well under the theoretical one at the rated power, while the one made with the Markov's theory is much closer. This demonstrates the flaw, explained in section 1.2, of averaging instead of taking the stationary power. The power curve obtained for Klondike-10 with Markov's theory is obviously not good. Indeed, the power found at the bin speed of 6,25 m/s is too high of what it was supposed to be. In fact,

the power curve needs to follow a cubic curve before the rated power. Moreover, once the power curve has reached the rated power, the power curve following Markov's theory stops, which is another sign of bad power curve.

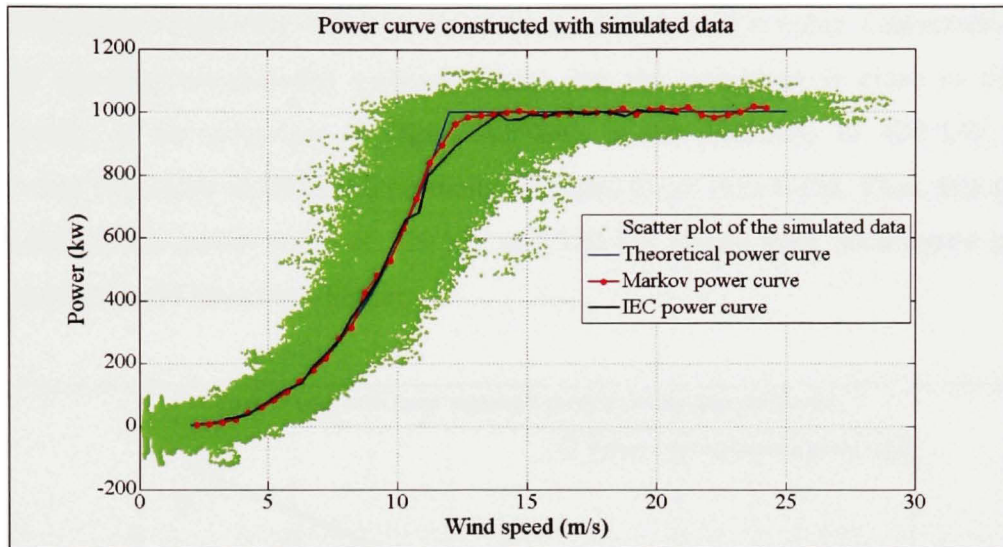


Figure 4.2 *Default power-curve for the simulated data.*

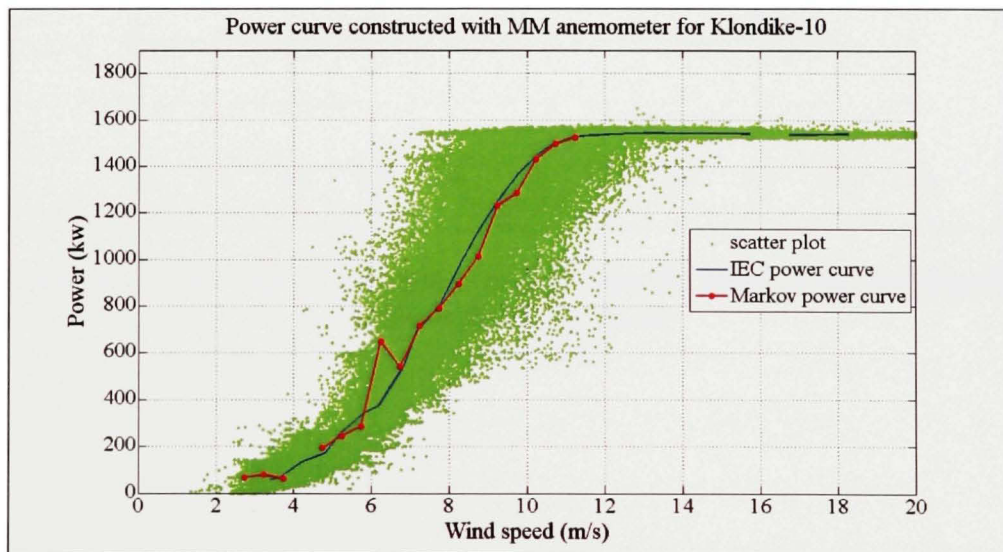


Figure 4.3 *Default power-curve for the MM anemometer of Klondike-10.*

In order to understand the problem which occurs at 6,25 m/s, it is required to go one step deeper into the problem. The stochastic power has been calculated at this bin speed, where the potential is minimal in the equation of the drift in function of the power. Figure 4.4 shows, with the linear-regression method at the bin speed of 6,25 m/s, that the stationary power should have been near 400 kW, since it crosses zero at this value. Conversely Figure 4.5, with the minimal-potential method, shows that the minimum is close to 650 kW. Consequently, if the minimum in Figure 4.5 isn't in the proximity of 400 kW, then it signifies that this curve should have normally ascended faster than it did. Thus, this suggests that the drift at the power states of 579 kW and 720 kW would have been lower and then their potential would have been higher.

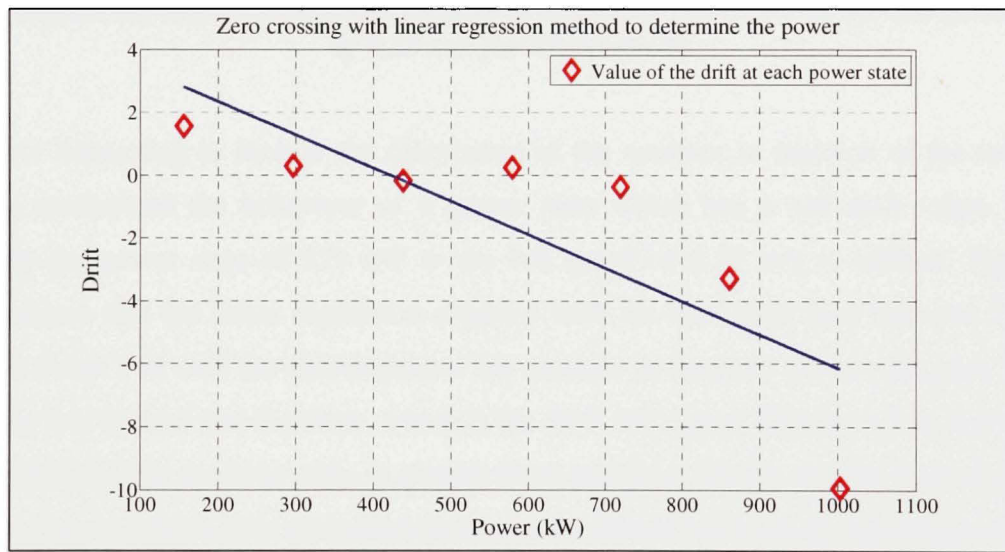


Figure 4.4 *Linear-regression method to determine the power at the bin speed of 6,25 m/s for Klondike-10.*

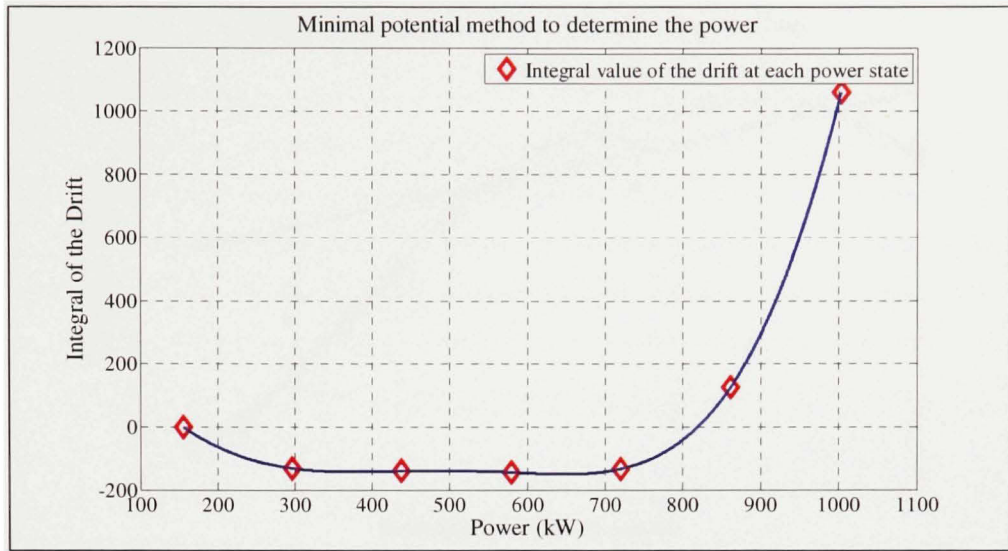


Figure 4.5 *Minimal-potential method to determine the power at the bin speed of 6,25 m/s for Klondike-10.*

It is now interesting to look at the calculation of the moment in function of the relaxation time to understand the behaviour of a power state which has a bad drift value. For the example the power state of 579 kW at the bin speed of 6,25 m/s is utilised. Figure 4.6 demonstrates that the linear regression obtained with the relaxation time between 5 and 15 seconds doesn't fit well the distribution of the moment in function of the relaxation time. In that case it is normal that the slope, which is the drift, isn't good. Further works and analysis will be done in this thesis in order to correct those problems. Moreover, the recommendation section proposes that a new relaxation-time interval should be found at some power states in order to obtain a good power inside a bin speed. However, this problem isn't present at each bin speed. Generally, when this problem occurs, it is easy to spot on the Markov power-curve. For the moment, we will put our effort to increase the shape of the Markov power-curve, and also to get some points beyond the rated power for the real data.

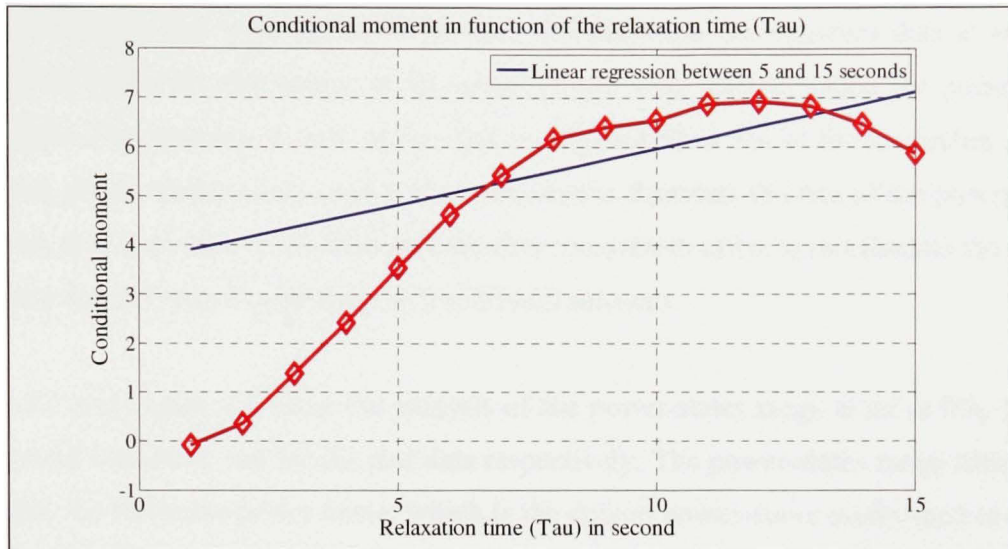


Figure 4.6 *Conditional moment in function of the relaxation time at the bin speed of 6,25 m/s at the power state of 579 kW for Klondike-10.*

4.2 Power-states range filter

Yet, the calculation of the power curve following Markov's theory has shown that there are no points beyond the rated power. Indeed the power curve stops at the bin speed of 11,25 m/s, like illustrated at Figure 4.3. The main reason of that is because the scatter plot isn't as large at the rated power, than anywhere before it. In fact, the sizes of the power states are variable from a bin to another, but are the same size inside a certain bin, and the power-states number is also constant. Therefore, if there are some data, for any reasons, which are a little bit offset of the scatter plot at the rated power, then the power-states size will adjust to that. Thus, there are less power states covering the data beyond the rated power and the number isn't enough to calculate the appropriate stationary power at those bins speed. The extremes data in the scatter plot occurs when the measurement system record erroneous data, the turbine doesn't work properly, or there is high turbulence intensity on that turbine.

A way to correct that is to create a filter that will eliminate the extremes data at each bin speed to re-adjust the dimension of the power states. This filter is called the power-states range filter. For instance, if 10% of the data are filtered, then 5% of the maximum and the minimum power inside a bin speed will be removed to calculate the size of the power states. However, it is important to mention that the data removed in order to re-calculate the power-states size are still kept to calculate the conditional moment.

Figure 4.7 and Figure 4.8 show the analysis of the power-states range filter at 0%, 5% and 10% for the simulated and for the real data respectively. The power-states range filter at 0% is, in fact, the reference power curve, which is the default power-curve established in section 4.1. To lighten the graphics, the plot of the power curve at other percentage isn't shown, while the yellow dots show the powers removed to calculate the power-states size.

Nevertheless, these graphics demonstrate that the power-states range filter is necessary to eliminate extremes powers, especially for real data, in order to construct a good power curve. The best power curve found with this analysis, for all five turbines and the simulated data, occurs when around 15% of the data are filtered. Therefore, the new default power-curve will have the power-states range filter, which will filter 15% of the data at each bin speed to calculate the power-states size.

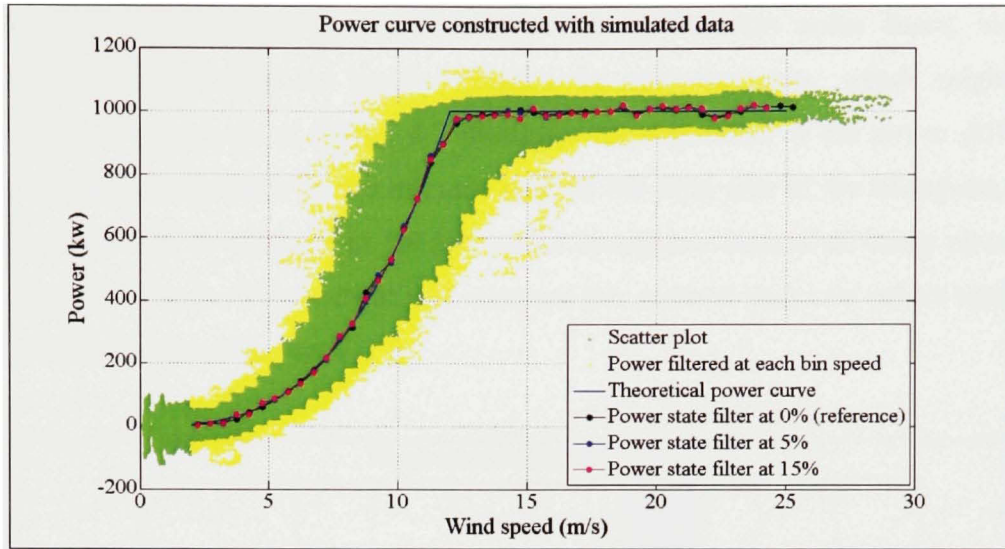


Figure 4.7 Comparison of different power-states range filter for the simulated data.

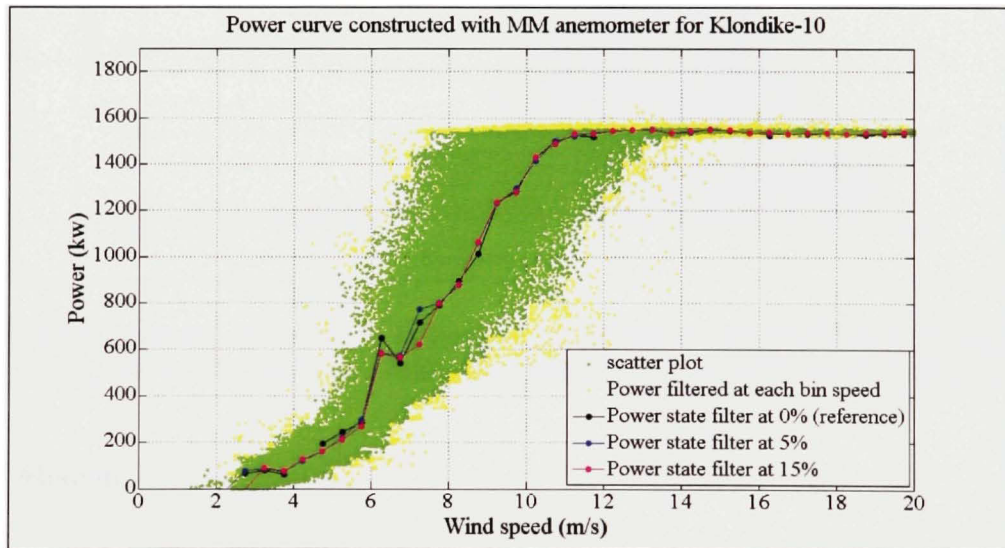


Figure 4.8 Comparison of different power-states range filter for the MM anemometer of Klondike-10.

4.3 Method to calculate the conditional moment

The basic method to calculate the conditional moment is to take the mean of the power differences, at a certain bin speed, at a certain power state and at a certain relaxation time,

like shown in the equation (2.24). However, this method has some flaws, since the conditional moment might be greatly affected by extremes data, which might occur frequently on a wind turbine. Figure 4.9 illustrates the dispersion of the power differences and there is more dispersion on the left side than on the right side of the histogram. In that case, the mean will be affected to the left of the histogram, instead of being close to the highest amount of data. This section will compare this method with two others methods to calculate the conditional moment.

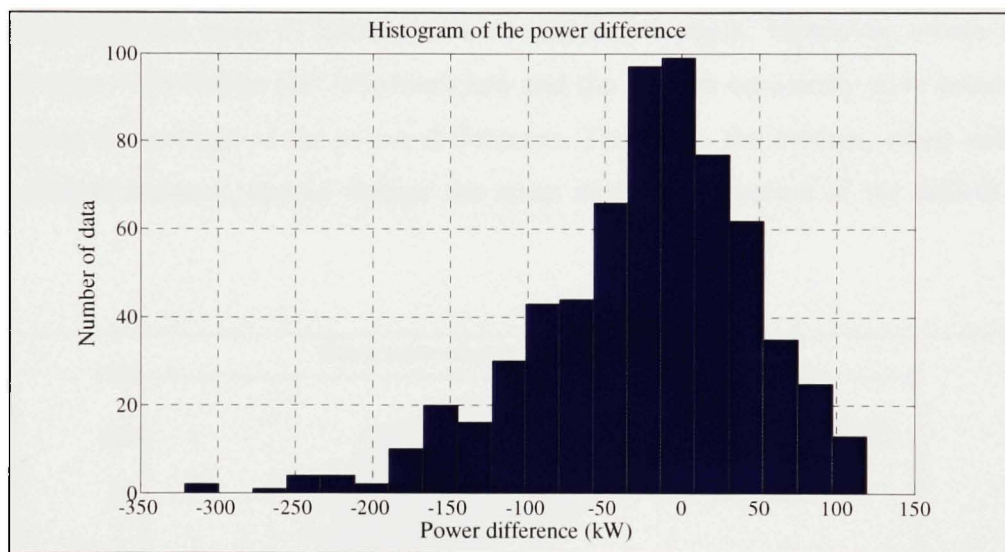


Figure 4.9 *Histogram of the power difference for the bin speed of 9,25 m/s, for the power state of 1450 kW and for the relaxation time (τ) of 5 seconds for Klondike-10.*

4.3.1 Median

The first method to compare with the mean is the median, since it is less affected by extremes data, than the mean. In fact, in a perfect Gaussian distribution, the mean and the median will give the same value. However, when this distribution isn't perfect the mean and the median won't have the same value. For instance, the median won't be affected by the values at the extreme left or right, but only by the amount of points on each side, which is not the case when utilising the mean method. The comparison of the mean and the median has been done for the simulated data (Figure 4.10), for the MM anemometer of Klondike-10 (Figure 4.11)

and for Prettin and Wietmarschen turbines, which aren't presented here. The power curve constructed with the mean is the reference power curve for simulated and real data.

The comparison between the mean and the median shows approximately no difference for the simulated data, and the reason might be because these data are theoretical and we can assume that this is a perfect Gaussian distribution, and therefore there is no extremes data in that group. However, the power curve made with Klondike-10 did greatly improve with the median. In fact, the shape of the power curve is smoother and more cubic than the one constructed with the mean to calculate the conditional moment. Moreover, others analysis has been done with Prettin and Wietmarschen and the median constantly gave better results than making the average of the power differences. Therefore, the median, when calculating the conditional moment, should replace the mean in the construction of the default power-curve.

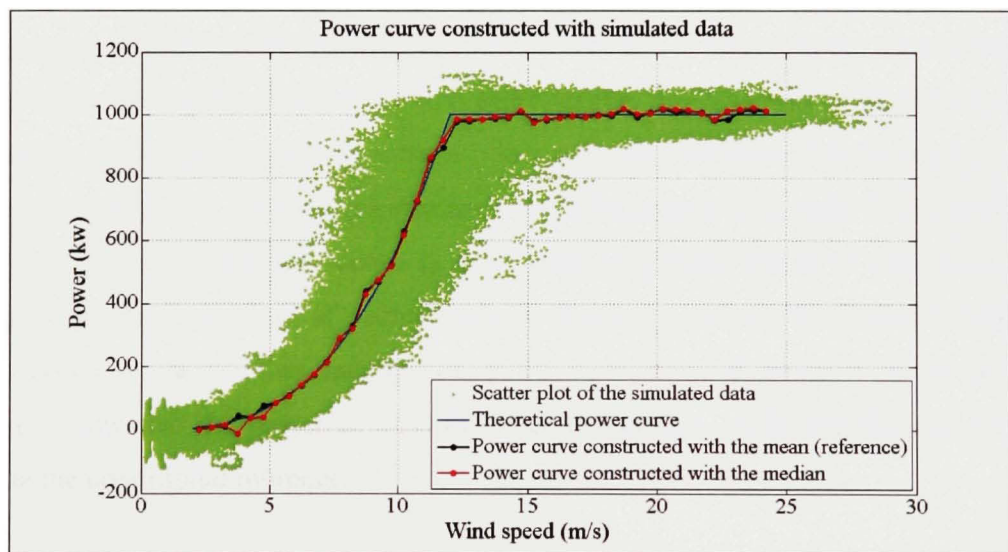


Figure 4.10 *Comparison of the mean with the median to calculate the power curve for the simulated data.*

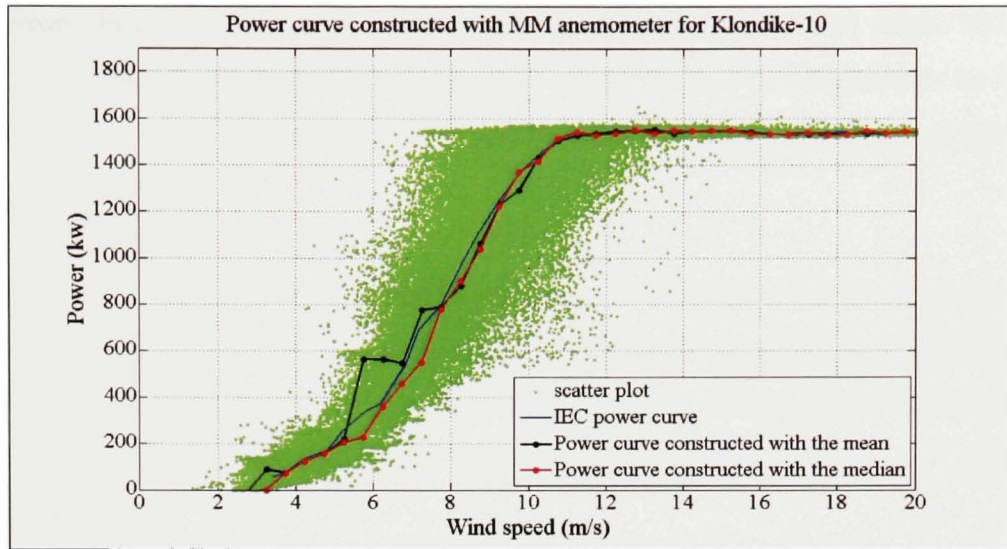


Figure 4.11 *Comparison of the mean with the median to calculate the power curve for the MM anemometer of Klondike-10.*

However, we can see that the power curve constructed with the median is a little bit lower than the one constructed with the IEC standard. In fact this is normal at the start of the curve, because of the averaging effect of the IEC power-curve, but it should be higher close to the rated power. There can be multiple reasons it is not. Firstly, we know that the Markov power-curve isn't perfect yet, so other parameters should be analysed in order to ameliorate this curve. And secondly, this IEC curve is done with only three weeks of data so it can be influenced by the short time of acquisition. Nevertheless, for the four other turbines, the Markov power-curve is higher than the IEC power-curve close to the rated power, so we will continue to improve the power curve with other parameters, while keeping the median to calculate the conditional moment.

4.3.2 Most frequent power-difference

The second method to compare with the default power-curve will be to take the most frequent power-difference. Mainly, this method consists in binning the power differences, taking the bin with the highest amount of data, then averaging the power differences in that bin. On the other hand, only keeping the bin with the highest amount of data might lead to

some errors. In reality, the bin with the second highest number of data might be in a big proportion of the one with the highest amount of data. Figure 4.12 demonstrates an example when a power-difference bin, next to one with the highest number of data, is proportionally high.

Therefore, it is necessary to fix a certain percentage to only keep the bin higher than this proportion of the highest amount of data. Figure 4.12 shows an example of the distribution for the power differences, while Figure 4.13 illustrates the bins kept after filtering the bins lower than the fixed percentage. These percentages are constant and we will analyse the proportion values.

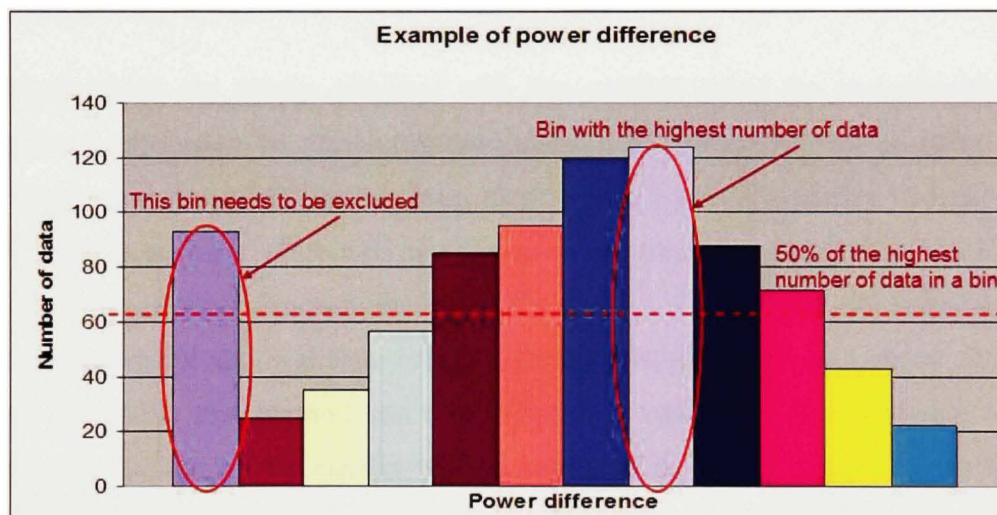


Figure 4.12 *Example of distribution for the power difference.*

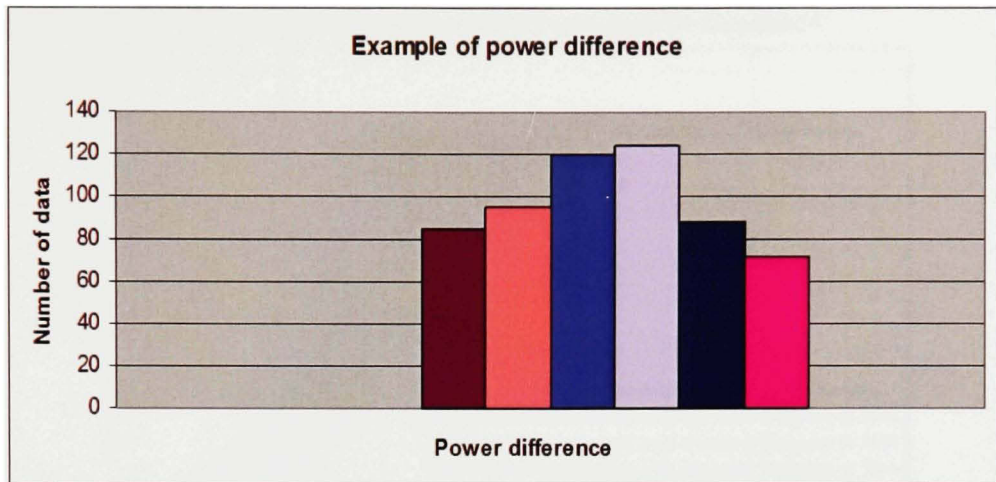


Figure 4.13 *Example of distribution for the power difference at 50% of the highest number of data.*

Figure 4.14 shows the results obtained with this method using the meteorological-mast anemometer for Klondike-10. Obviously this method doesn't seem to work properly. Indeed, by removing some power-differences bins, there is also a great possibility to remove good values inside those bins. Moreover, the Gaussian distribution is clearly reduced by this method, like the example demonstrates at the Figure 4.13. Furthermore, the reduction of the number of data inside a power state brings inaccuracy in the calculation of the conditional moment. Therefore, this method can't be utilised to calculate the conditional moment. Consequently, the use of the median will be kept as a default parameter to construct the power curve, since the most frequent method is far from being a good method.

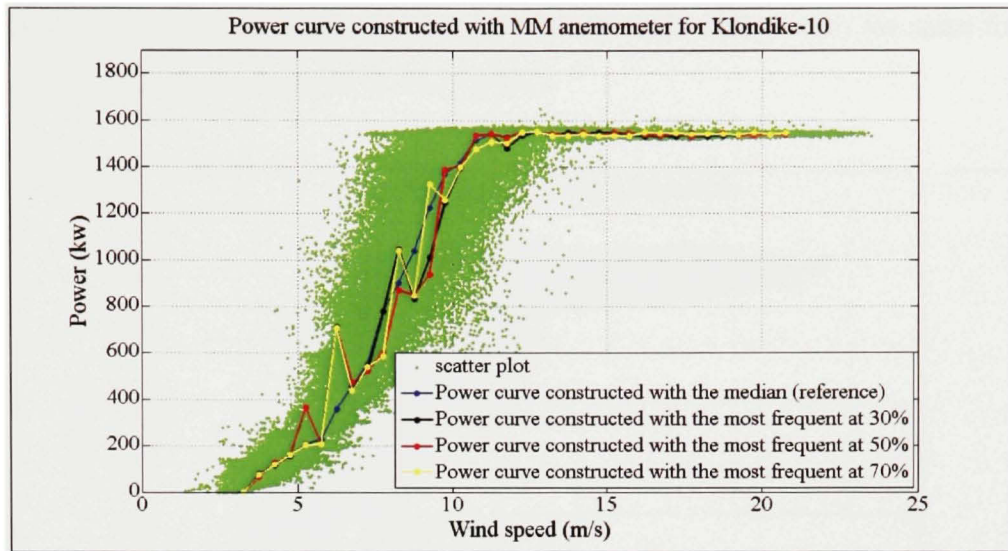


Figure 4.14 *Comparison of the median with the most frequent to calculate the power curve for the MM anemometer of Klondike-10.*

4.3.3 Power-differences filter

After trying different methods to calculate the conditional moment, it might be advantageous to only filter the power differences, because if there are extremes data inside a certain power state, then the power-differences filter might help getting good results.

Basically, this method consists in filtering a certain proportion of data at both end of the power-differences variable. However, this kind of filtering is not required when calculating the conditional moment with the median, since the median takes the middle point of a variable, and removing a certain proportion at both end of this variable will lead to the same value. Therefore, this filtering can only be analysed when utilising the mean to calculate the conditional moment.

For the simulated data (Figure 4.15) and for the meteorological-mast anemometer of Klondike-10 (Figure 4.16), there is no significant differences between the use of the median, and the use of the power-differences filter when constructing a power curve. Moreover, the difference is close to null when comparing the power-differences filter percentage. These

graphics show that the results are the same for 5% and 10%. This is also the same for others percentages, which are not shown in the graphics.

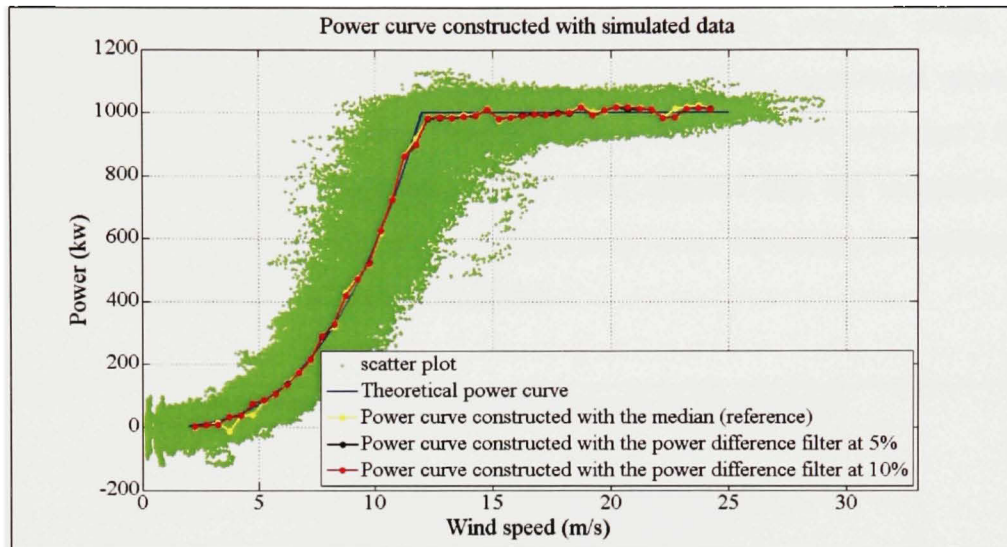


Figure 4.15 *Comparison of the median with the power-differences filter to calculate the power curve for the simulated data.*

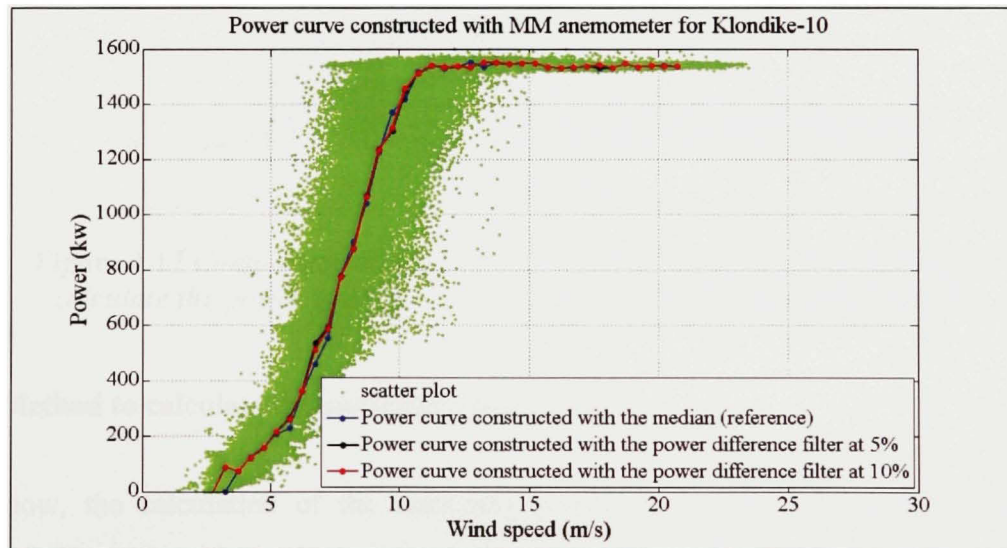


Figure 4.16 *Comparison of the median with the power-differences filter to calculate the power curve for the MM anemometer of Klondike-10.*

However, when utilising the Prettin and the Wietmarschen data, the median is far better than the power-differences filter. Figure 4.17 illustrates that using the power-differences filter isn't as good as the median for Wietmarschen-2; this is also true for Prettin and Wietmarschen-1 turbines. In fact, the main problem with this method, which is also explained in section 4.3.1, is that we use the mean to calculate the conditional moment, but this time with a filter. As soon as the power differences inside a power state don't follow a perfect Gaussian distribution, the mean will be more affected than the utilisation of the median, which lead to a higher risk of getting the wrong value. Therefore, the median should be kept when calculating the conditional moment.

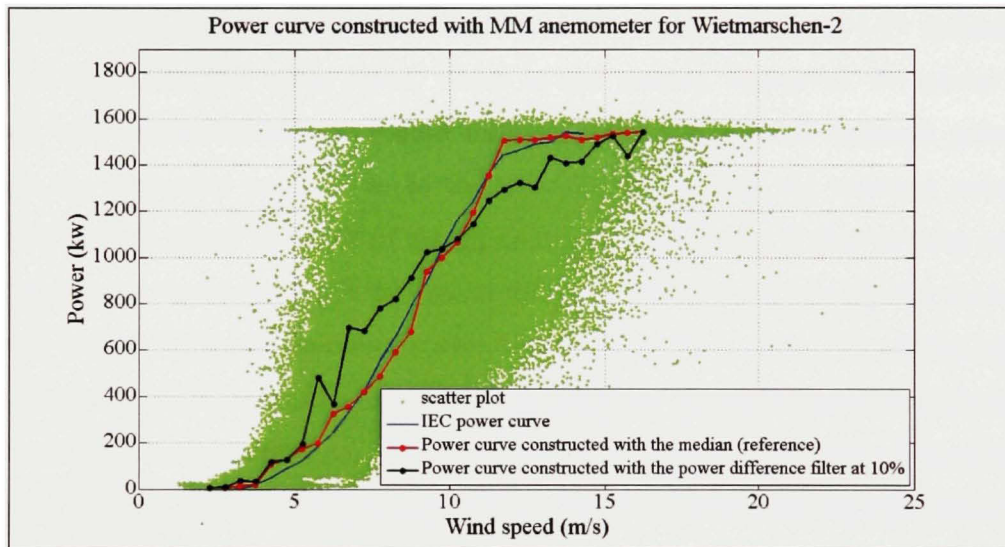


Figure 4.17 *Comparison of the median with the power-differences filter to calculate the power curve for the MM anemometer of Wietmarschen-2.*

4.4 Method to calculate the stationary power curve

Until now, the calculation of the stationary power curve was made with the minimal potential. However, this method seems to have some problems when a second minimum arises (see Figure 4.5). Even though the second minimum problem might be solved for Klondike-10 turbine with the use of the median, the Wietmarschen-1, Wietmarschen-2 and Prettin-4 turbines still does have this problem.

The apparition of the second minimums is difficult to eliminate, since we need to find which points aren't good in the graphic of the drift in function of the power. In fact, the wrongs drift values close to zero might create a second minimum when calculating the integral. Therefore, using the linear-regression method instead of the minimal-potential method might solve the problem, because it will be less affected by the bad drift values close to zero. However, the results could be even worst for the drift values far from zero.

After calculating the power curve with both methods, the minimal potential is still the best way to construct a power curve. Figure 4.18 shows that there is no considerable difference between these two methods for the simulated data. However, the Figure 4.19 illustrates that the linear regression has some peaks, which is not wanted. Moreover, the power curves obtained with Wietmarschen and Prettin turbines are better with the minimal potential to calculate the stationary power. The reason it works better with the minimal potential is because it doesn't adjust to the fit of the linear regression. In fact, if there is only one point wrong, the linear regression might be greatly affected, which is not the case for the minimal potential, unless that point re-crosses zero which will give a second minimum problem. Consequently, a method should be found to eliminate that problem and will be investigated in section 4.5. For the moment, the calculation of the power curve with the minimal potential will remains, because theoretically it should give the best results, and experimentally it does too.

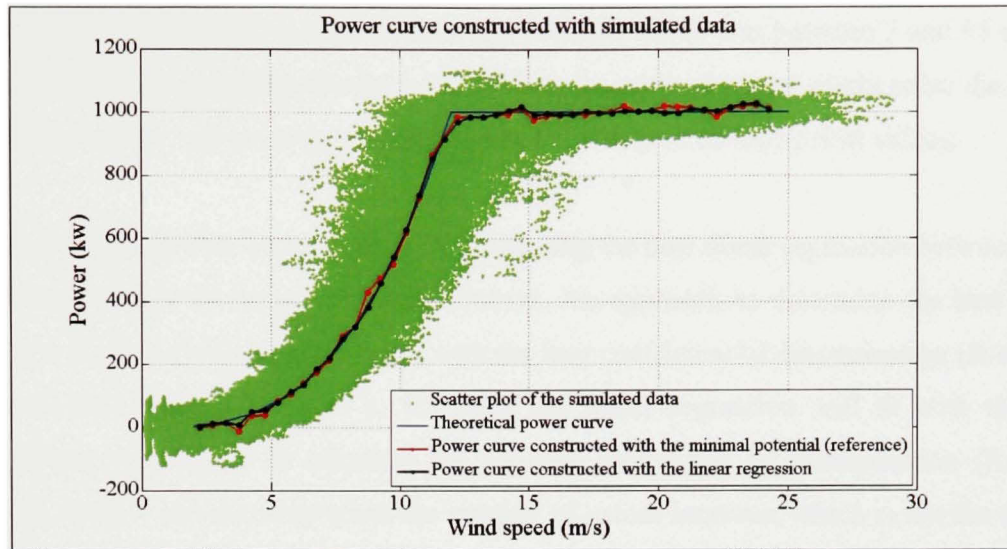


Figure 4.18 *Comparison of the minimal potential with the linear regression to calculate the power curve for the simulated data.*

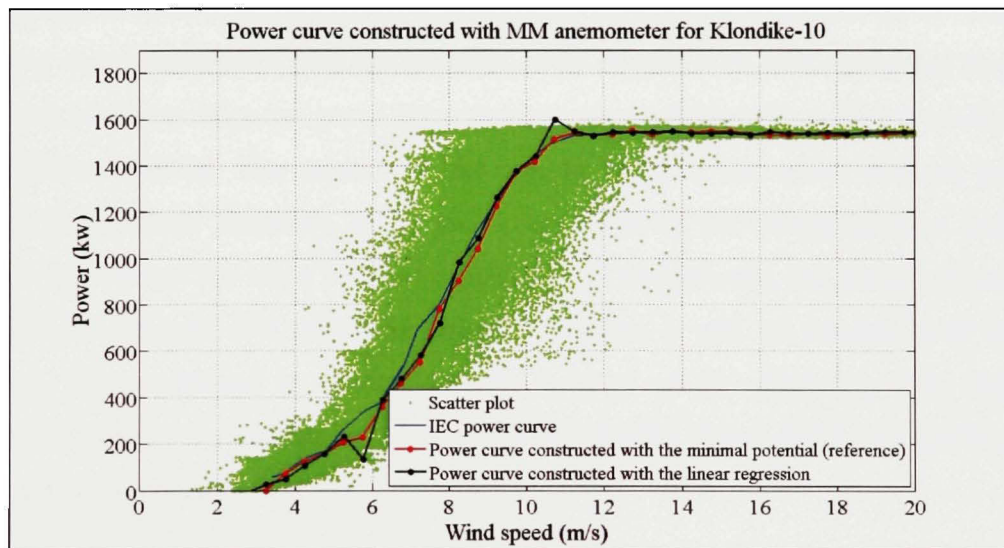


Figure 4.19 *Comparison of the minimal potential with the linear regression to calculate the power curve for the MM anemometer of Klondike-10.*

4.5 Method to calculate the drift

The calculation of the drift is done by calculating the slope of the linear regression in the graphic of the conditional moment in function of the relaxation time, like shown in Figure

2.1. Until now, the relaxation time was already defined, which was between 5 and 15 seconds [8]. Nonetheless, in applying another interval than the original one, it might solve the second minimum problem explained in section 4.4, since it will give different drift values.

A method to change this interval might be by finding the best linear regression between 5 and 15 seconds, instead of taking the entire interval. An approach to determine the best linear-regression curve is by finding the curve with the best coefficient of determination (R-square). The more this value is close to 1, the more the linear regression will fit with the data. Nevertheless, it is better to calculate the adjusted coefficient of determination (R-square adjusted), since it can decrease when the number of values increase, which is not the case for the standard coefficient of determination.

The difference between these two methods is negligible for the simulated data. Figure 4.20 demonstrates that every points of one curve overlap all points of the other curve. Moreover, the power curve constructed with the real data, at the Figure 4.21, still shows that there is no conclusive evidence of power curve improvement when utilising the adjusted coefficient of determination method. The reason of that can be because the entire interval generally contains good value. Therefore, if we utilise any value of the relaxation time inside this interval, we will get the same results or close to it. Consequently, the default power-curve shouldn't be changed and the entire interval between 5 and 15 seconds will be kept. However, like mentioned in section 4.1, the interval of the relaxation time should be modified at some power states in order to obtain a perfect power value at each bin speed, which is also proposed in the recommendation section.

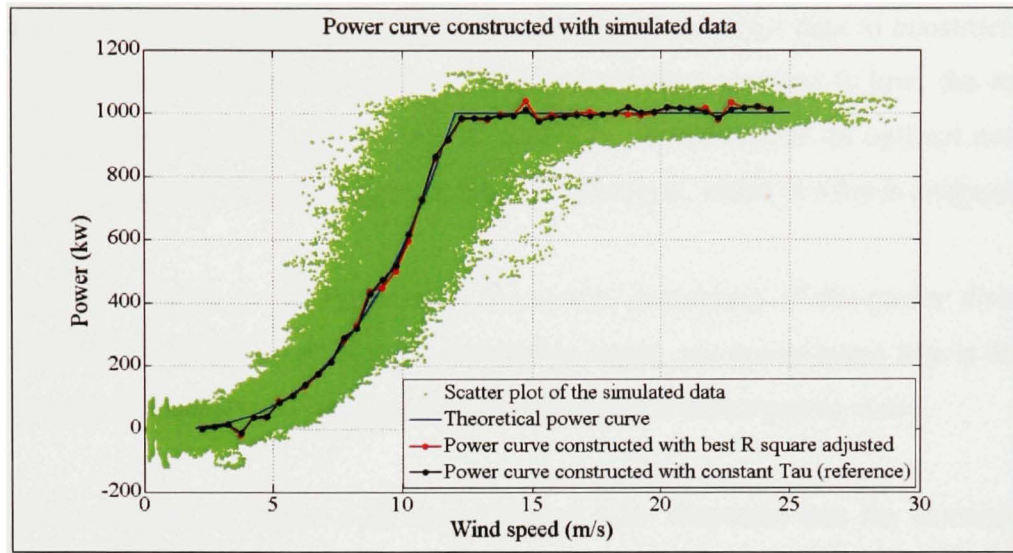


Figure 4.20 *Comparison of the power curve with different methods to calculate the drift for the simulated data.*

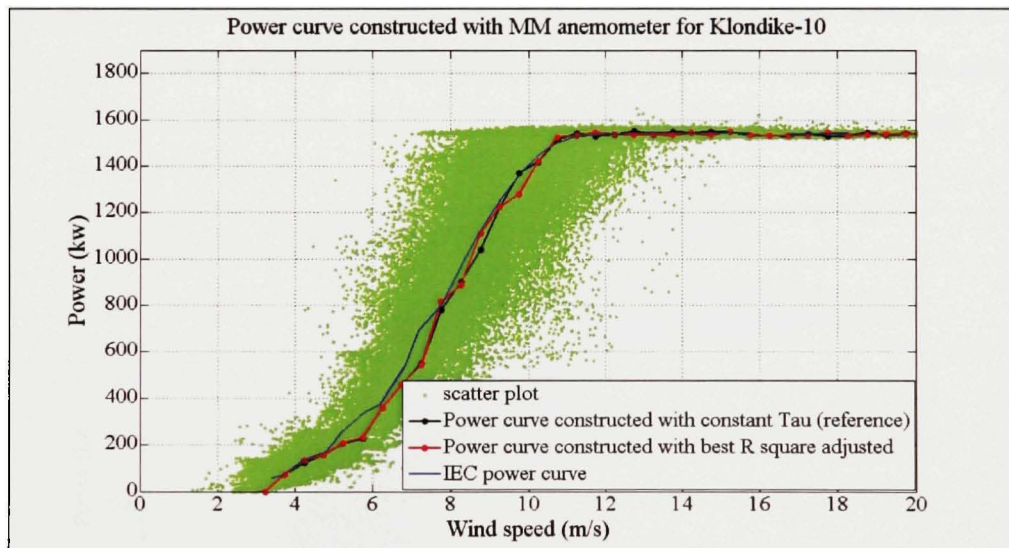


Figure 4.21 *Comparison of the power curve with different methods to calculate the drift for the MM anemometer of Klondike-10.*

4.6 Power-states number

Defining the number of power states is necessary since the acquisition time of the data and the success of the power-curve construction depend on it. Indeed, the more the power-states

number is high; the more the recording time can be long to obtain data to construct a good power curve. On the other hand, the more the power-states number is low; the more the quality of the power curve can be reduced. Therefore, it can require an optimal number of power states to construct a good power curve in a short time, which is what is analysed here.

The power-states size is variable at each bin speed, depending of the power distribution inside that bin speed. However, inside a certain bin speed, the power-states size is the same. Until now, the construction of the power curve was made with ten power states.

The results obtained, at Figure 4.22 and at Figure 4.23, illustrates that the construction of power curve following Markov's theory needs at least eight power states. Indeed, there is an asymptote starting from the moment the power-state number reaches eight, which means that higher than this value the stationary power at each bin speed is approximately the same. Moreover, the Wietmarschen and Prettin data confirm that eight power states are enough to construct a good power curve following Markov's theory, but more power states also can be utilised. For the rest of this thesis, all analysis will be done with eight power states.

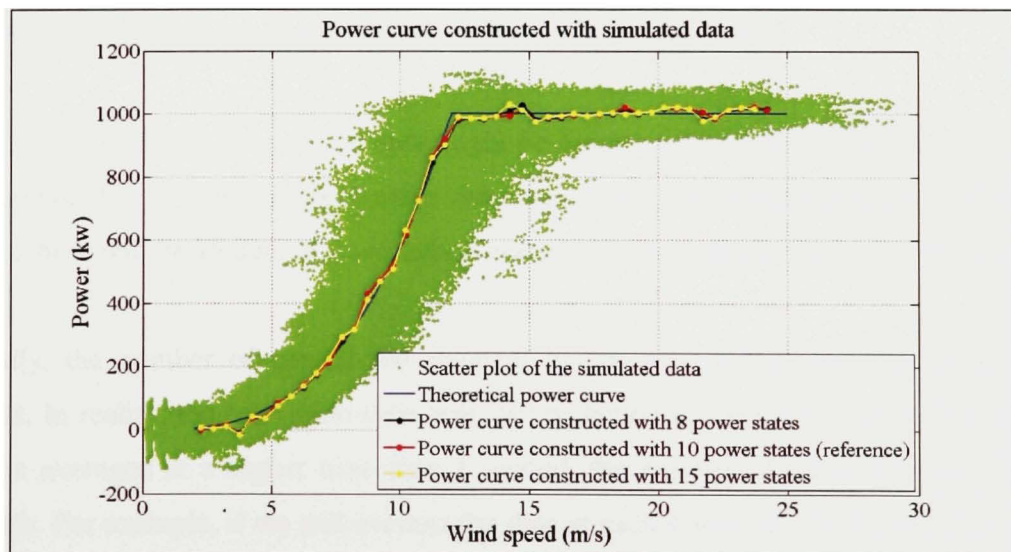


Figure 4.22 Comparison of different number of power states to calculate the power curve for the simulated data.

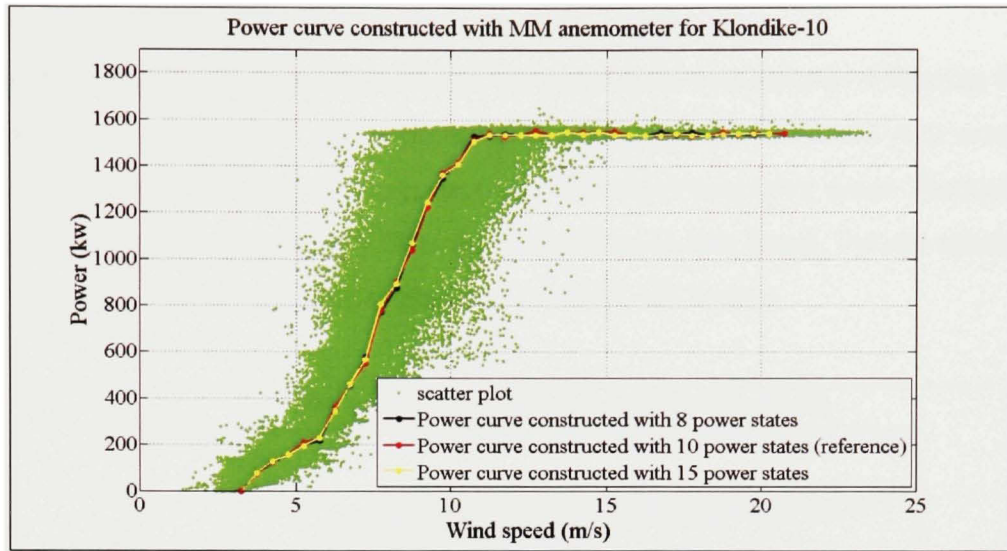


Figure 4.23 *Comparison of different number of power states to calculate the power curve for the MM anemometer of Klondike-10.*

4.7 Averaging time

Since the start of this thesis, the averaging time of data was 1 second. However, there is a possibility to average the data over a longer period. Nonetheless, those averaging times higher than the default one aren't recommended for various reasons.

Firstly, the acquisition time of the data might be longer, since there will be less data over a same period. For example if we average the data at each 4 seconds, then over a period of 1 minute, there will be 15 data of 4 seconds average, instead of 60 data of 1 second average.

Secondly, the number of conditional moment in function of the relaxation time will be reduced. In reality, the relaxation time will still be between 5 and 15 seconds, but since the data are averaged at a higher time than 1 second, the number of conditional moment will diminish. For example, if we still average the data at each 4 seconds, the conditional moment can only be calculated at 4, 8, 12 and 16 seconds, which gives four values of conditional moment instead of ten values. Therefore, the precision of the slope, when calculating the drift, will be reduced.

The results obtained at Figure 4.24 illustrate that there is no considerable difference between the power curves constructed with different averaging times. However, the data averaged at one second might require less time to collect, than the others averaging times. The analysis of the minimal time to acquire data will be presented later in this thesis. For the moment, the power curve constructed with data averaged at 1 second will be kept.

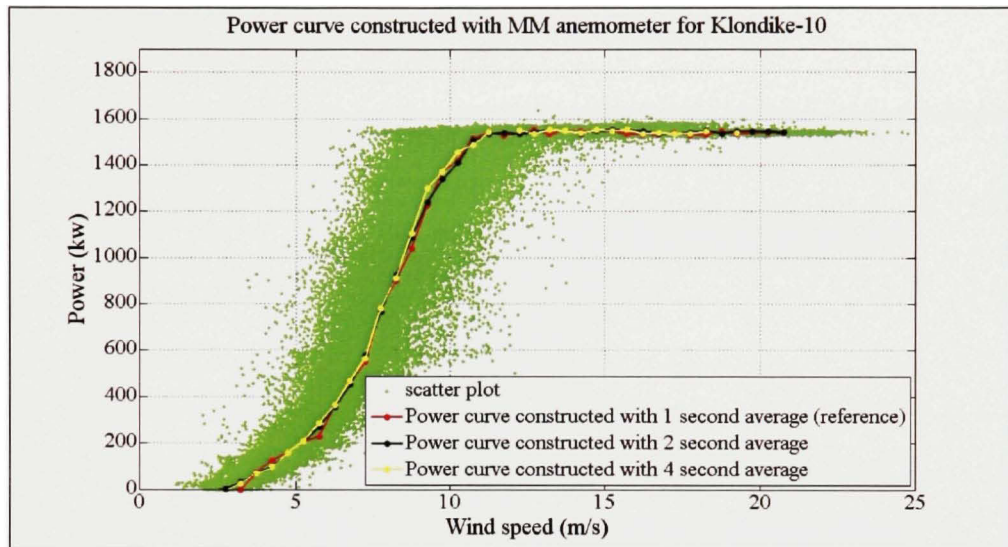


Figure 4.24 *Comparison between the averaging times higher than 1 second to construct the power curve for the MM anemometer of Klondike-10.*

According to the last results, it might be advantageous to utilise an averaging time shorter than 1 second. In that case, the time to collect data could be even more reduced. The Klondike-10 and the Wietmarschen measurements systems collect the power at a rate of 50 Hz, which means that it can collect 50 data per second. However, the data averaged at 0,02 second aren't available for the Prettin turbines. Thus, the construction of the power curves with data averaged at 0,1 and 0,2 second can be analysed for the Wietmarschen and the Klondike turbines. The reason why the data averaged at 0,02 second isn't considered in this analysis is because it requires a lot of space in the memory of the computer. Therefore, the periods examined were too short to give at least a good scatter plot to construct a power curve.

Figure 4.25 illustrates the power curves constructed with the averaging times shorter than 1 second. The results obtained demonstrate that the power curve can be constructed, with good results, at different averaging time shorter than 1 second. Moreover, there is no difference between those averaging times. Therefore, it is preferable to utilise the data averaged at 0,1 second, since it might give the advantage to construct the same power curve in less time. More details on the analysis of the minimal recording time for the Markov power-curves will be given in Chapter 7.

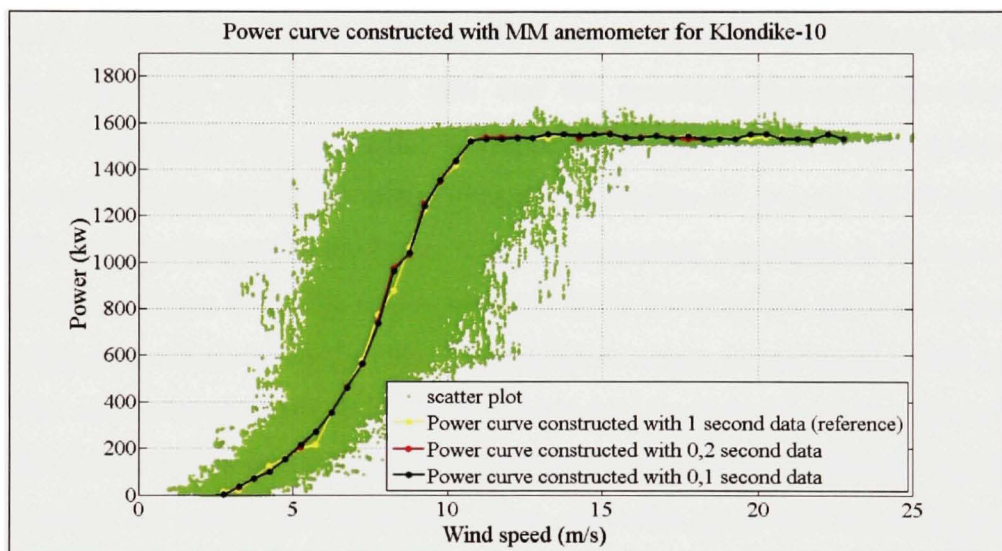


Figure 4.25 *Comparison between the averaging times shorter than 1 second to construct the power curve for the MM anemometer of Klondike-10.*

4.8 Wind speed averaging

When the MM anemometer reads the wind speed, the power output of the turbine doesn't react instantly. Indeed, there is an algorithm inside the turbine, which averages the wind speeds over a certain period of time to determine the power output. This algorithm is present in the system because the wind speed fluctuates over a short period of time. The construction of the power curve following Markov's theory is made with the data averaged at each second. Therefore, the wind speed changes bin constantly, which causes that the power

output of the turbine might be in the wrong bin. Moreover, when the wind speed is obtained from the nacelle anemometer, there is more fluctuation because of the addition of blade passage.

A solution to counter this problem is to average the wind speeds over a certain period of time, then replace the wind speeds read over this period by the wind speed averaged. For example, if we decide to average the wind speeds over 60 seconds, then the wind speeds from 1 second to 60 seconds will take the value of the averaged one.

Figure 4.26 and Figure 4.27 show that the difference is negligible for different wind speed averaging times with the simulated data and the meteorological-mast anemometer of Klondike-10. However, this parameter is important to keep in the default power-curve, because it gives better results on others sites than Klondike-10. Indeed, for Wietmarschen and Prettin turbines the results are better with this parameter, especially at 30 seconds, like demonstrated in Figure 4.28. The reason why it is better for those two sites is because of the large scatter plot, which is mostly caused by turbulent winds. In reality, the wind speed on those sites can fluctuate really fast, which causes that the power output might be on the wrong bin speed. On Klondike-10 turbine, the wind speed isn't as turbulent as the other two sites, therefore the scatter plot is smaller. Thus, the wind speed will be averaged over a period of 30 seconds in the default MM power-curve.

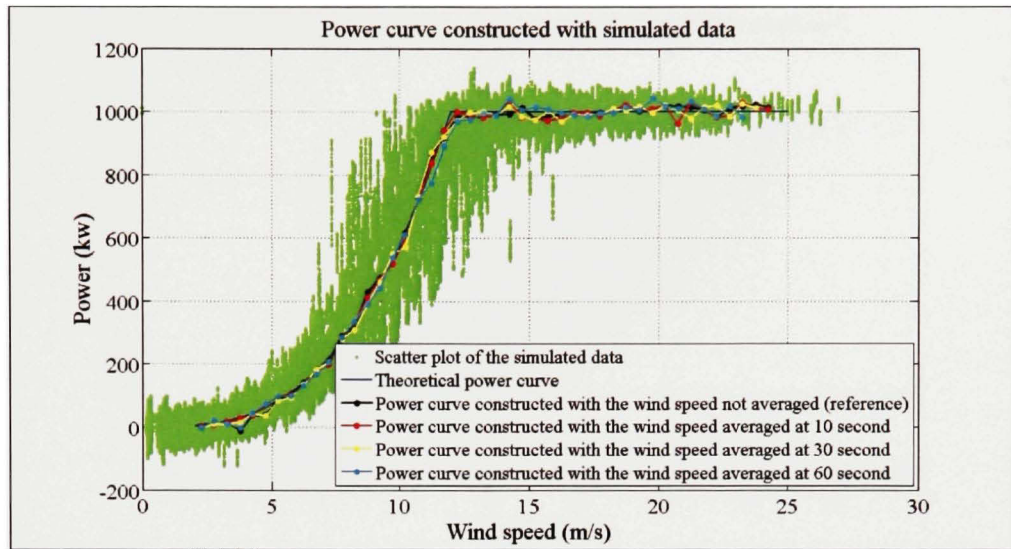


Figure 4.26 Comparison of different averaging times of the wind speed to construct the power curve for the simulated data.

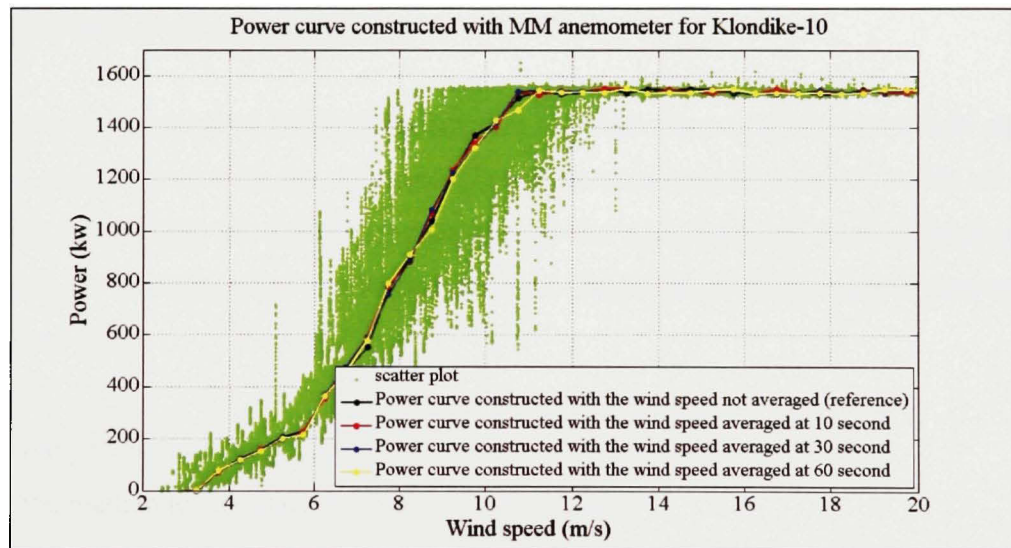


Figure 4.27 Comparison of different averaging times of the wind speed to construct the power curve for the MM anemometer of Klondike-10.

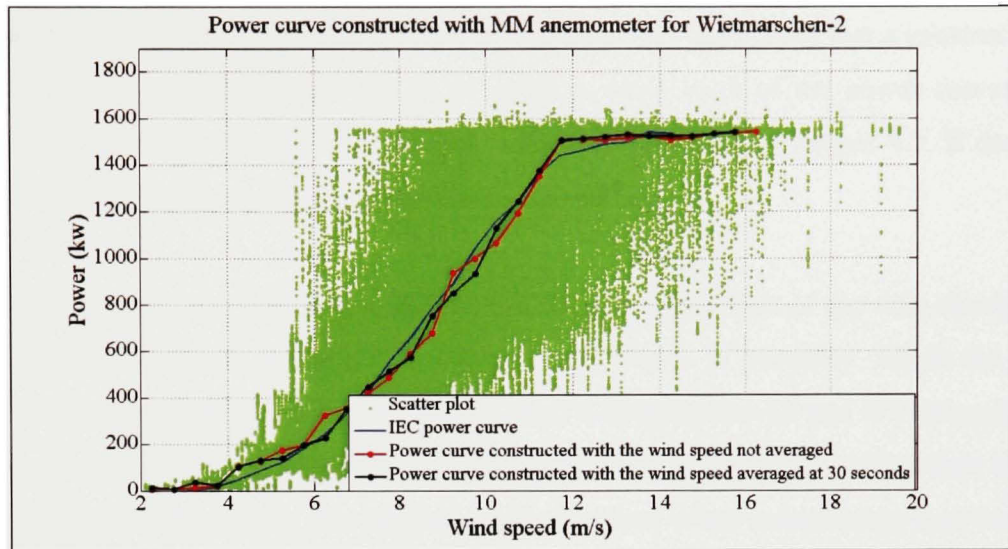


Figure 4.28 *Comparison of different averaging times of the wind speed to construct the power curve for the MM anemometer of Wietmarschen-2.*

4.9 Synthesis of all parameters

Until now, the analysis of different parameters has been done to determine which ones give the best power curve with the meteorological-mast anemometer. Even if nearly all figures shown in this chapter are from Klondike-10 and the simulated data, this analysis also has been done for Wietmarschen and Prettin turbines. Therefore, the default power-curve is now constituted with:

- the power-state range filter of 15%;
- the median to calculate the conditional moment;
- eight power states to calculate the stationary power at each bin speed;
- the minimal potential to calculate the stationary power;
- the relaxation time between 5 and 15 seconds to calculate the drift coefficient;
- the bins speed set at 0,5 m/s;
- the wind speed averaged over a period of 30 seconds;
- the data averaged on a period of 1 second or less.

Besides, the previous analysis made with the simulated data has shown that a construction of power curve following Markov's theory is possible, since most of the power curves made with these data are on the theoretical curve, like the one shown in Figure 4.1. It does also confirm that the Markov power-curve software is working.

Furthermore, it also has been demonstrated that the averaging time of the data shouldn't be over 1 second, since the power curve will eventually loose in accuracy. Albeit the results with the averaging time under 1 second seem good with Klondike-10 and Wietmarschen-site turbines, it can't be proven with Prettin-site turbines, because it doesn't collect data at a rate under 1 second. Nonetheless, this method could save time when constructing a power curve following Markov's theory. An analysis of the time required will be done in the Chapter 7.

CHAPTER 5

POWER CURVE CONSTRUCTED WITH THE NACELLE ANEMOMETER

To construct the nacelle power-curve following Markov's theory, it is necessary to keep the parameters obtained with the meteorological-mast anemometer. However, there are some differences between the MM and the nacelle anemometer. Indeed, there is a transfer function to pass the construction of the power curve from the MM anemometer to the nacelle anemometer. In fact, this transfer function is required because the blade passage affects the wind speed recorded at the nacelle anemometer.

First a correlation between the MM wind-speed and the nacelle wind-speed is required. This correlation should be done following the bin-correlation method, which is explained in section 1.1.1. Figure 5.1 illustrates this correlation. The blue line is the normal correlation, which is done with all the data, while the red dot-line is the bin correlation, which is done at each bin speed. The last correlation is the oncoming standard procedure according to the IEC standard [12].

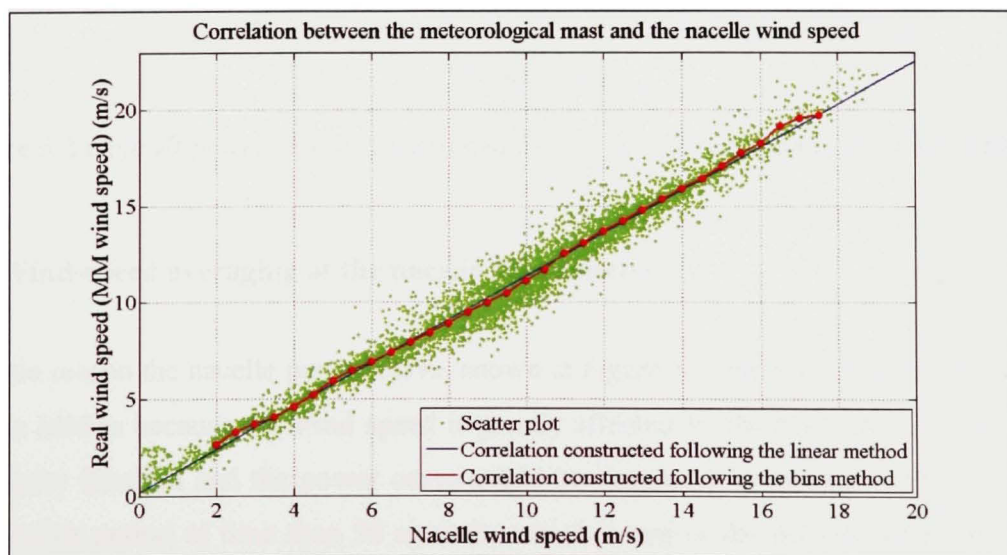


Figure 5.1 *Correlation between the MM and the nacelle anemometer for Klondike-10.*

Then, the construction of the nacelle power-curve following Markov's theory can be done with the defaults parameters. Therefore, we assume that the relaxation time (τ) is the same than the one utilised for the MM anemometer. Figure 5.2 shows the nacelle power-curve obtained, while keeping the optimal parameters found from the MM power-curve. The power curve constructed with the nacelle anemometer isn't as good as the one made with the MM anemometer. Indeed, this power curve is a little bit erratic below the rated power. Consequently, the transfer function might require more parameters, than only the bin-correlation method.

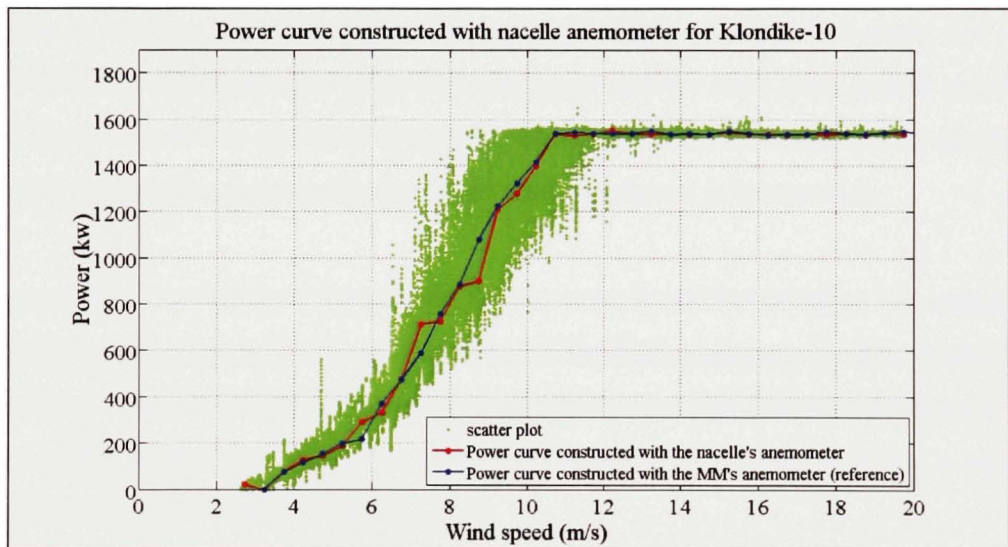


Figure 5.2 *Default power-curve constructed for the nacelle anemometer of Klondike-10.*

5.1 Wind-speed averaging at the nacelle anemometer

The main reason the nacelle power-curve, shown at Figure 5.2, isn't as good as the one made with the MM is because the wind speed is greatly affected by the blade passage. Therefore, the transfer function and the power curve might be improved by averaging the wind speed over another period of time than 30 seconds, which is one of the default parameters for the MM anemometer.

Moreover, it is also important to mention that we can't average the data on a period like 0,5 or 1 second, because in this interval we don't know if we do have the effect of blade passage or not. In fact, the rotor speed can be between 10 and 20 rpm, which means between 30 and 60 blade passages per minute, which is at least one blade passage per 2 seconds. This is why it is preferable to average on longer period of time for the nacelle anemometer, because we do know that we do have the effect of blade passage.

Figure 5.3 illustrates the comparison of different wind speed averaging times, when constructing a power curve with the nacelle anemometer. The results show that it is preferable to average the wind speed over a period of two minutes. Moreover, the analysis with Prettin and Wietmarschen gives also the same results, since their power curves have greatly improve and they are close to perfect. The graphics of the construction of the power curve with the nacelle anemometer, for those sites, are shown in section 6.2.

The reason why the wind speed averaging times passes from 30 seconds to two minutes with the nacelle anemometer is because of the effect of the blades passage. In fact, the addition of the blades passage with the high variation of the wind speed in a short time causes that the average of the wind speed should be done on a longer period in order to get a significant value of the wind speed in the interval.

Thus, the transfer function is better when the wind speed is averaged over a period of two minutes, and it should be incorporated in the default power-curve constructed with the nacelle anemometer.

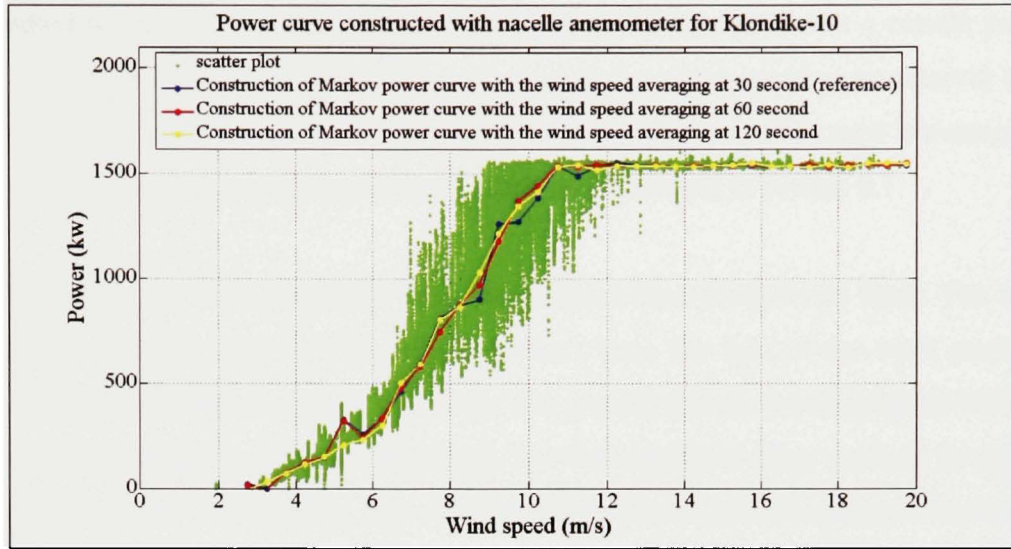


Figure 5.3 *Comparison of different wind-speed averaging time for the power curve constructed for the nacelle anemometer of Klondike-10.*

5.2 Rotor-position filter

Another method to decrease the effect of blade passage might be by filtering with the rotor position, because the wind passes through the blades before reaching the nacelle anemometer. Consequently, the wind is affected by that, and removing the data that are affected by the blade passage could provide a better power curve.

However, the rotor position to filter is dependent of the wind speed, and the distance between the rotor and the nacelle anemometer. In reality, there is a difference of time between the moment the wind reaches the blade and the moment the wind reaches the nacelle anemometer. This time difference changes in function of the wind speed. Consequently, the calculation of the influenced rotor position (φ) will be in function of these two parameters [10].

$$\varphi = \frac{360 * d * \omega}{V_{avg} * \eta_{GB} * 60} \quad (5.1)$$

The method to use the equation (5.1) is to average the wind speed over a certain period of time, calculate the influenced rotor position, remove the wind speed at an interval of ± 40 degrees of φ , and re-calculate the averaged wind speed [10]. The wind speed is averaged over a two minutes period, since it was the best period of time found in section 5.1.

Figure 5.4 illustrates the comparison with and without the rotor-position filter. The analysis can only be done for Klondike-10, since we don't have the data of the rotor position for Wietmarschen and Prettin turbines. Moreover, the graphic shows no or negligible differences between these two power curves. Therefore, the rotor-position filter can not be kept as a default parameter for constructing a power curve with the nacelle anemometer. However, the study of this filter should be done with more sites and more turbines, which will produce a better conclusion. For all these reasons this analysis is, for the moment, inconclusive.

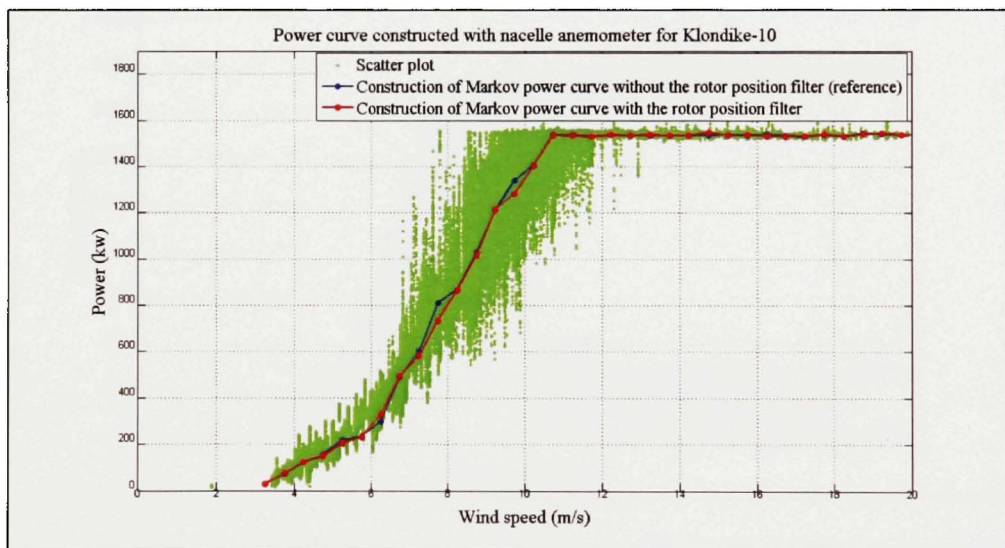


Figure 5.4 Comparison of the rotor-position filter for the power curve constructed for the nacelle anemometer of Klondike-10.

5.3 Averaging time below 1 second

Like demonstrated in section 4.7, if the averaging time is reduced, then the recording time might also be reduced, which is the primary goal of this thesis. That section has also shown

that there is no considerable difference between the power curve constructed with the MM anemometer for 0,1 and 1 second averaged. However, it is important to verify it for the nacelle anemometer, since there is a transfer function to pass from the MM wind-speed towards the nacelle wind-speed.

The comparison of the time averaging for the nacelle anemometer is shown at Figure 5.5. Akin to the analysis obtained with the MM power-curve, the nacelle power-curve shows no difference between the data at different averaging times. It is also the same for Wietmarschen turbines, but those two power curves will be illustrated in the section 6.2. Therefore, there is a possibility to average the power at a shorter time than 1 second and to obtain a good power curve, with the nacelle anemometer.

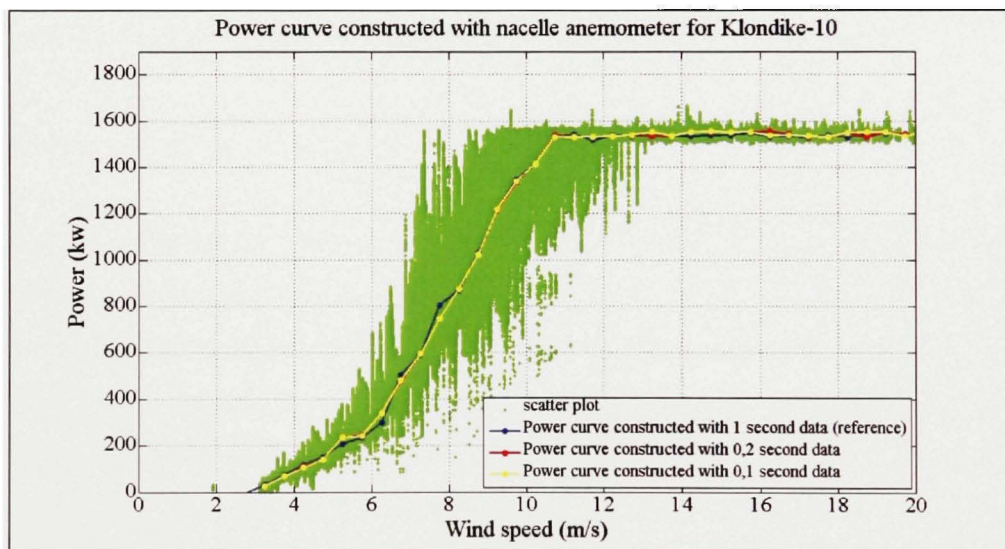


Figure 5.5 Comparison of the time averaging for the power curve constructed for the nacelle anemometer of Klondike-10.

This chapter has presented the construction of the nacelle power-curve following Markov's theory. The results obtained for Klondike-10 turbine are good, but not great. Generally, the power curve constructed with the MM anemometer is better than the one obtained with the nacelle anemometer for this site. Moreover, until now the power curves aren't stable. One of the reasons is because the Markov power-curve software isn't perfect yet and more

improvements need to be done. More meteorological-mast and nacelle power-curves from others sites will be shown in the Chapter 6, which will verify the efficiency of this novel method.

CHAPTER 6

VALIDATION OF THE POWER CURVE WITH WIETMARSCHEN AND PRETTIN TURBINES

The validation of the parameters with Wietmarschen and Prettin turbines was included in Chapter 4 for the meteorological-mast anemometer, and in Chapter 5 for the nacelle anemometer, even though the majority of the graphics are from the Klondike-10 turbine. However, now it is necessary to prove that the construction of the power curve following Markov's theory works for others sites than Klondike-10. Consequently, the others sites validation is done for the meteorological-mast anemometer and the nacelle anemometer. Afterward, it will be possible to determine the minimal number of data required per bins speed, and then deduce the minimal time to construct a Markov power-curve.

6.1 Meteorological-mast anemometer

The parameters utilised to construct the power curve for Wietmarschen and Prettin turbines are the same as the optimal ones found in the Chapter 4. However, Wietmarschen and Prettin turbines are a little bit different than Klondike-10 since the scattering of the power at each bin speed is more dispersed. This great dispersion might be caused by the distance between the turbines and their respective MM. Indeed, these distances are much higher than the Klondike-10 one. We need to mention that Prettin measurement-systems don't have the advantage to collect data on a shorter period than 1 second. Therefore, the analysis can only be done with 1 second data for those turbines.

The power curve constructed with the default parameters for the MM anemometer of Prettin-4 and Prettin-5 are represented by Figure 6.1 and Figure 6.2 respectively. The results of those power curves show that it is not perfect for this site, when applying the Markov's theory to the MM. In fact, there are some abrupt changes in those power curves, which confirm that perfection is not reached yet. The large scatter plot doesn't affect that much the Markov

power-curve. However, there is not enough data once the wind speed has reached the rated power. In fact, the IEC power curves are also not perfect, since there are some abrupt changes and they both stop close to 14 m/s. On a positive note, the powers obtained at the rated power give better results than the IEC ones. Moreover, there are only a couple of points on each of those power curves that aren't good. Other than that, the curves seem to follow a cubic function of the wind speed.

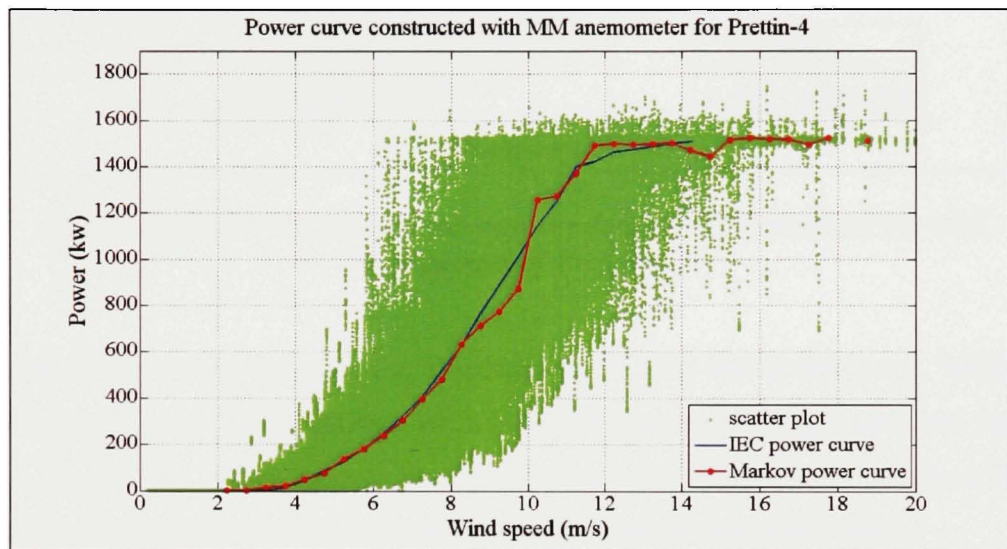


Figure 6.1 *Power curve obtained with the default parameters for the MM anemometer of Prettin-4.*

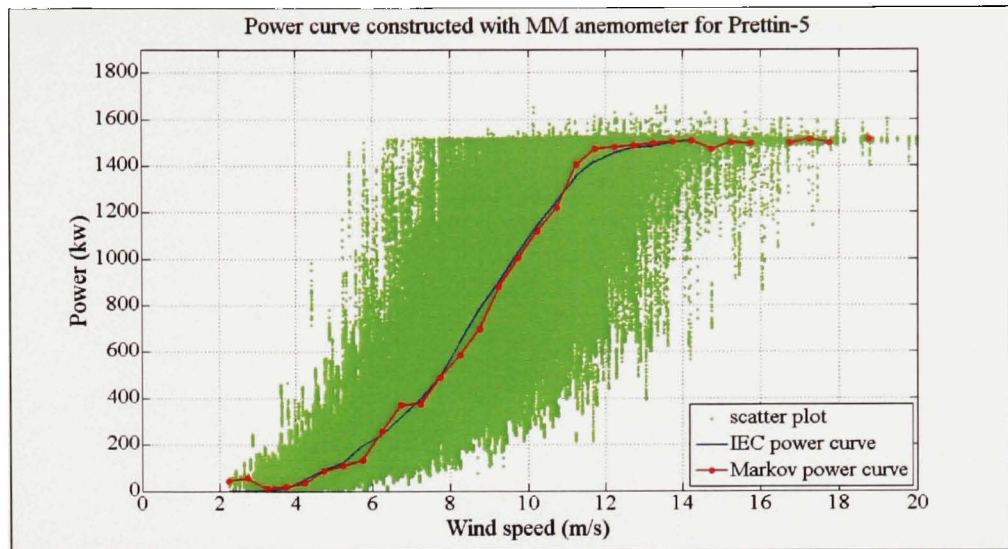


Figure 6.2 *Power curve obtained with the default parameters for the MM anemometer of Prettin-5.*

The MM power-curves obtained for Wietmarschen-1 and Wietmarschen-2, illustrated at Figure 6.3 and Figure 6.4 respectively are a little bit better than the ones obtained for Prettin turbines. In fact, the curves seem to be cubic before the rated power and sharp at the rated power. Nonetheless, like Prettin, there are two or three points that aren't good.

Like mentioned before, the height of the scatter plot is mainly due to the distance between the MM anemometer and the turbine. Therefore, the correlation between the power output of the turbine and the wind speed is greatly reduced. However, that doesn't seem to affect greatly the MM power-curve. The analysis with the nacelle anemometer might give better results, than the one made with the meteorological-mast anemometer.

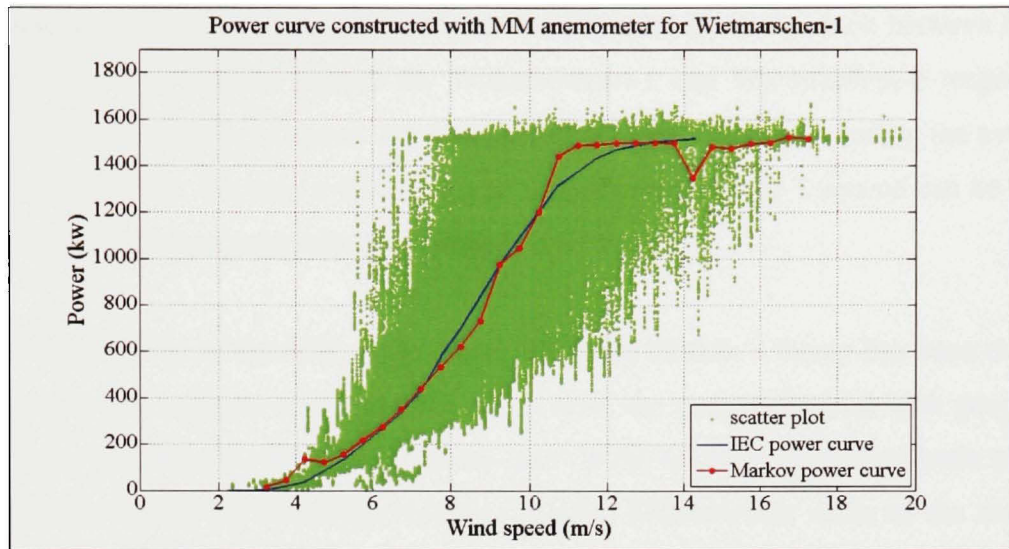


Figure 6.3 *Power curve obtained with the default parameters for the MM anemometer of Wietmarschen-1.*

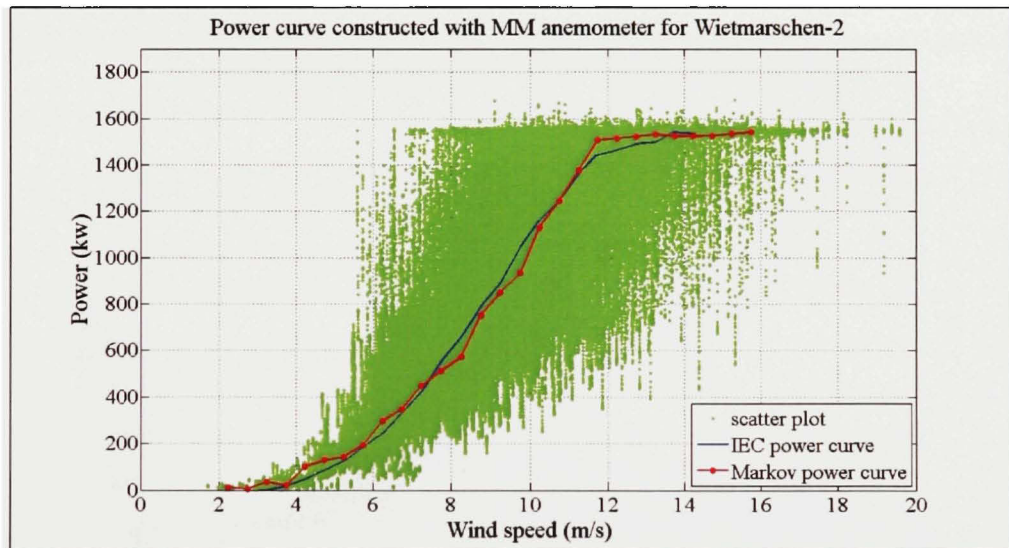


Figure 6.4 *Power curve obtained with the default parameters for the MM anemometer of Wietmarschen-2.*

Before moving to the verification with the nacelle anemometer for those two sites, we will compare the results obtained at different averaging time for Wietmarschen turbines. The previous analysis has proven that the averaging time shorter than 1 second had no influence on the power curve. Therefore, it will be appropriate to verify it with the MM anemometer of

Wietmarschen turbines. Figure 6.5 and Figure 6.6 illustrate the comparison between the data averaged at 1, 0,2 and 0,1 second for Wietmarschen-1 and Wietmarshen-2 respectively. Again, the results obtained confirm that there are little or no differences among the averaging times. Consequently, the data averaged at a period of time less than 1 second can be used to construct a MM power curve following Markov's theory.

Yet, the construction of the MM power curve following Markov's theory has been done and verified with five turbines and three sites. Until now, the results obtained look good at the rated power, even though there is large scatter plot for the Wietmarschen and Prettin turbines. That does prove that the turbulence intensity doesn't influence the value of the stochastic power calculated by Markov's theory, which is not the case with the IEC standard. However, the power curves aren't stable, since there are some points that are a little bit offset of a cubic curve.

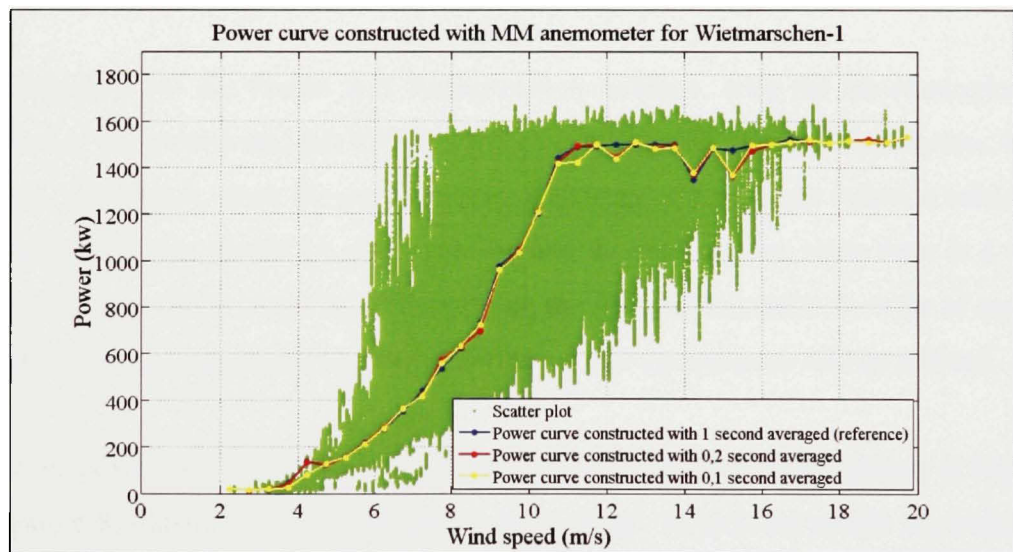


Figure 6.5 *Comparison of the time averaging for the power curve constructed for the MM anemometer of Wietmarschen-1.*

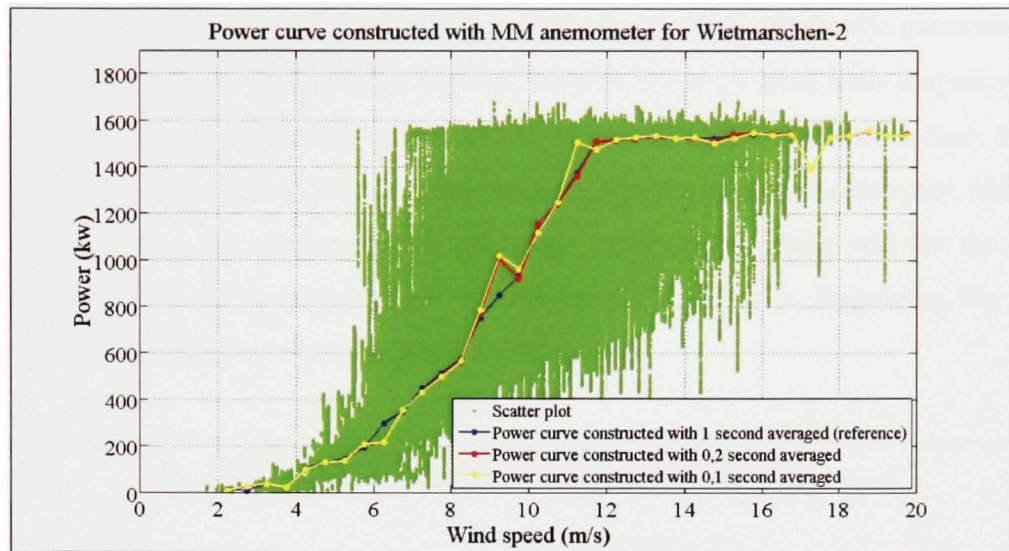


Figure 6.6 *Comparison of the time averaging for the power curve constructed for the MM anemometer of Wietmarschen-2.*

6.2 Nacelle anemometer

The verification for the Prettin and Wietmarschen turbines, with the meteorological-mast anemometer, has proven that this new method gives acceptable results. Nevertheless, it is not stable yet, nor perfect, since the power curves obtained don't perfectly follow a cubic curve. This verification also should be done with the nacelle anemometer, since there is a transfer function, and the results might be different than the MM anemometer. In order to make this verification, the default parameters found for the nacelle anemometer will be utilised.

The nacelle power-curve of Prettin-4 and Prettin-5 turbines, shown respectively at Figure 6.7 and Figure 6.8, illustrate that it does have a great shape. In fact, the results are better when the power curve is constructed with the nacelle anemometer than with the meteorological-mast anemometer. Furthermore, it is the same thing for the nacelle power-curve of Wietmarschen-1 and Wietmarschen-2 turbines (Figure 6.9 and Figure 6.10). However, the nacelle power-curve for Prettin-4 turbine has some points offset of the cubic curve, which confirm that the results are still not stable.

The reason why the behaviour of the power curve is better with the nacelle anemometer for these two sites might be because the turbines are too far away from their respective MM. Thus, the correlation between the power of the turbine and the wind speed, from the MM anemometer, is a little bit lost, which is not the case with the nacelle anemometer. Moreover, it is also caused by the power curves not being stable for the MM and for the nacelle anemometer, which might lead to some random results. Therefore, improving the power-curve software will lead to better and more stable results.

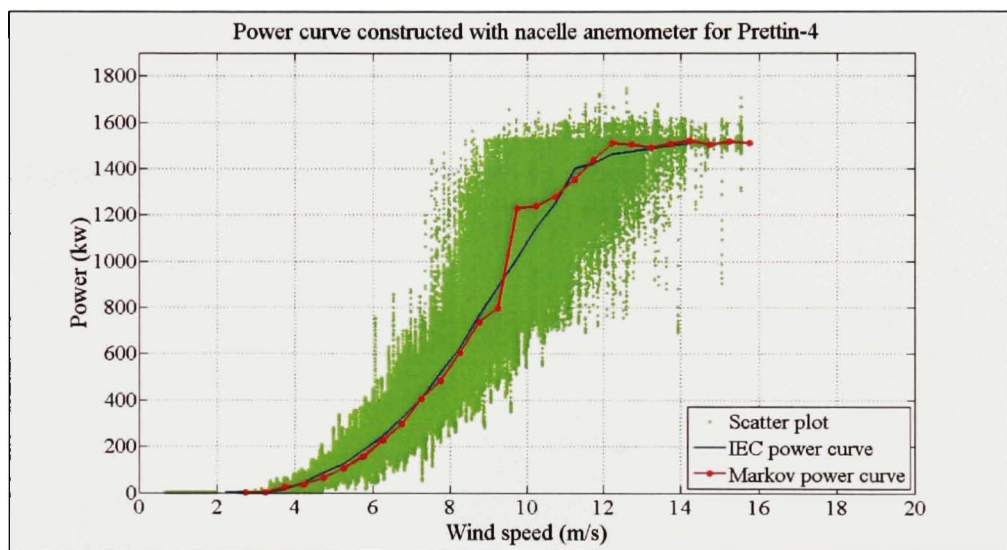


Figure 6.7 *Power curve obtained with the default parameters for the nacelle anemometer of Prettin-4.*

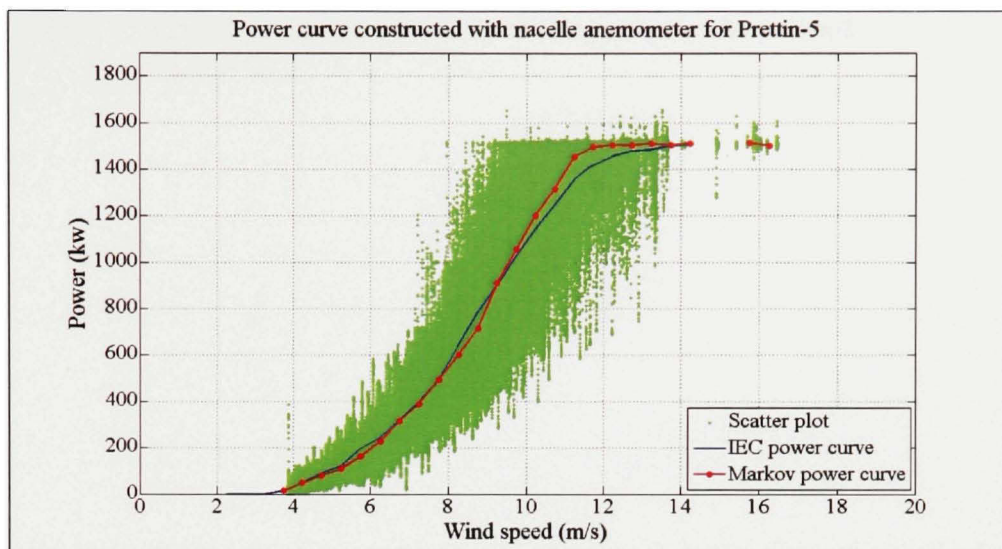


Figure 6.8 *Power curve obtained with the default parameters for the nacelle anemometer of Prettin-5.*

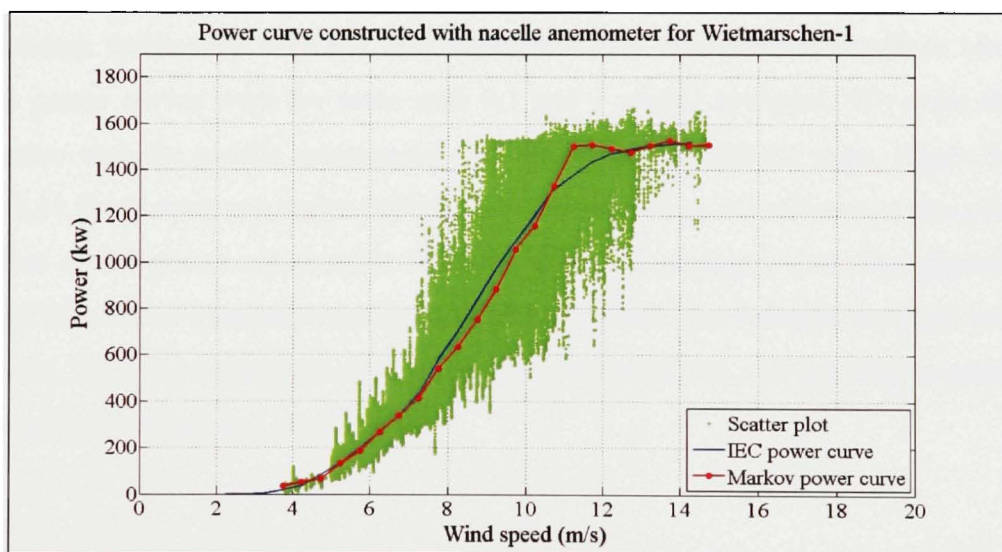


Figure 6.9 *Power curve obtained with the default parameters for the nacelle anemometer of Wietmarschen-1.*

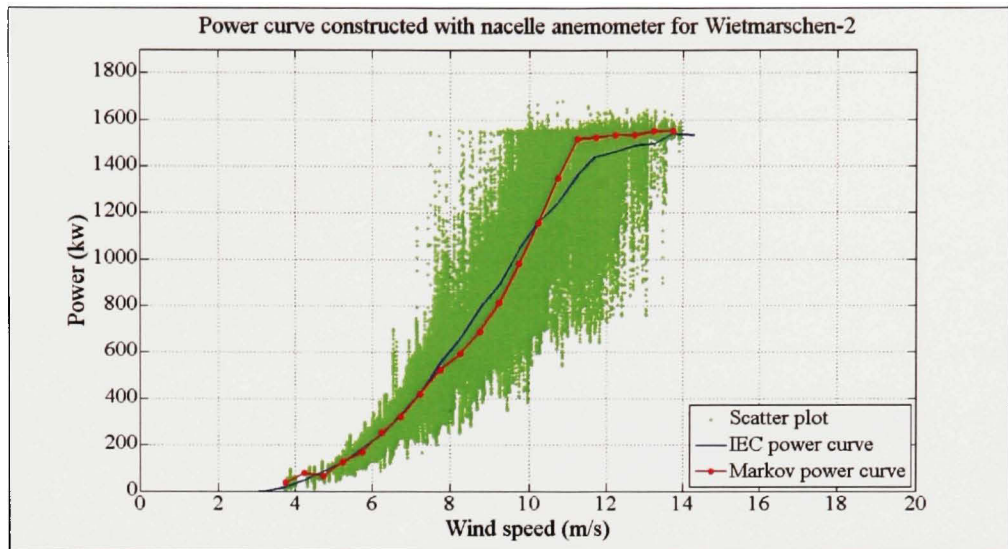


Figure 6.10 *Power curve obtained with the default parameters for the nacelle anemometer of Wietmarschen-2.*

The previous verification with the MM anemometer of Wietmarschen turbines has shown that the power curves were the same with 0,1 and 1 second averaged. We made the same verification with the nacelle anemometer and the results are still the same. Figure 6.11 and Figure 6.12 don't show any major differences. However, there are still one or two points that are offset of the power curve made with the 1 second averaged data. But generally, the averaged time under 1 second is good, and looking towards this direction in future work isn't a bad idea, since the acquisition time of the data might reduce, and therefore a good power curve would be created in a shorter time.

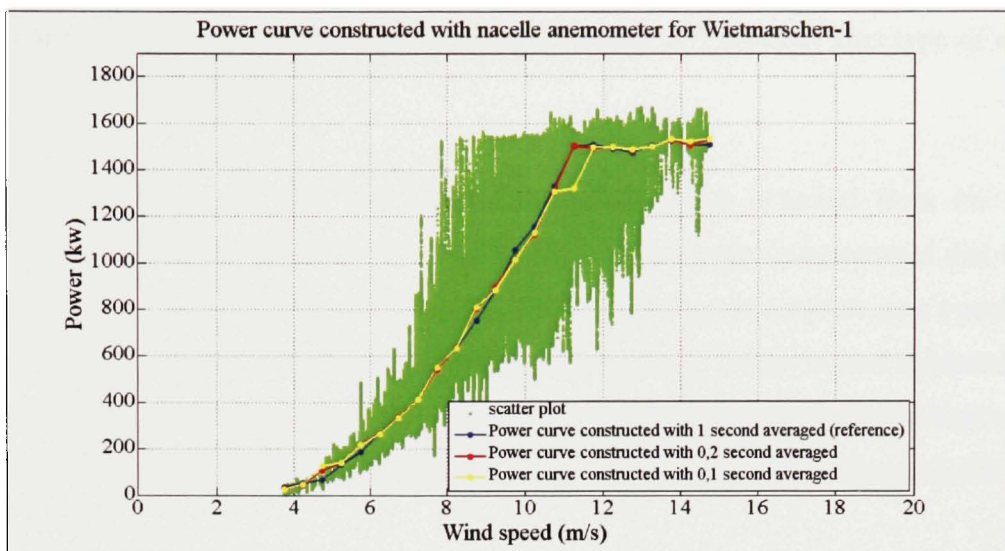


Figure 6.11 *Comparison of the time averaging for the power curve constructed for the nacelle anemometer of Wietmarschen-1.*

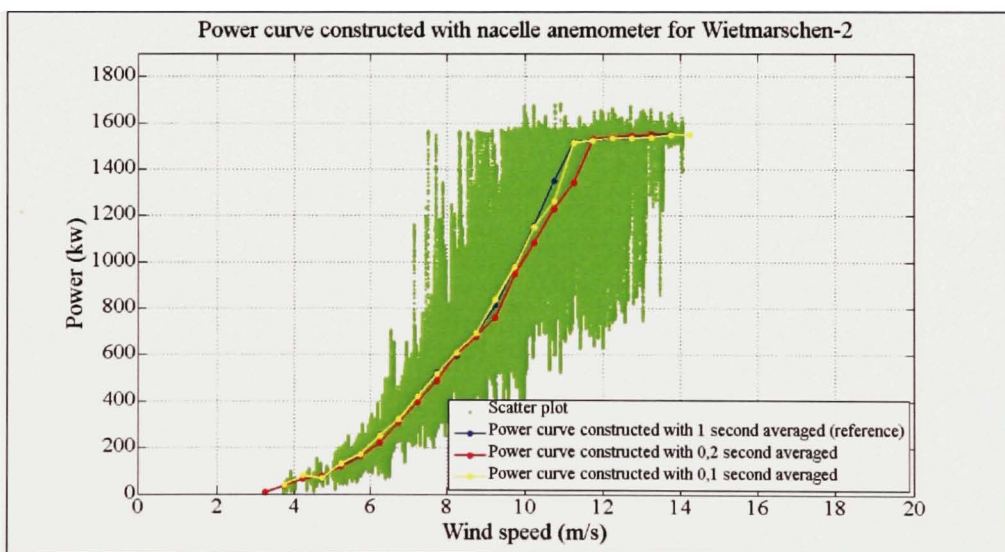


Figure 6.12 *Comparison of the time averaging for the power curve constructed for the nacelle anemometer of Wietmarschen-2.*

Overall, constructing a power curve with the data averaged on a shorter time than 1 second gives the same results as the power curve constructed with the data averaged at 1 second. Indeed, this fact has been verified with Klondike-10 and with Wietmarschen turbines. Therefore, it might be advantageous to utilise the data averaged at 0,1 second, since they

might require less time to collect than the data averaged at 1 second. This type of analysis will be done in the Chapter 7.

Furthermore, this section also has verified the power curve obtained from the nacelle anemometer with Wietmarschen and Prettin turbines. It has been demonstrated that it gives good results with the default parameters. Nonetheless, those power curves aren't perfect nor stable and can not be utilised as a new standard yet. This thesis brings a great enhancement of what was done before, but more improvements need to be done before considering utilising this novel method and this software to construct a power curve as a reference procedure.

CHAPTER 7

TIME REQUIRED TO CONSTRUCT A NACELLE POWER-CURVE FOLLOWING MARKOV'S THEORY

The main goals of this thesis are to save money by diminishing the recording time of the data, to avoid seasonal fluctuation when analysing the effect of different settings, and to construct a more accurate power curve. In order to do that, we need to analyse the minimal number of data required to construct a good power curve. This total amount of data is directly proportional to the minimal number of data per bin speed. Therefore, the analysis of the minimal number of data per bin speed is done for all five turbines. However, this analysis, for the data averaged on shorter period than 1 second, can't be done for Prettin turbines.

In order to do that, we first should take the stationary power obtained with all the data at a certain bin speed and on a certain turbine. Then, we must calculate that power with different numbers of data and evaluate the error between those stationary powers and the stationary power found with all the data. These errors are expressed in percentage, since the difference of powers will inevitably be less important at lower wind speed, while it will be more important at higher wind speed. Afterwards, it will be possible to illustrate them on a graphic, and then deducing the minimal number of data required, with an asymptote close to zero percent.

First, the analysis has been done with the data averaged at 1 second with the nacelle anemometer. Thus, all 5 turbines of the three wind sites were analysed. The APPENDIX II contains the tables of the power error in function of the number of data for the data averaged at 1 second with different wind turbines. With those tables, the graphic at Figure 7.1 was constructed. This graphic shows the asymptote starting close to 4000 seconds. Indeed, all the power errors are under 5 % over this value. Consequently, the minimal time required to find

the stationary power inside a certain bin speed is 4000 seconds, with the data averaged at 1 second, which is a little bit over than one hour.

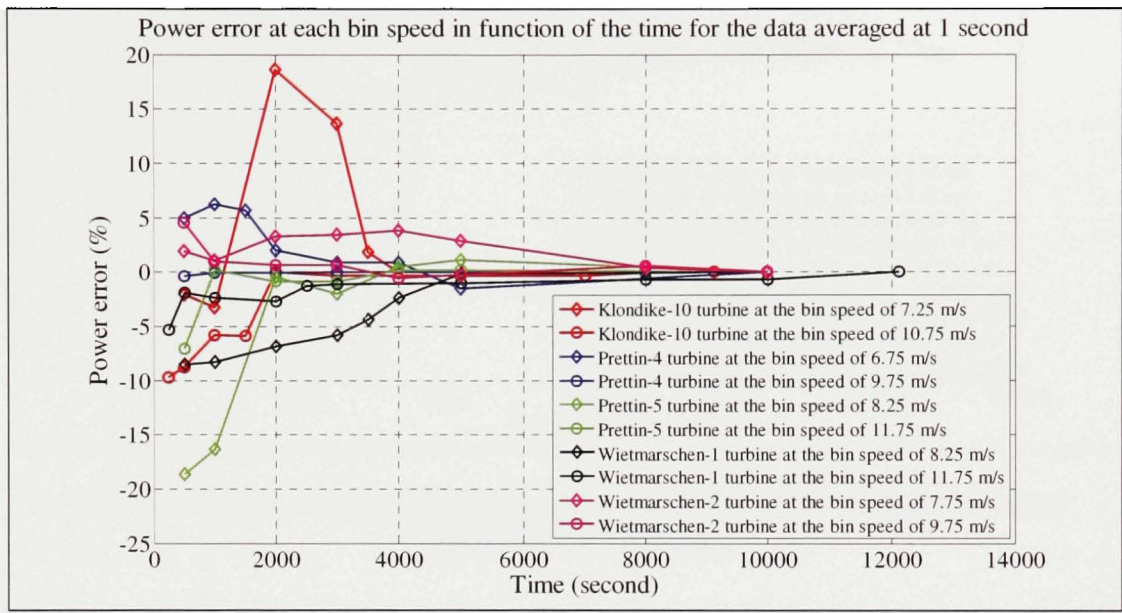


Figure 7.1 *Power error at each bin speed in function of the time for the data averaged at 1 second.*

Then, the same analysis has been done for the data averaged at 0,1 second. The tables which contain the results are found in the APPENDIX III. Then, Figure 7.2 was created with the values obtained in those tables. In opposition to what was expected, the minimal time required to obtain the stationary power inside a certain bin speed, for data averaged at 0,1 second, is the same than for data averaged at 1 second. In fact, the asymptote found at Figure 7.2, albeit less clear, starts at 4000 seconds, which is again over 1 hour. The averaged time is 10 time shorter, but the number of data to construct a good power curve has decupled. Thus, the acquisition times to collect data are the same, however the results are more trustful with the data averaged at 1 second because the error decrease further than 4000 seconds, which is not the case with the data averaged at 0,1 second.

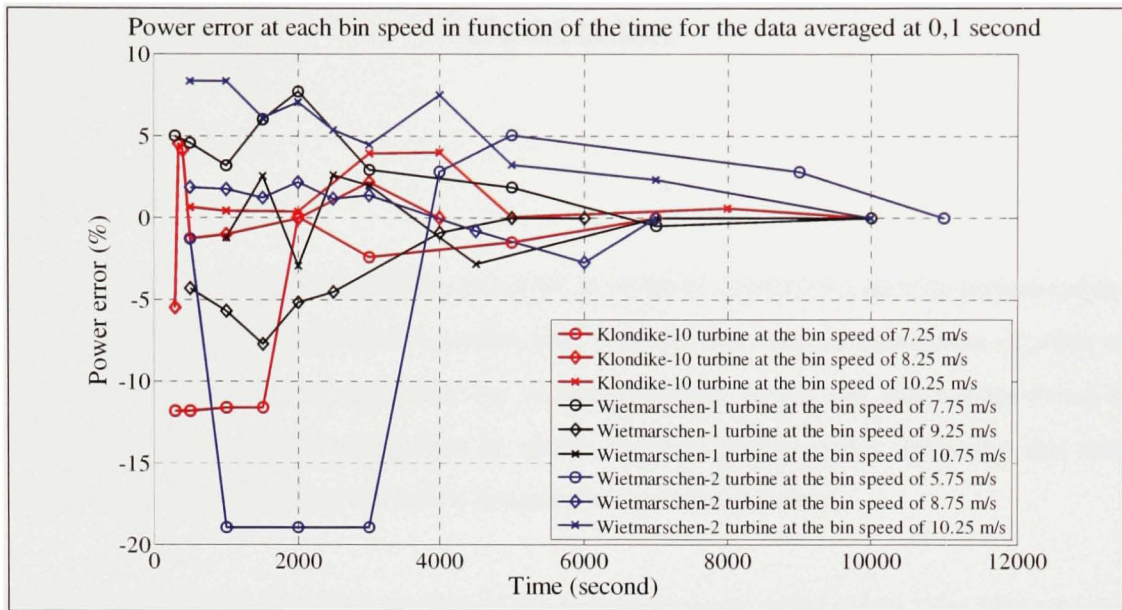


Figure 7.2 *Power error at each bin speed in function of the time for the data averaged at 0,1 second.*

The minimal time required to determine the stationary power inside a certain bin speed, obtained for the data averaged at 0,1 and 1 second, is a little bit more than 1 hour. The IEC standard stipulates that it requires at least 30 minutes per bin speed in order to get the correct power. However, below the rated power this value is absolutely not enough because of the large scatter plot. Therefore, if 20 points is enough below the rated power with the IEC standard, it means that it will require 200 minutes to calculate the accurate power per bin speed. Consequently, in that case, the construction of the nacelle power-curve following Markov's theory is little bit more than 3 times faster than the standard procedure. Nevertheless, the Markov power-curves aren't stable yet, since it doesn't follow a perfect cubic curve. More improvements should be done to improve the parameters of this novel method, and then stabilize the results. Once it will be stabilized, the speed at which a power curve can be reached with Markov's theory will surely increase again.

CONCLUSION

Thesis review

This work has permitted to develop a program in order to construct a nacelle power-curve in a more accurate method. Albeit the results aren't stable, this is an improvement of what was realised before in this field, especially for General Electric. Moreover, this master thesis has also evaluated the optimal parameters to obtain the best power curve following this novel method. A résumé of each of the seven chapters are presented below.

Chapter 1 presented a literature review of the previous works in this field. The IEC standard, along with their flaws, has been explained. In addition, the works of different contributors, concerning the construction of a power curve following a stochastic approach, have been described.

Chapter 2 demonstrated a mathematical model to construct a power curve following the Markov's theory. The method to determine different coefficients and parameters also has been exposed.

Chapter 3 introduced the turbines and the wind farms analysed in this thesis. Consequently, the location, the operating data and the limitation of those turbines have been presented.

Chapter 4 identified the influence of each parameter to construct a Markov power-curve with the MM anemometer. The results of those analysis lead to construct a power curve with the following parameters:

- a power-state range filter set at 15%;
- the median to calculate the conditional moment;
- eight power states to calculate the stationary power at each bin speed;
- the minimal potential to calculate the stationary power;

- the relaxation time between 5 and 15 seconds to calculate the drift coefficient;
- the bins speed set at 0,5 m/s;
- the wind speed averaged over a period of 30 seconds;
- the data averaged at 1 second or less.

Chapter 5 determined the best parameters to construct a Markov power-curve, but this time with the nacelle anemometer. The results demonstrated that the only different parameter from the MM anemometer is the period of time to average the wind speed. Indeed, the best period of time found to average the wind speed with the nacelle anemometer is two minutes.

Chapter 6 verified the power curve obtained with the default parameters for Wietmarschen and Prettin turbines, and this for the data averaged at 0,1 and 1 second. The results found prove that the power curves constructed with this novel method are good, but aren't stable yet. Therefore, more improvements in the Markov power-curve program need to be done in order to obtain perfect and stable results.

Chapter 7 analysed the minimal amount of data required per bin speed to construct a nacelle power-curve following Markov's theory. The results obtained demonstrate that the Markov power-curves require less time than the IEC procedure for the data averaged at 0,1 and 1 second. In fact, it requires a little bit more than an hour to calculate the power inside a certain bin speed for the Markov's theory, while most of the time it requires at least 200 minutes with the IEC standard. Moreover, by improving and stabilizing the power curve, the speed to construct a Markov power-curve will increase, and thus become more interesting to apply it to the IEC standard.

Contribution

The overall contribution of this master project is the development of a program, which can construct a MM or a nacelle power-curve by following the Markov's theory. This method is a stochastic one, and eventually might lead to a more precise power curve in a shorter time.

Furthermore, this thesis also analysed different parameters in order to obtain the best power curve from the MM and the nacelle anemometer. Finally, the evaluation of the minimal amount of time required to construct a Markov power-curve has been tested and analysed.

RECOMMENDATIONS

The recommendations for future efforts to invest in the continuance of this work mainly concern the improvement of the Markov power-curve software. In order to do that, some points are required to be investigated.

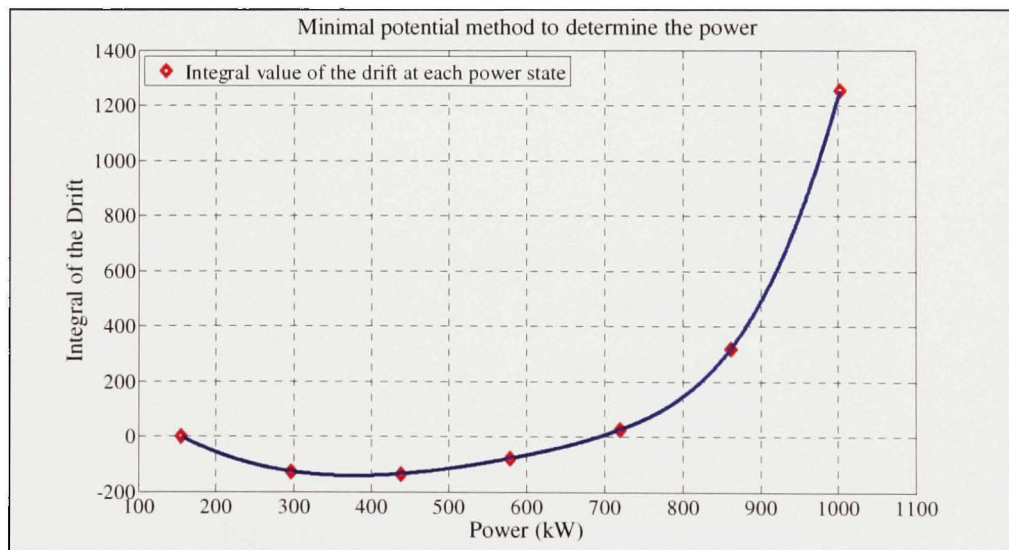
The first recommendation is to utilise more data set to analyse the rotor-position filter, when using the nacelle anemometer to calculate the Markov power-curve. Then, it will be possible to determine if this filter gives better results or not.

The second recommendation is based when the Markov power-curve is constructed with the meteorological-mast anemometer. In that case, it is important that the MM is not too far away from the turbine, otherwise the correlation between the MM wind speed and the power output might be lost, since the stochastic powers have more chance to be in the wrong bin speed. Thus, in respecting the distances recommended by the IEC standard, and in averaging the wind speed over a certain period of time, the MM power curves should give good results, even though they aren't stable yet.

The final recommendation is based on the second minimum problem, when calculating the stationary power with the minimal potential. A method should be found to pass through this problem and to have more constancy when calculating the stationary power. One way to perhaps solve this dilemma might be in the values of the relaxation time to calculate the drift. Indeed, this thesis utilised only a relaxation time constant between 5 and 15 seconds. Further improvements need to be done on this relaxation time, since it might also depend of parameters like the wind speed, the algorithm of the turbine, the blade angle, the measurement system or the value of the turbulent intensity.

An experiment has been executed in order to help future searchers to understand the investigation concerning the relaxation time. Mainly, this test takes the best linear regression in the graphic of the moment in function of the relaxation time, but this time with other

interval than the one between 5 and 15 seconds. If we go back to the power curve obtained at Figure 4.3, it shows that the power at 6,25 m/s isn't correct. For all power state of this bin speed, the best regressions are found in the plots of the conditional moment in function of the relaxation time, which are presented in APPENDIX IV. For five of those seven graphics the interval between 5 and 15 seconds was correct. Nevertheless, for the two others graphics, at power state of 579 and 720 kW, it wasn't the optimal interval, and therefore it has been corrected. We also remember that the drift is the slope of this linear regression. Thus, a new graphic of the integral of the drift in function of the power for this bin speed was constructed, which is in fact the same graphic like the one shown at Figure 4.5, but this time with the interval of the linear regression corrected, and the results are definitively better. Figure below shows that the minimal potential is reached at 377 kW, instead of 650 kW. According to the graphic at Figure 4.3, it is a better approximation of the power at the bin speed of 6,25 m/s.



Corrected power in function of the integral of the drift at the bin speed of 6,25 m/s.

However, this test wasn't done for an entire power curve but demonstrates that it can be possible to reach a great stochastic power at a certain bin speed by modifying the interval of the relaxation time at some power states. Like mentioned before, more investigation on that problem should be done, and once solved a perfect Markov power-curve, constructed in a short time, might be possible to reach.

APPENDIX I

FLOW CHART: SOFTWARE TO CONSTRUCT THE STATIONARY POWER CURVE

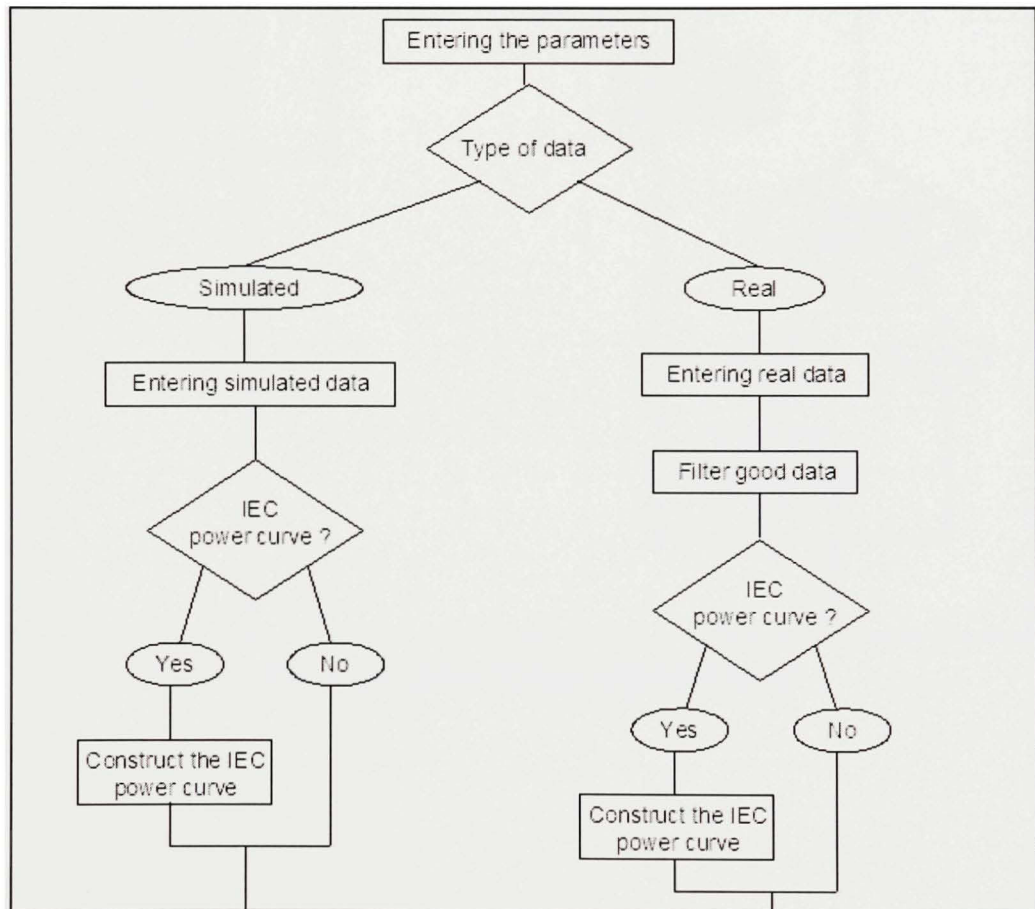
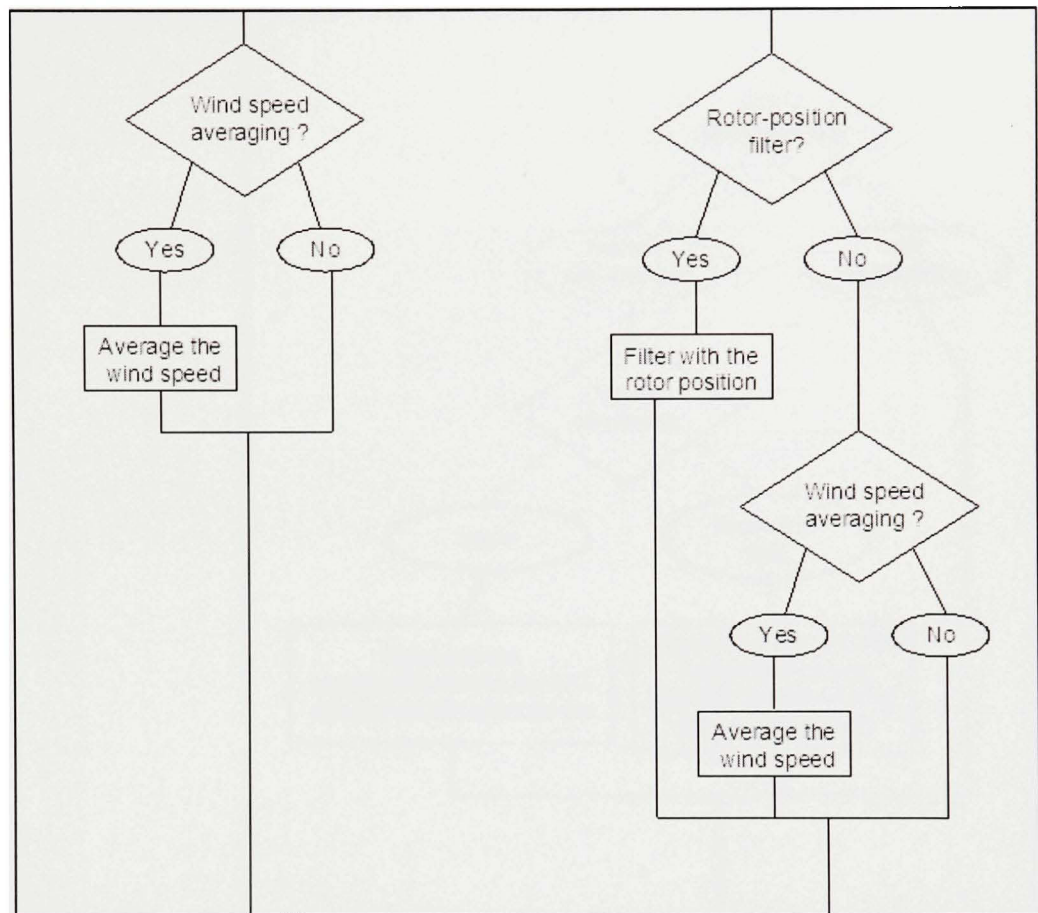
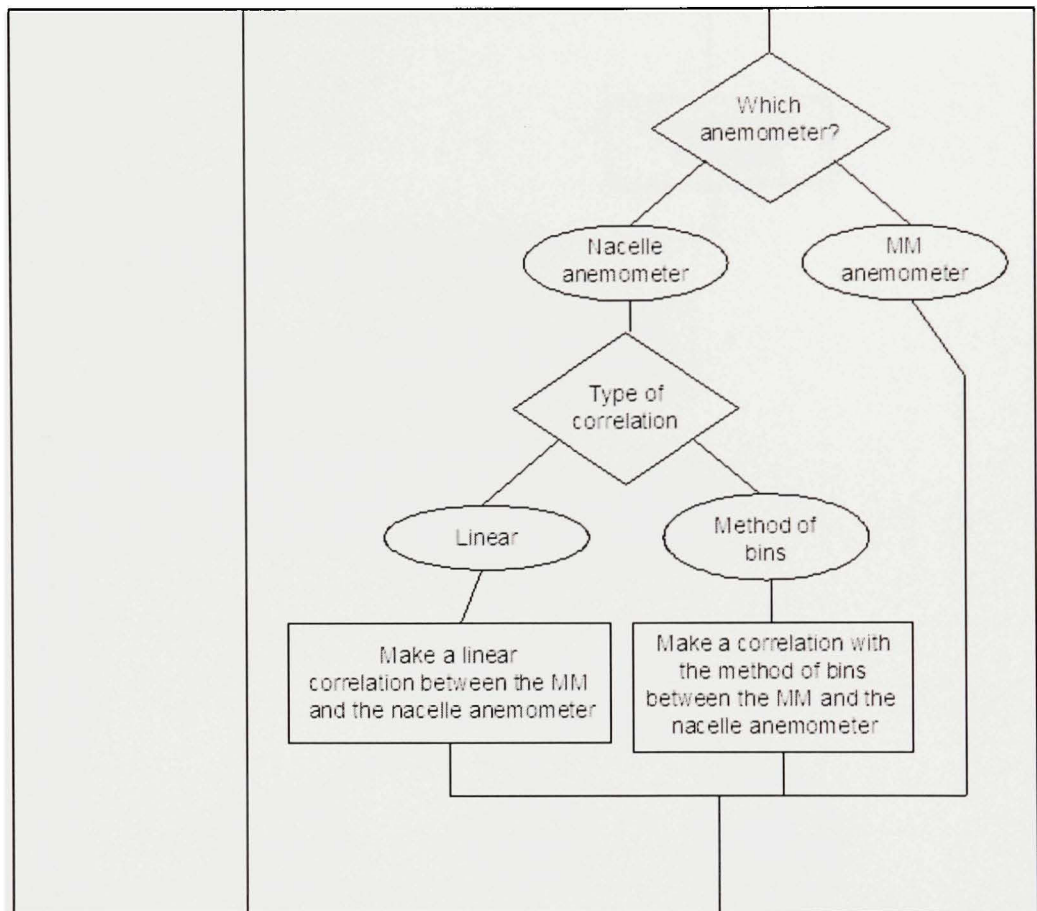


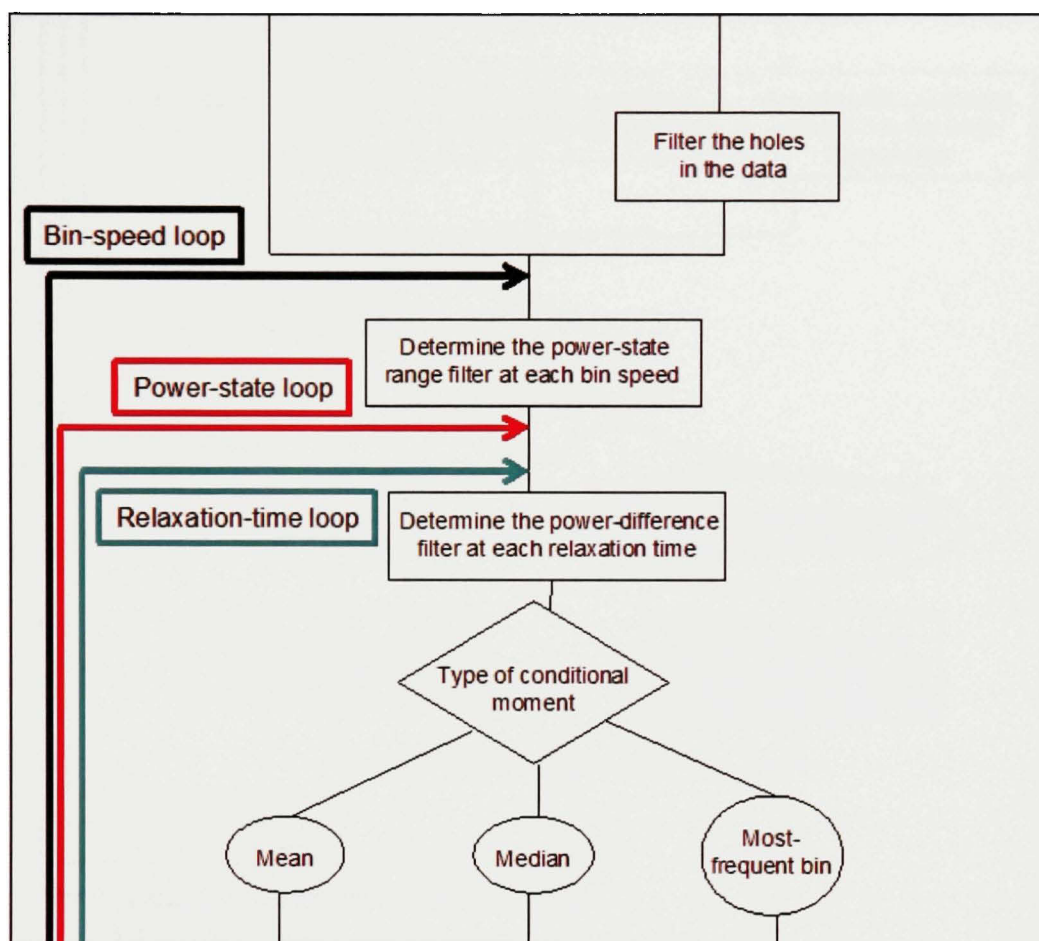
Figure I.1 *Flowchart of the Markov software*



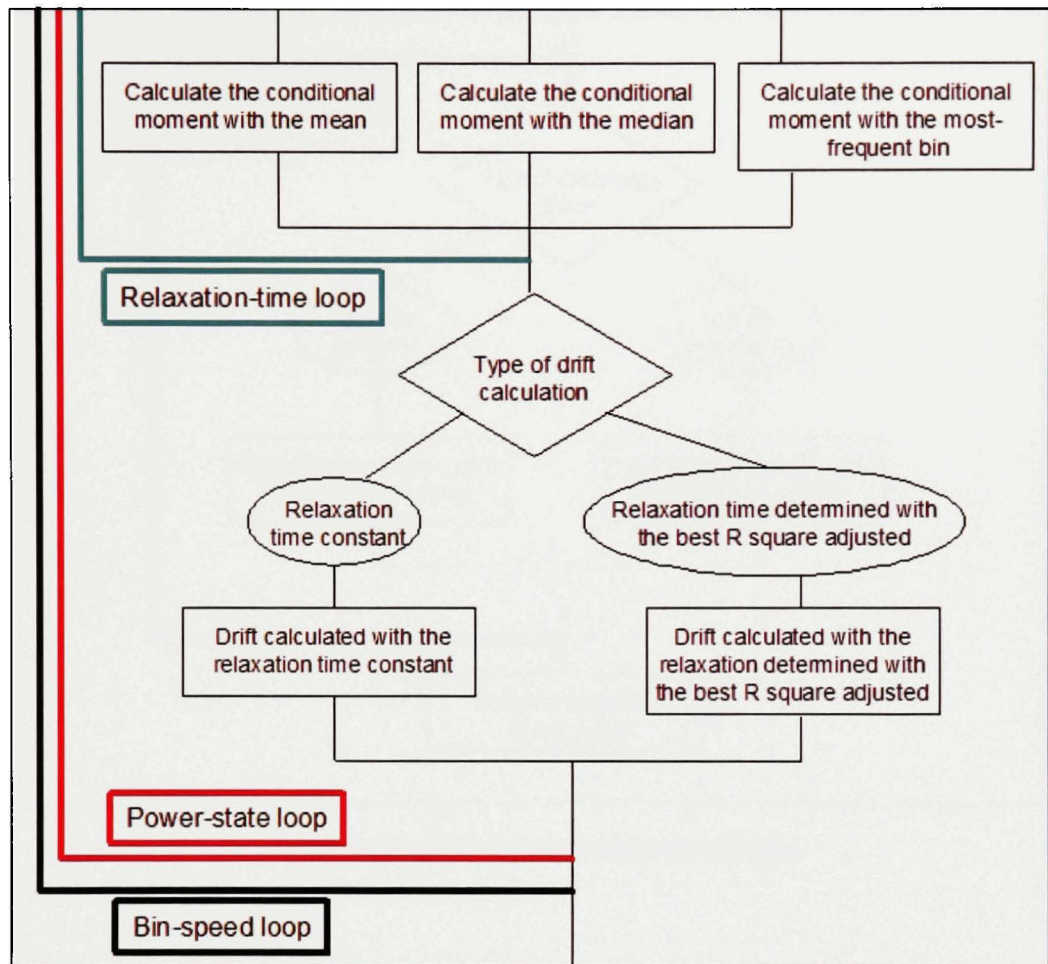
Flowchart of the Markov software (cont.)



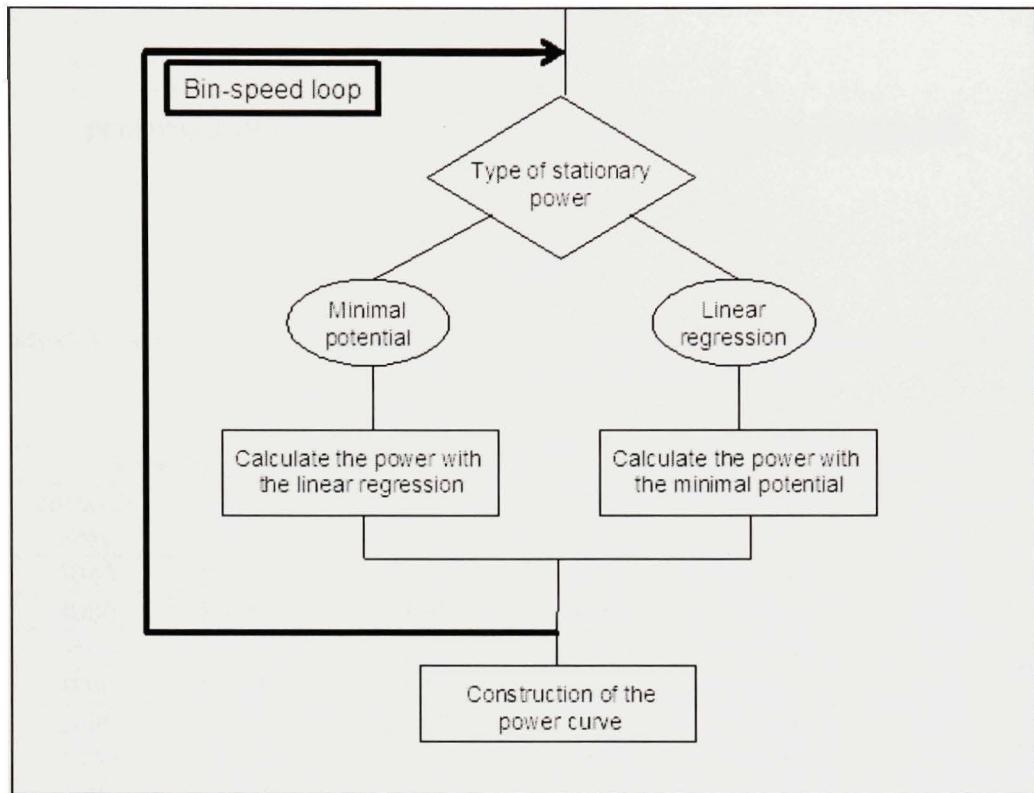
Flowchart of the Markov software (cont.)



Flowchart of the Markov software (cont.)



Flowchart of the Markov software (cont.)



Flowchart of the Markov software (cont.)

APPENDIX II

POWER ERROR FOR THE DATA AVERAGED AT 1 SECOND

Table II.1

Stationary power output in function of the number of data per bin speed, with the data averaged at 1 second for the Klondike-10 turbine

Klondike-10 at 7,25 m/s			Klondike-10 at 10,75 m/s		
Number data	Power (kW)	Power error (%)	Number data	Power (kW)	Power error (%)
5040	601,02	0,00	9118	1538,40	0,00
4000	600,97	-0,01	8000	1536,80	-0,10
3500	612,02	1,83	7000	1533,90	-0,29
3000	682,85	13,62	5000	1533,60	-0,31
2000	712,95	18,62	3000	1533,90	-0,29
1000	581,60	-3,23	2000	1538,30	-0,01
500	588,84	-2,03	1500	1448,30	-5,86
			1000	1449,00	-5,81
			500	1403,40	-8,78
			250	1388,70	-9,73

Table II.2

Stationary power output in function of the number of data per bin speed, with the data averaged at 1 second for the Wietmarschen-1 turbine

Wietmarschen-1 at 11,75 m/s			Wietmarschen-1 at 8,25 m/s		
Number data	Power (kW)	Power error (%)	Number data	Power (kW)	Power error (%)
12120	1508,50	0,00	10000	635,83	0,00
10000	1498,20	-0,68	5000	634,93	-0,14
8000	1497,80	-0,71	4000	620,80	-2,36
5000	1492,60	-1,05	3500	608,09	-4,36
3000	1492,40	-1,07	3000	598,86	-5,81
2500	1489,80	-1,24	2000	592,48	-6,82
2000	1468,20	-2,67	1000	583,18	-8,28
1000	1472,20	-2,41	500	581,61	-8,53
500	1479,60	-1,92			
250	1428,60	-5,30			

Table II.3

Stationary power output in function of the number of data per bin speed, with the data averaged at 1 second for the Wietmarschen-2 turbine

Wietmarschen-2 at 9,75 m/s			Wietmarschen-2 at 7,75 m/s		
Number data	Power (kW)	Power error (%)	Number data	Power (kW)	Power error (%)
10000	1010,90	0,00	10000	544,67	0,00
8000	1016,70	0,57	8000	546,80	0,39
5000	1008,50	-0,24	5000	560,36	2,88
4000	1005,70	-0,51	4000	565,74	3,87
3000	1017,50	0,65	3000	563,64	3,48
2000	1017,70	0,67	2000	562,43	3,26
1000	1021,10	1,01	1000	550,40	1,05
500	1057,10	4,57	500	555,02	1,90

Table II.4

Stationary power output in function of the number of data per bin speed, with the data averaged at 1 second for the Prettin-4 turbine

Prettin-4 at 6,75 m/s			Prettin-4 at 9,75 m/s		
Number data	Power (kW)	Power error (%)	Number data	Power (kW)	Power error (%)
10000	275,20	0,00	10000	1277,70	0,00
5000	271,01	-1,52	8000	1277,70	0,00
4000	277,68	0,90	3000	1277,70	0,00
3000	277,74	0,92	2000	1276,70	-0,08
2000	280,68	1,99	1000	1276,90	-0,06
1500	290,80	5,67	500	1272,60	-0,40
1000	292,44	6,26			
500	288,80	4,94			

Table II.5

Stationary power output in function of the number of data per bin speed, with the data averaged at 1 second for the Prettin-5 turbine

Prettin-5 at 8,25 m/s			Prettin-5 at 11,75 m/s		
Number data	Power (kW)	Power error (%)	Number data	Power (kW)	Power error (%)
10000	602,13	0,00	10000	1495,90	0,00
5000	608,79	1,11	5000	1498,90	0,20
4000	605,15	0,50	4000	1498,90	0,20
3000	590,34	-1,96	3000	1483,00	-0,86
2000	599,28	-0,47	2000	1483,40	-0,84
1000	503,54	-16,37	1000	1499,10	0,21
500	489,69	-18,67	500	1389,90	-7,09

APPENDIX III

POWER ERROR FOR THE DATA AVERAGED AT 0,1 SECOND

Table III.1

Stationary power output in function of the number of data per bin speed, with the data averaged at 0,1 second for the Klondike-10 turbine

Klondike-10 at 7,25 m/s			Klondike-10 at 8,25 m/s		
Number data	Power (kW)	Power error (%)	Number data	Power (kW)	Power error (%)
70000	595,05	0,00	40000	881,53	0,00
50000	585,93	-1,53	30000	900,46	2,15
30000	580,63	-2,42	20000	880,75	-0,09
20000	595,12	0,01	10000	872,35	-1,04
15000	525,85	-11,63	5000	869,88	-1,32
10000	525,82	-11,63	4000	918,06	4,14
5000	524,45	-11,86	3500	921,05	4,48
3000	524,45	-11,86	3000	833,16	-5,49

Stationary power output in function of the number of data per bin speed, with the data averaged at 0,1 second for the Klondike-10 turbine (cont.)

Klondike-10 at 10,25 m/s		
Number data	Power (kW)	Power error (%)
100000	1416,6	0,00
80000	1424,3	0,54
50000	1417,3	0,05
40000	1472,40	3,94
30000	1471,90	3,90
20000	1421,80	0,37
10000	1422,30	0,40
5000	1425,30	0,61

Table III.2

Stationary power output in function of the number of data per bin speed, with the data averaged at 0,1 second for the Wietmarschen-1 turbine

Wietmarschen-1 at 7,75 m/s			Wietmarschen-1 at 9,25 m/s		
Number data	Power (kW)	Power error (%)	Number data	Power (kW)	Power error (%)
100000	551,54	0,00	60000	886,38	0,00
70000	548,69	-0,52	50000	886,33	-0,01
50000	561,50	1,81	40000	877,93	-0,95
30000	567,43	2,88	25000	846,25	-4,53
20000	593,80	7,66	20000	840,27	-5,20
15000	584,41	5,96	15000	817,85	-7,73
10000	568,89	3,15	10000	835,70	-5,72
5000	576,68	4,56	5000	847,72	-4,36
3000	579,14	5,00			

Stationary power output in function of the number of data per bin speed, with the data averaged at 0,1 second for the Wietmarschen-2 turbine (cont.)

Wietmarschen-1 at 10,75 m/s		
Number data	Power (kW)	Power error (%)
100000	1266,70	0,00
70000	1266,30	-0,03
45000	1230,70	-2,84
30000	1291,00	1,92
25000	1299,60	2,60
20000	1229,20	-2,96
15000	1299,00	2,55
10000	1250,80	-1,26

Table III.3

Stationary power output in function of the number of data per bin speed, with the data averaged at 0,1 second for the Wietmarschen-2 turbine

Wietmarschen-2 at 5,75 m/s			Wietmarschen-2 at 8,75 m/s		
Number data	Power (kW)	Power error (%)	Number data	Power (kW)	Power error (%)
110000	167,53	0,00	70000	690,89	0,00
90000	172,21	2,79	60000	672,03	-2,73
50000	175,92	5,01	45000	685,18	-0,83
40000	172,21	2,79	30000	700,14	1,34
30000	135,76	-18,96	25000	698,61	1,12
20000	135,76	-18,96	20000	705,79	2,16
10000	135,77	-18,96	15000	699,10	1,19
5000	165,34	-1,31	10000	702,76	1,72
			5000	703,39	1,81

Stationary power output in function of the number of data per bin speed, with the data averaged at 0,1 second for the Wietmarschen-2 turbine (cont.)

Wietmarschen-2 at 10,25 m/s		
Number data	Power (kW)	Power error (%)
100000	1155,8	0,00
70000	1182,4	2,30
50000	1193,00	3,22
40000	1242,50	7,50
30000	1207,00	4,43
25000	1217,90	5,37
20000	1237,40	7,06
15000	1226,40	6,11
10000	1251,9	8,31
5000	1252,3	8,35

APPENDIX IV

CONDITIONAL MOMENT IN FUNCTION OF THE RELAXATION TIME

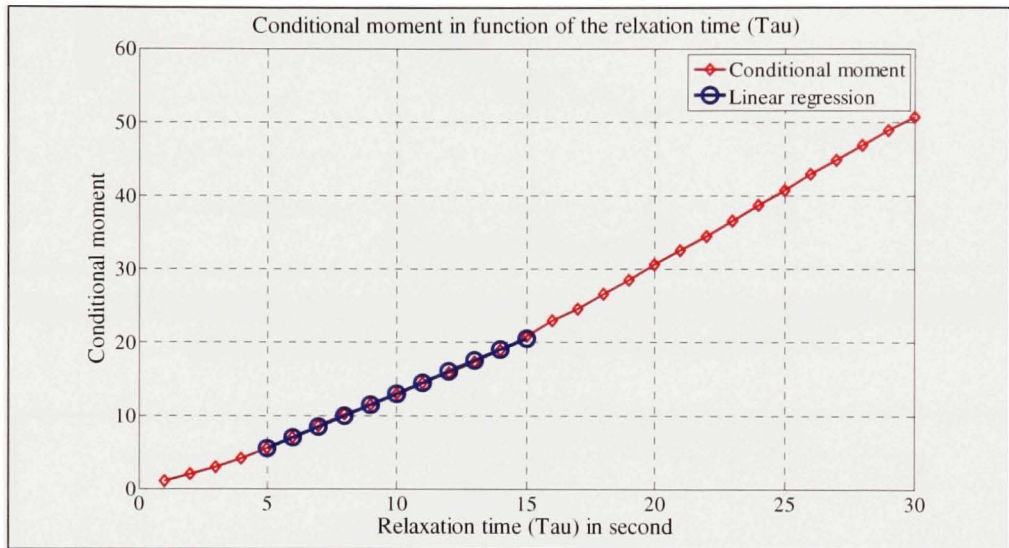


Figure IV.1 *Conditional moment in function of the relaxation time at the bin speed of 6,25 m/s and at the power state of 156 kW.*

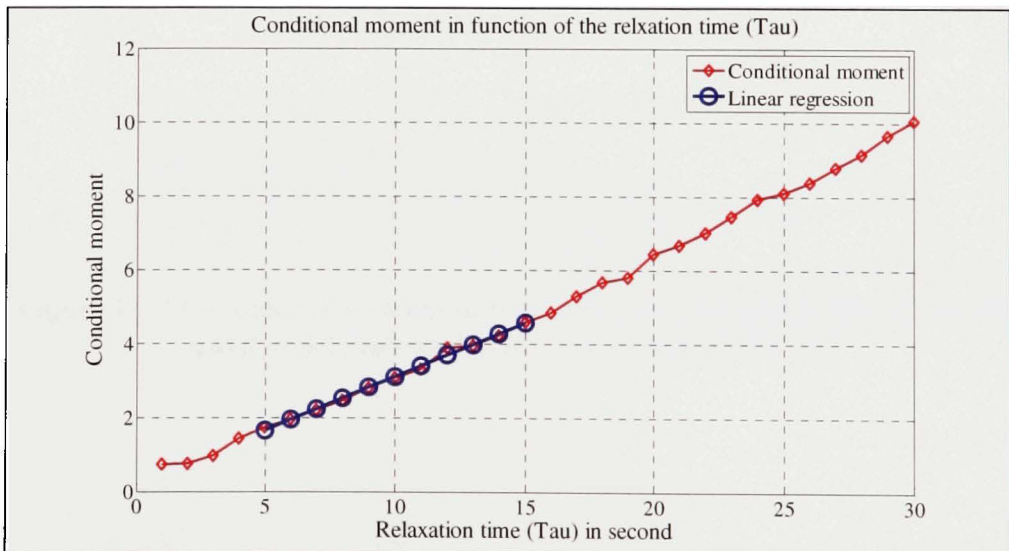


Figure IV.2 *Conditional moment in function of the relaxation time at the bin speed of 6,25 m/s and at the power state of 297 kW.*

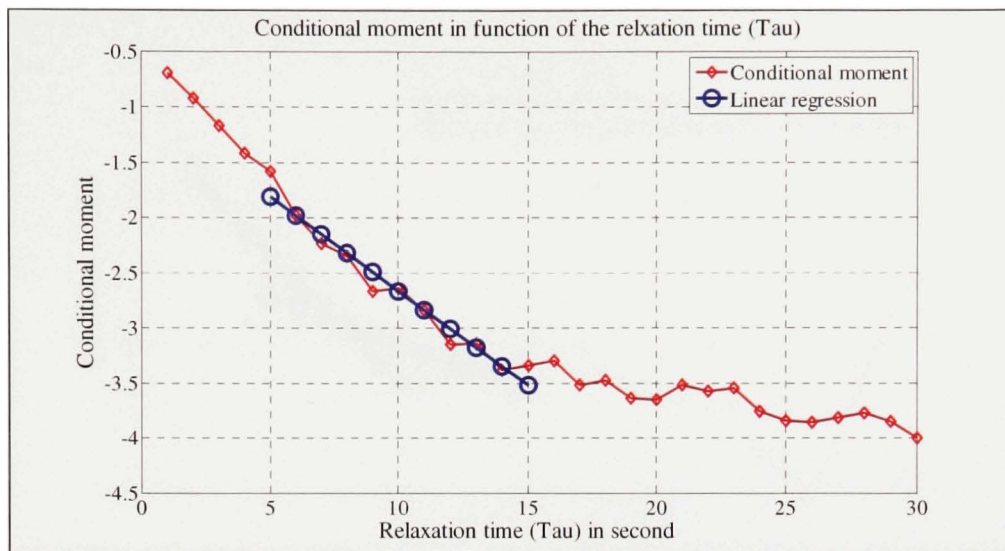


Figure IV.3 *Conditional moment in function of the relaxation time at the bin speed of 6,25 m/s and at the power state of 438 kW.*

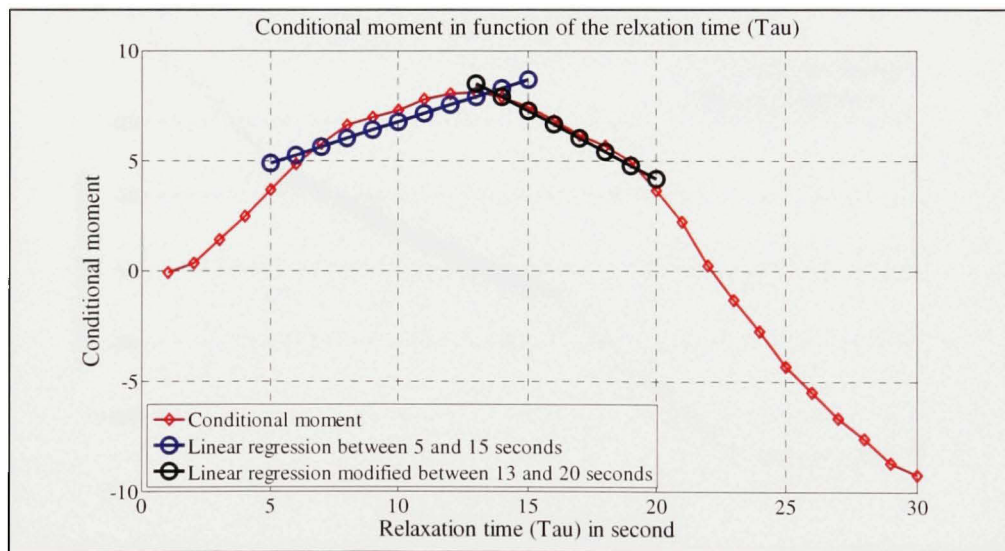


Figure IV.4 *Conditional moment in function of the relaxation time at the bin speed of 6,25 m/s and at the power state of 579 kW.*

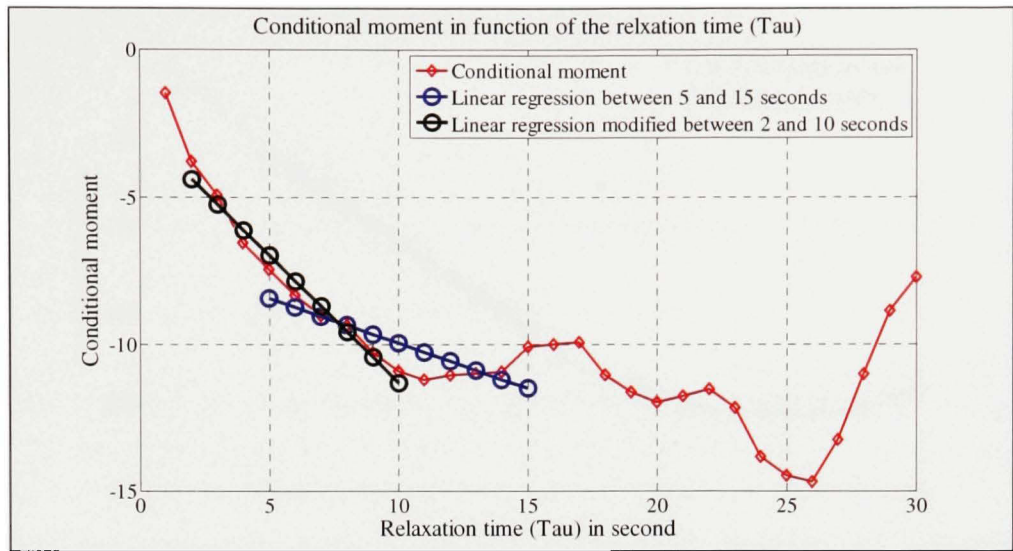


Figure IV.5 *Conditional moment in function of the relaxation time at the bin speed of 6,25 m/s and at the power state of 720 kW.*

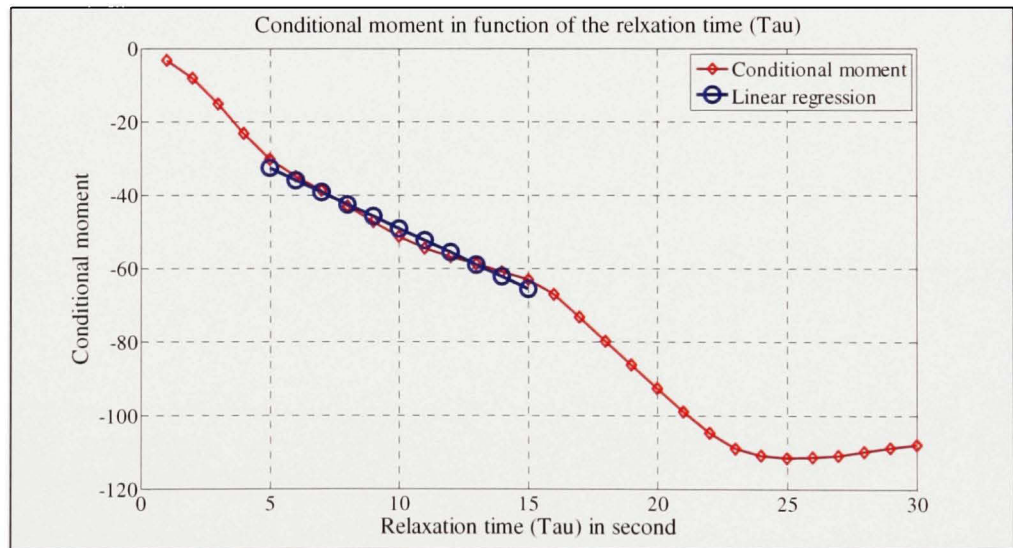


Figure IV.6 *Conditional moment in function of the relaxation time at the bin speed of 6,25 m/s and at the power state of 862 kW.*

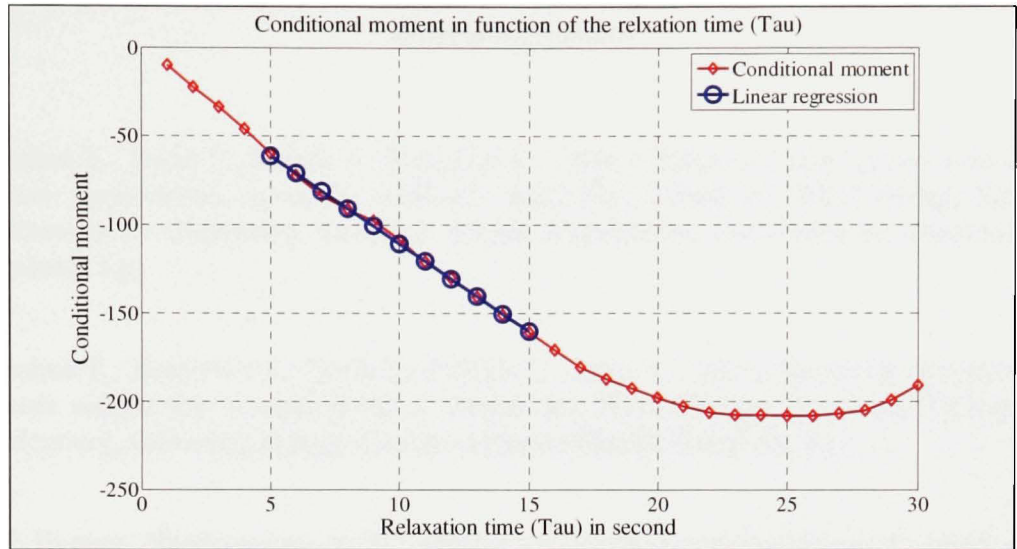


Figure IV.7 *Conditional moment in function of the relaxation time at the bin speed of 6,25 m/s and at the power state of 1003 kW.*

BIBLIOGRAPHY

- [1] Anahua E., Barth S., Peinke J., Boettcher F., 2006, *Characterization of the wind turbine power performance curve by stochastic modeling*, Center for Wind Energy Research, University of Oldenburg, Germany, Physic Department, University of Auckland, New Zealand, 5 p.
- [2] Anahua E., Boettcher F., Barth S., Peinke J., Lange L., 2006, *Stochastic analysis of the power output for a wind turbine*, Center for Wind Energy Research, University of Oldenburg, Germany, energy & meteo systems GmbH, Germany, 4 p.
- [3] GE Energy, *Wind energy at GE*, http://www.gepower.com/businesses/ge_wind_energy/en/about_wind_ener.htm, consulted on June 20th, 2007.
- [4] GE Energy, *Wind energy at GE*, http://www.gepower.com/businesses/ge_wind_energy/en/index.htm, consulted on May 30th, 2007.
- [5] Global Wind Energy Council, *About global industry*, <http://www.gwec.net/index.php?id=31>, consulted on October 8th, 2007.
- [6] Gottschall J., *Provide the simulated data in this thesis*, Center for Wind Energy Research, University of Oldenburg, Germany, 2006.
- [7] Gottschall J., Anahua E., Barth S., Peinke J., 2006, *Stochastic modelling of wind speed power production correlations*, Center for Wind Energy Research, University of Oldenburg, Germany, 2 p.
- [8] Honhoff S., *Obtained from a phone discussion which was initiated by her with the University of Oldenburg*, General Electric, September 2006.
- [9] IEC, 2005, *Power performance measurements of electricity producing wind turbines*, Ed.1, IEC 61400-12-1, Switzerland, International electrotechnical Commission, 90 p.
- [10] Landwehr F., *Formula found by him and obtained from email discussion with Saskia Honhoff*, General Electric, March 2007.

- [11] Manwell J.F., McGowan J.G., Rogers A.L., 2002, *Wind Energy Explained*, John Wiley and sons, 577 p.
- [12] Masson C., *Discussion with him about the new IEC procedure oncoming (61400-12-2)*, École de technologie supérieure, March 2006.
- [13] Pilar Alvarez D., 2006, *Characterization of the wind turbine power performance curve by stochastic modelling*, Diploma thesis, University of Applied Sciences, Germany, 83 p.
- [14] Rauh A., Peinke J., 2003, *A phenomenological model for the dynamic response of wind turbines to turbulent wind*, Institute of physic, University of Oldenburg, Germany, 23 p.
- [15] Risken H., 1989, *The Fokker-Planck Equation*, Ed. 2, Springer Series in Synergetic, Germany, 472 p.
- [16] Wikipedia, 2007, *Brownian motion*, http://en.wikipedia.org/wiki/Brownian_motion, consulted on May 14th, 2007.
- [17] Wikipedia, 2007, *Equipartition theorem*, http://en.wikipedia.org/wiki/Equipartition_theorem, consulted on May 10th, 2007.
- [18] Wikipedia, 2007, *Langevin equation*, http://en.wikipedia.org/wiki/Langevin_equation, consulted on August 13th, 2007.
- [19] Wikipedia, 2007, *Markov property*, http://en.wikipedia.org/wiki/Markov_property, consulted on June 5th, 2007.